

Republic of Iraq
Ministry of Higher Education &
Scientific Research
University of Diyala
College of Science
Department of Physics



**Studying the Properties of Ceramic Bodies Prepared From
Micro and Nano Powders by Slip Casting Technique**

A Thesis

*Submitted to The Council of the College of Sciences, University of Diyala in Partial
Fulfillment of the Requirements for the Degree of Master of sciences in Physics*

By

Haydar Ali Salman Al-obaidy

B.Sc. in Physics (2010-2011)

Supervised by

Prof. Dr.

Sabah A. Salman

Assist. Prof. Dr.

Shehab A. Z. Al-jubouri

2013 AD

1435 AH

إِنَّمَا لِلذَّالِمِينَ فِيهَا عَذَابٌ أَلِيمٌ
فَوَيْلٌ لِلَّذِينَ كَفَرُوا مِنْ عَذَابِ اللَّهِ
الَّذِي هُوَ يُصِيبُكَ مِنَ الدُّنْيَا وَأَحْسِنَ كَمَا
أَحْسَنَ اللَّهُ إِلَيْكَ وَلَا تَبْغِ الْفَسَادَ فِي الْأَرْضِ إِنَّ اللَّهَ لَا يُحِبُّ الْمُفْسِدِينَ (77)

وَابْتَغِ فِيمَا آتَاكَ اللَّهُ الدَّارَ الْآخِرَةَ وَلَا تَنْسَ نَصِيبَكَ مِنَ الدُّنْيَا وَأَحْسِنَ كَمَا
أَحْسَنَ اللَّهُ إِلَيْكَ وَلَا تَبْغِ الْفَسَادَ فِي الْأَرْضِ إِنَّ اللَّهَ لَا يُحِبُّ الْمُفْسِدِينَ (77)

“But seek, through that which Allah has given you, the home of the Hereafter; and [yet], do not forget your share of the world. And do good as Allah has done good to you. And desire not corruption in the land. Indeed, Allah does not like corrupters (77).”

سورة القصص (77)

Surat Al-Qaṣaṣ (77)

CERTIFICATION

CERTIFICATION

We certify that this thesis has been prepared under our supervision at the University of Diyala / College of Sciences / Department of Physics as a partial fulfillment of the requirements for the Degree of Master of sciences in Physics.

Signature:

Name: Dr. Sabah A. Salman

Title: Professor

Date: / / 2014

Signature:

Name: Dr. Sheahab A. Zaidan

Title: Assistant Professor

Date: / / 2014

Head of the Physics Department

In view of the available recommendation, I forward this thesis for debate by the examining committee.

Signature:

Name: Dr. Ziad T. khudair

Title: Lecturer

Date: / / 2014

Committee Certification

Examination Committee Certificate

We certify, that we have read the thesis entitle (*Studying the properties of ceramic bodies prepared from Micro and Nano powders by slip casting technique*), presented by (*Haydar Ali Salman Alobaidy*) and as an examining committee, we examined the student in its contents, and in what is related to it, and that in our opinion it meets the standard of a thesis for the degree of master in Physics Sciences with (**Excellent**) degree.

(Chairman)

Signature:

Name: Dr. Tahseen H. Mubarak

Title: Assistant Professor

(Member)

Signature:

Name: Dr. Abd-ulkhaluq F. Hamood

Title: Assistant Professor

(Member)

Signature:

Name: Dr. Farouq I. Hussain

Title: Assistant Professor

(Member/ Supervisor)

Signature:

Name: Dr. Sabah A. Salman

Title: Professor

(Member/ Supervisor)

Signature:

Name: Dr. Sheahab A. Z. Al jubouri

Title: Assistant Professor

Approved by the Deanery of the College of Science

(The Dean)

Signature:

Name: Dr. Tahseen H. Mubarak

Title: Assistant Professor



Dedication

This thesis is dedicated to my God and lord through this journey has given me Strength, my lovely and respectable parents who are the light of my eyes. To my father who supported my decision for higher education, and my mother who encouraged me all the time. To my brothers: Ibrahim, Asaad and Haseeb. To my lovely sisters & their kind husbands and sons. To my lovely young brother Khalid.

I would like to dedicate this work to all my respectable and authentic teachers especially my supervisors **Dr. Shehab. A. Z. Aljeboori & Dr. Sabah A. Salman** who have helped me a lot on my way to finish my thesis.

Special mention must be made here for my dear friends and especially for my Group: Fuad Al-dulaimy, Aws Al-ezzi, Ali Al-jumaily, Muhammad Al-awssy, Alaa Al-obaidy, Ali Al-rashedy, Alaa Altaay, Aise Karakus, Wadhah Al-jubury and S. Al-dury !

Thanks for inspiring. We made it...

Haydar

Acknowledgments

First and foremost, I thank Allah (SWT) for letting me live to see this thesis through and gave me chance and courage to complete this work, and our prophet Muhammad (peace and blessings of Allah be upon him) who invites us to science and knowledge.

There are a number of people without whom this thesis might not have been written, and to whom I am greatly indebted.

It has been a long road for me to be right here. It is the love, encouragement, support, and help that take me here. Therefore, I would like to express my thanks first to Our God and then to all of my family members, my friends and my teachers.

My greatest indebtedness goes to my Parents for their valuable advice, my Brothers and my Sisters (Adawiya, Shaima Khadija, suha, and rana) and their families (especially my dear Hummady I. Al-mahdawy) for their endless support.

I would like to express my sincere gratitude to my supervisors Prof. Dr. Sabah A. Salman and Assist Prof. Dr. Shehab A. Zaidan who granted me the opportunity to do this research. I am indebted to them for their suggestions and valuable remarks.

Special thank are extended to the Dean of the College of Science and all the Staff of the Department of Physics for their assistance. I am also grateful to the Materials Department at the University of Technology for their kind help during the laboratory work and I would like to express my appreciation to Mr.Duraid for his suggestions and valuable remarks.

Finally, my deepest gratitude is dedicated to my Studying Partners: Ahmed, Zainab, Nisreen, Asmaa, Naowar, Noor, Rudaina, Cheya, Muhammad and especially Aws K. Al-Ezzi who share every happy and sad moment with me..!

Published and Accepted Research Articles

- S. A. Salman, S. A. Z. Aljubouri, H. A. Salman, “**Studying the Physical Properties of Ceramic Bodies Prepared by Slip Casting Technique**”, Diyala journal for pure science, (7 / Jan / 2014).

Abstract

Abstract

In this work, physical phenomena related to the growth and phase formation of alumina, (Al_2O_3), are investigated by experiments and computer calculations.

The specimens were formed by slip casting technique. These specimens were fired at various temperatures of (500, 1100, 1450, 1550 and 1600) °C.

Alumina samples with different dopant percentage were prepared to study their various mechanical and physical properties. Before casting, slurries with different particles size gradation were prepared with different solid content (50 - 70) wt. % and different percentage of dopant additions. The primary dopant used here is kaolinite with a (0, 5, 10 and 15) percentage addition, where kaolinite is one of many types of raw materials that have plasticity and advantage of securing.

Sodium carboxymethylcellulose (Na-CMC) solution was used as dispersant. The stability of the slip which clearly depends on the percentage of dispersant added and the best ratio is found to be (0.33 ml) for each gram of solids.

Increasing the solid concentration percentage leads to decrease the porosity, density, and water absorption, and leads to increase the shrinkage.

Kaolinite percentage increases lead to decreasing the porosity, water absorption and mass losses. But it leads to increase thermal conductivity, density, shrinkage and mechanical properties (compressive strength, bending strength and hardness).

Also, the effect of particle size (nano size of particles) on the physical and mechanical properties is studied together with sintering temperature.

Contents

Contents	Page
Contents	I
List of Figures	V
List of Tables	VIII
List of Symbols and Abbreviations	IX
Abstract	X
1. Chapter one: Introduction	
1.1 Introduction	1
1.2 Previous Studies	4
1.3 Aims of Study	9
2. Chapter Two: Theoretical concept	
2.1 Advanced Ceramics	10
2.2 Slip casting forming method	11
2.2.1 Mould making	12
2.2.2 Slurry preparation	13
2.2.3 Casting the slip	19
2.3 Crystal Structure of Materials	22
2.3.1 Alumina	22
2.3.1.1 γ-Alumina	24
2.3.1.2 α-Alumina	25
2.3.2 Kaolin	26
2.4 Characteristic of α- alumina	28
2.5 Mullite	29

2.6 Physical Properties	31
2.6.1 Density of Powder	31
2.6.2 Mass Losses	32
2.6.3 Shrinkage	33
2.6.4 Density, Porosity and Water absorption	34
2.6.4.1 Bulk density	35
2.6.4.2 Apparent porosity	35
2.6.4.3 Water absorption	35
2.6.5 Thermal conductivity	36
2.7 mechanical Properties	40
2.7.1 Hardness	40
2.7.2 Strength and Compressive Strength	41
2.7.3 Bending Strength	42
2.8 Factors Affecting Mechanical Properties	44
2.8.1 Grain size and distribution	44
2.8.2 Porosity Effects	45
 3. Chapter Three: Experimental Procedure	
3.1 Introduction	48
3.2 Materials	51
3.2.1 Micro Alumina	51
3.2.2 Nano Alumina Powder	52
3.2.3 Kaolinite	53
3.3 Obtainment of Alpha Phase Alumina	54
3.4 Green Body Fabrication by slip casting	55
3.4.1 Mould Making	55
3.4.2 Optimization of the Slurry	56

3.4.3 Casting Process and De-moulding	59
3.5 Drying and Shaping	60
3.6 Firing Program	61
3.7 Procedure of Measurements	63
3.7.1 Physical Testing	63
3.7.1.1 Mass Losses	63
3.7.1.2 Linear Shrinkage	63
3.7.1.3 Bulk Density (BD)	63
3.7.1.4 Apparent Porosity (% AP)	63
3.7.1.5 Water Absorption	64
3.7.1.6 Thermal Conductivity	64
3.7.1.7 Density of Powder	65
3.7.2 Mechanical Testing	66
3.7.2.1 Compressive Strength	66
3.7.2.2 Flexural Strength	67
3.7.2.3 Hardness	68
 4. Chapter Four: Results and Discussion	
4.1 Introduction	69
4.2 Effects of Solid Concentration	69
4.3 Effects of Kaolinite Additions	72
4.3.1 Linear Shrinkage	72
4.3.2 Loss of Ignition	73
4.3.3 Density, Porosity and Water Absorption	74
4.3.4 Thermal Conductivity	76
4.3.5 Mechanical Properties	77
4.4 Effects of Nano Powder	80

4.5 Effects of Sintering Temperature	81
---	----

5. Chapter Five: Conclusions and Recommendations

5.1 Conclusions	84
------------------------	----

5.2 Recommendations	85
----------------------------	----

References	86
-------------------	----

List of Figures

No.	Title	page
1-1	The most widespread ceramics forming methods.	2
2-1	The sample preparation steps by slip casting technique.	11
2-2	Unstable and stable colloidal dispersion	14
2-3	Zeta potential vs. pH for slurries.	16
2-4	Double layer colloidal process.	17
2-5	Schematic energy versus distance curves for double layer repulsion and van der Waals attraction.	18
2-6	Water distribution in slip casting.	19
2-7	Schematic diagram of the drain casting system.	20
2-8	Schematic diagram of the solid casting system.	21
2-9	The alumina phases and the transition stages at different temperatures.	23
2-10	Lattice structure for the (γ -alumina) phase.	24
2-11	The unit cell for the (α -alumina) phase.	25
2-12	Structure of kaolinite.	27
2-13	Schematic representation of kaolinite structure.	27
2-14	Kaolinite plates.	27
2-15	Kaolinite phases transformation in the time of kaolin heating.	30
2-16	Pycnometer.	32
2-17	Laboratory Archimedes setup.	34
2-18	Lee's Disk, for measurement of the thermal conductivity.	39
2-19	Durometer hardness testers (A and D).	41
2-20	Compression strength test.	42
2-21	Three Points loading for modulus of rupture test.	43

List of Figures

2-22	Schematic relationship between grain size and strength for a number of ceramics.	45
2-23	Effect of porosity on the fracture strength of ceramics.	47
2-24	The influence of porosity on the flexural strength for ceramics (Al_2O_3).	47
3-1	Flow chart of the overall experimentation.	49
3-2	Flow chart of the slip casting process in general.	50
3-3	XRD pattern for the micro gamma alumina powder.	51
3-4	XRD pattern for the nano alpha alumina powder.	52
3-5	XRD pattern for the micro kaolinite powder fired at 1300 °C.	53
3-6	X-ray analysis of the (α phase) micro alumina .	54
3-7	Pictures of mould preparation and the mould prepared for a bar sample.	56
3-8	Obtainment of the preferable dispersant.	57
3-9	Obtainment of the preferable value of (Na-CMC) dispersant.	57
3-10	Pictures depicting the slip preparation.	59
3-11	The cast in the mould and after de-moulding.	59
3-12	Samples oven drying.	60
3-13	Samples firing.	61
3-14	The firing program.	62
3-15	The Lee's disk apparatus.	64
3-16	Pycnometer (25ml).	65
3-17	Hydraulic testing compression machine.	66
3-18	A (3-Point) bending tester.	67
3-19	Shore (D) hardness tester.	68
4-1	Effect of solid concentration on the linear shrinkage.	70

List of Figures

4-2	Effect of solid concentration on the bulk density.	71
4-3	Effect of solid concentration on the apparent porosity.	71
4-4	Effect of solid concentration on the water absorption.	72
4-5	Effect of kaolinite percentage additions on shrinkage.	73
4-6	Effect of kaolinite percentage additions on loss on ignition.	74
4-7	Effect of kaolinite percentage additions on bulk density.	75
4-8	Effect of kaolinite percentage additions on apparent porosity.	76
4-9	Effect of kaolinite percentage additions on water absorption.	76
4-10	Effect of kaolinite percentage additions on thermal conductivity.	77
4-11	Effect of kaolinite percentage additions on compressive strength.	78
4-12	Effect of kaolinite percentage additions on bending strength.	79
4-13	Effect of kaolinite percentage additions on hardness.	80

List of Tables

No.	Title	page
2-1	The phases of the alumina and their physical properties at different melting temperatures.	23
2-2	(99.9%) alumina mechanical and physical properties.	28
3-1	Specifications of micro alumina.	51
3-2	Specifications of nano alumina by the manufacturer.	52
3-3	Specifications of micro Kaolinite.	53
3-4	The raw materials compositions of samples.	58
3-5	The sintering temperature of each sample's type.	62
4-1	Effects of nano alumina on the (alumina-kaolinite) samples.	81
4-2	Effects of sintering temperature on the (alumina-kaolinite) samples.	82

List of Symbols and Abbreviations

Symbol	Definition	Unit
γ - Al ₂ O ₃	Gamma phase Alumina	-
θ - Al ₂ O ₃	Theta phase Alumina	-
α - Al ₂ O ₃	Alpha phase Alumina	-
ϵ	The dielectric constant	-
z	Zeta potential	mV
η	Viscosity	-
Na-CMC	Sodium carboxymethylcellulose	-
G_t	Density of powder	g/cm ³
MOI	moisture	%
LOI	Loss on ignition	%
L.S	Linear shrinkage	%
BD	Bulk Density	g/cm ³
AP	Apparent porosity	%
A	Water absorption	%
W _d	Dry weight	Gram
W _s	Soaked weight	Gram
W _i	Suspended weight	Gram
K	Thermal conductivity	W/m.k
G	Average grain size	m
σ	True strength	MPa
σ_0	Strength with no micro pores	MPa
H	Hardness (Shore D)	-
XRD	X-Ray Diffraction	-



Chapter One: Introduction

1. Chapter one: Introduction

1.1 Introduction

The word ceramic is derived from the Greek words ‘kéramos’ - ground, clay; kerameoús - made of clay. The term covers inorganic non-metallic materials that have been permanently hardened by firing at a high temperature [1].

The first step in ceramic processing is preparing the ceramic powder, the second step is moulding (forming). There are many methods of forming ceramics, mainly depending on the final desired shape of a product. The most widespread methods of forming ceramics can be divided into several groups as shown in figure (1-1) [1].

Some of the mechanical properties of ceramics have always been attractive to manufacturers. Their hardness, durability, and ability to operate effectively at high temperatures are unsurpassed by any metal, but their brittleness and difficulty in manufacturing complex shapes have been repelling factors to manufacturers [2].

Slip casting is an old and traditional process which comprises casting a slip (slurry) of particles such as ceramic particles, metallic particles, etc. which can be used as long as they are insoluble in solvents, and in particular it is a method suitable for forming a cast article of high quality complex shaped bodies [3].

The common casting methods involve drain casting and solid casting; hollow bodies such as crucibles are prepared by drain casting whereas non hollow bodies are prepared by solid casting. Casting process begins by filling a mould with ceramic slurry having a pourable consistency. The cast is produced when a physical and/or thermal changes causes the slurry to develop a yield strength. These common casting methods are based on colloidal system in which removal of the liquid is used to consolidate particles suspended in slurry. slip casting

INTRODUCTION

consolidation of particles is accomplished as the liquid flows through a porous medium under a pressure gradient [4].

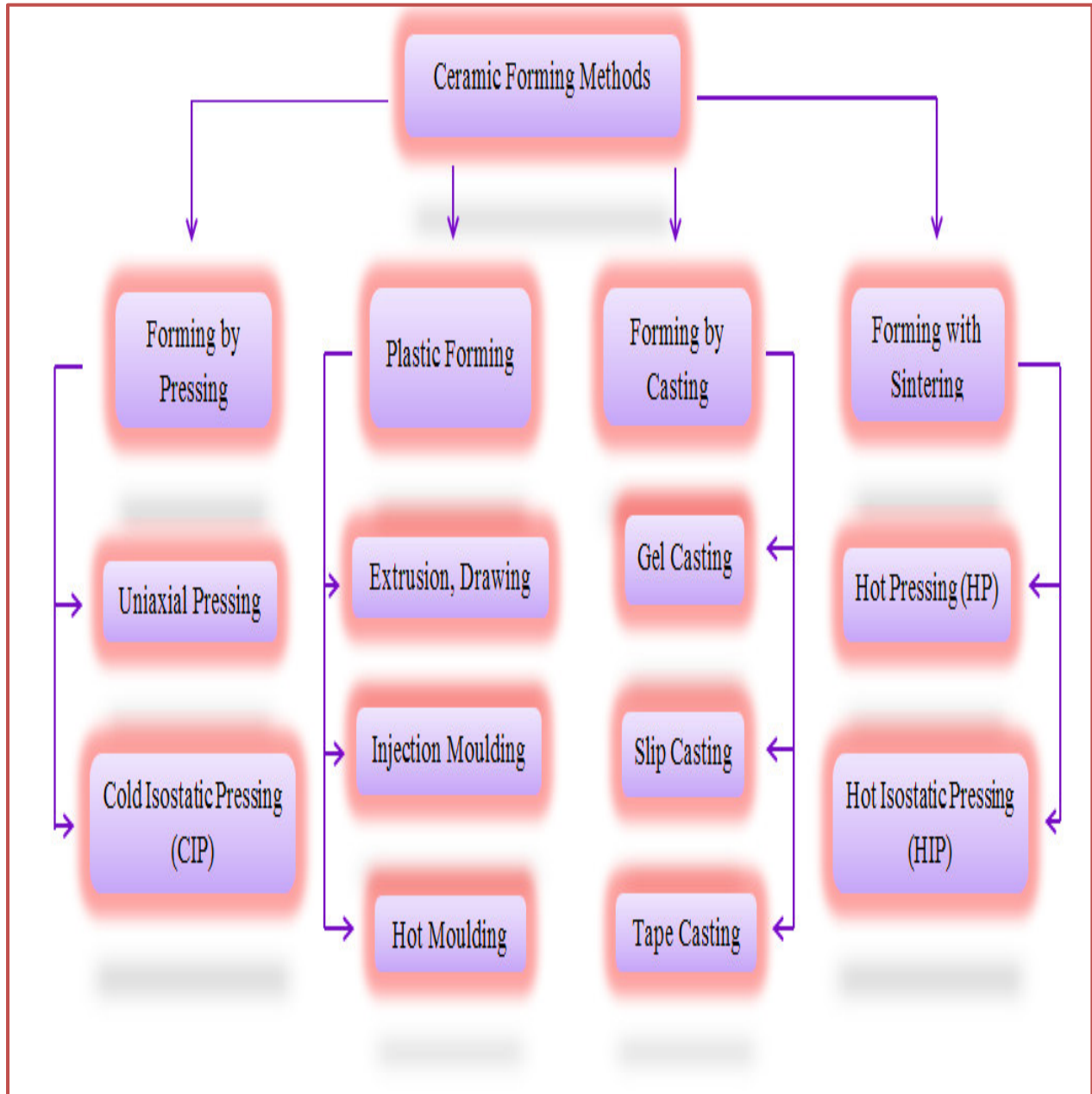


Figure (1-1): The most widespread ceramics forming methods.

INTRODUCTION

The Alumina (Al_2O_3) is old and a tremendous amount of research work has been done over the years. For example, a database (INSPEC) search with the keywords “alumina” or “ Al_2O_3 ” results in (91,700) hits from (1969-2013), i.e., more than (5) published works per day for the last (44 years). However, alumina was known long before that. Even in antiquity several naturally occurring forms of alumina were known, such as the mineral corundum and the gemstones emery, ruby, and sapphire [5]. Due to this long history of research most intrinsic properties of alumina are known, but even today a significant part of the published work deals with alumina materials science on a fundamental level. The main reason is arguably the complexity (and usefulness) of the alumina polymorphs (i.e., crystalline phases). The most important, and common, polymorphs are denoted α , γ , θ , and κ). In addition to these, there are reports on more than twenty other crystalline phases [5]. The (α) phase is the thermodynamically stable polymorph and occurs naturally as corundum or sapphire, while the other phases are metastable in bulk form (but can still be produced in certain processes where thermal equilibrium is not reached, e.g., thin film growth) [6].

Aluminum oxide (alumina; Al_2O_3) has advantages such as its thermal, chemical, and physical properties when compared with several ceramics materials, and is widely used for firebricks, abrasives and integrated circuit (IC) packages. Industrially, more than about (45 million) tons of (Al_2O_3) are produced in the world, which are mainly manufactured by the Bayer method using bauxite, and about (40 million) tons are consumed for refining aluminum [7]. Furthermore about (5 million) tons of (Al_2O_3) are produced as chemical grade and used for various purposes. Moreover about (1.5 million) ton (Al_2O_3) is used as raw powder in the world [7, 8].

1.2 Previous Studies:

A. Tsetsekou et al (2000) [9] identified the conditions for the preparation of stable alumina slurries with high solids content for the production of slip-cast objects with improved properties, as well as to correlate the slurry properties to the final object properties. For slurry stabilization, three commercial dispersants were compared. It was found that for each dispersant there exists an optimum concentration range within which low viscosity is achieved for a slurry of high solids content. In addition to the slurry solids content, the choice of a particular dispersant also affects the slurry viscosity and through that the casting rate. The combination of high slurry solids content and slower casting rate results in objects with higher densities both in the green and fired state.

C. Y. Chen et al (2000) [10] mullite specimens and mullite/alumina composites are prepared by reaction sintering kaolinite and alumina at a temperature above (1000 °C). The phase and microstructural evolution of the specimens and their mechanical properties are investigated. Primary mullite appears at a temperature around (1200 °C). The alumina particles are inert to the formation of primary mullite. Alumina starts to react with the silica in glassy phase to form secondary mullite above (1300 °C). The formation of secondary mullite decreases the amount of glassy phase. Furthermore, the addition of alumina reduces the size of mullite grains and their aspect ratio. The strength and toughness of the resulting mullite increase with the increase of alumina content; however, the mechanical properties of the mullite and mullite/alumina composites are lower than those of alumina for their relatively low density.

INTRODUCTION

Y. Zhang and J. Binner (2001) [11] Raising the slip temperature during slip casting is known to increase the casting rate, this is believed to be via a decrease in water viscosity. However, differences have been observed when using convection and microwave heating to raise the temperature. In the present work, it has been found that the use of short-pulses of microwave energy to heat the casting system dynamically causes a greater degree of acceleration than when using conventional radiant heating. The increased uptake of water from the slip by the porous mould is believed to be indicative of a vaporisation–condensation cycle mechanism. A negative pressure would be created during the condensation stage of the cycle, acting as an additional suction force to the capillary action and hence accelerating the casting process.

L. Braginsky et al (2004) [12] the temperature dependence of the thermal conductivity of porous, nanostructured alumina has been measured. It is shown that this dependence can be described with a single parameter, the value of which depends on the intergrain boundary structure and is independent of the grain size and porosity

M. Hashiba et al (2005) [13] the dispersion and fluidity of aqueous platelet (γ) alumina slurries were enhanced by addition of ammonium polyacrylate (PAA) as a dispersant at (PH 10). Magnesia powder was mixed with the slurries using a planetary mixer for (150 s) after ball milling of the slurries for (24 h). A porosity of about (60%) and strength of (45 MPa) were obtained in bodies fired at (1300 °C) and the mean pore diameter was (0.6 μm).

J. M. Andersson (2005) [6] in this work, physical phenomena related to the growth and phase formation of alumina, (Al_2O_3), are investigated by experiments

INTRODUCTION

and computer calculations. The metastable phases are involved in transition sequences, which all irreversibly end in the transformation to the stable (α) phase at about (1050 °C). As a consequence, the metastable aluminas, which can be grown at low temperatures, cannot be used in high temperature applications, since they are destroyed by the transformation into (α).

Y. Shin et al (2006) [14] investigate and report the effects of a cationic polyelectrolyte, polydiallyldimethylammonium chloride (PDADMAC), on the stability of nano-sized alumina (α -Al₂O₃) suspension. Free (PDADMAC) electrolyte in suspension results in increasing viscosity of (α - Al₂O₃) suspensions dispersed with (PDADMAC) at alkaline and neutral (pH). However, non-adsorbed free (PDADMAC) in suspension do not contribute to viscosity increase in acidic (α - Al₂O₃) suspensions and (α - Al₂O₃) suspensions dispersed with (PDADMAC) show the best flow behavior at acidic (pH).

I. ZEDNIKOVÁ et al (2007) [15] prepared functionally graded zirconia-alumina ceramics. The important factor in the preparation of these ceramics is the study of length changes. The first part of this work focuses on the preparation of bodies with variable zirconia-alumina composition. The optimal deflocculant content was proposed based on colloidal and rheological properties of the (Al₂O₃-ZrO₂) systems. It was observed that increasing volume of deflocculant causes the temperature of shrinkage to rise. In the next part two characteristics were studied on zirconia samples - whether the difference in dilatation changes is caused by firing of deflocculant or by porosity of bodies. It was observed that dilatation changes are caused by the porosity and distribution of pores within the dried samples at the low temperature range. The content of deflocculant influences the size of linear changes.

INTRODUCTION

S. Cava et al (2007) [16] Show that nanocrystalline (Al_2O_3) powders have been synthesized by the polymeric precursor method. A study of the evolution of crystalline phases of obtained powders was accomplished through X-ray diffraction, micro-Raman spectroscopy and refinement of the structures through the Rietveld method. The results obtained allow the identification of three steps on the (γ - Al_2O_3) to (α - Al_2O_3) phase transition. The single phase (α - Al_2O_3) powder was obtained after heat-treatment at (1050 °C) for (2 h). A study of the morphology of the particles was accomplished through measures of crystallite size, specific surface area and transmission electronic microscopy. The particle size is closely related to (γ - Al_2O_3) to (α - Al_2O_3) phase transition.

P. Silakate et al (2008) [17] have prepared tubular alumina filters by a slip casting process. The flocculation of alumina slip was studied as a function of (pH) and (PAM) concentrations. The particle size and viscosity of alumina slip were determined by using laser diffraction technique and Brookfield (DV III+) viscometer, respectively. Pore size and pore size distribution of the alumina filters were measured by using Mercury Porosimeter. From the experimental results, the isoelectric point (i.e.p.) of the alumina slip showed at (pH 7) and gave the largest particle size. Furthermore, the flocculation by (PAM) increased particle sizes, particle size distribution and viscosity of alumina slip due to polymer bridging on surface of particles. However, the addition of electrolyte in (PAM) solutions facilitate flocculation of particles due to the compression of electrical double layer and increase in the van der Waals attractive forces. The larger floc size resulted in bigger pore size in the filter. The average pore size of fired filter at (1500°C) is in the range of (0.32 – 0.34) μm .

INTRODUCTION

C. Falamaki and M. Beyhaghi (2009) [18] present slip casting process for the manufacture of tubular alumina microfiltration membranes. An initial powder of an average particle size of (2 μm) and broad size distribution (up to 10 μm) for imparting initial large pores during the slip casting process was used. The dispersing ability of sodium carboxymethylcellulose (Na-CMC) and Tiron ($\text{C}_6\text{H}_4\text{O}_8\text{S}_2\text{Na}_2 \cdot \text{H}_2\text{O}$) for slips containing (40, 50 and 60 wt. %) of alumina was studied. They show that (Na-CMC) is not able to act as a proper dispersant. The kinetics of the slip casting process and time dependences of cast twodimensional profile were investigated in function of slip concentration. The effect of sintering temperature on the pore microstructure of the final products was investigated.

S. Yi-hua et al (2009) [19] optimize the conditions of ($\text{ZnO-Al}_2\text{O}_3$) aqueous suspensions and slip casting to obtain dense green compacts and further to obtain high density ($\text{ZnO -Al}_2\text{O}_3$) ceramic composites. The Zeta potential of raw powders was measured. (ZnO and Al_2O_3) powders have lower Zeta potential than (-45 mV) commonly at (pH 8–10.3) with polyacrylic acid (PAA) added. They have investigate the influence of (pH) and the mass fraction of the additives on the stability and fluidity of the suspensions added with (PAA) and polyethylene glycol (PEG) by experiments of viscosity and sedimentation.

L. Zhang et al (2010) [20] have processed Textured (α -alumina) ceramics by slip casting suspensions with different mean-sized particles in a strong magnetic field of (9.4 T), followed by pressure less sintering at (1650 $^\circ\text{C}$) for (2 h) in air. The dispersed crystalline particles in the colloidal suspensions could be oriented in a strong magnet when the energy of the crystal anisotropy overcomes the thermal motion energy. They confirmed by the experimental results that the orientation in the green deposit increased with the increasing starting powder size. After

INTRODUCTION

sintering, however, anisotropic grain growth accompanied with excellent texture formation was observed for the ceramic fabricated from the finest starting powder grade, whereas the modest orientation factor of the largest starting powder-based ceramic hardly changed after sintering.

1.3 Aims of Study

- ❖ Preparing ceramic bodies from alumina powder by slip casting technique with high porosity as well as good mechanical properties and low thermal conductivity to make a possibility of using it in the thermal insulation, filters, light Blocks, spark plugs and furnaces lining.
- ❖ Using a plastic ceramic powder as a binder for alumina powder.
- ❖ Studying the effect of solid content on the physical properties.
- ❖ Studying the effects of kaolinite addition on the mechanical & physical properties.
- ❖ Studying the effects of nanoparticle alumina on the mechanical & physical properties.
- ❖ Studying the effects of porosity on the thermal conductivity & mechanical properties.
- ❖ Studying the effects of sintering temperature on the physical & mechanical properties.



Chapter Two: Theoretical Concept

2. Chapter Two: Theoretical Concept

2.1 Advanced Ceramics

Ceramic materials are utilized for many different applications in a variety of fields. There are many types of ceramics, each with unique individual properties. Some examples of common ceramics include glasses, cermets, heavy clays, abrasives, and some dielectric materials. Advanced ceramics have been used in many applications for the last (50 years). The possible uses of these ceramics are seemingly limitless [21].

These materials are compounds that are usually composed of metallic and nonmetallic elements. The classification of a ceramic falls into one of three categories: Oxides, such as alumina and zirconia; non-oxides, which include nitrides, borides, and silicides, and composites, which are reinforced combinations of oxides and non-oxides [22].

In order to use a ceramic for any application, ceramic materials must be formed into a desired shape by some processing method. This process is done by utilizing fine powders. There are many methods to obtain a desired ceramic structure of varying size and shape such as: Dry Pressing (Uniaxial Die Pressing and Isostatic Pressing), Spraying, Injection and Extrusion and Slurry Casting (Pressure Casting, Gel Casting, slip casting and Tape Casting), Each method utilizes various equipment and ingredients to create a desired result [23].

This research was specifically related to the slip casting technique.

2.2 Slip casting forming method

Slip-casting of ceramics has made it possible to create complex shapes while maintaining the desirable characteristics of the ceramic. Slip-casting is a relatively simple and inexpensive method used to produce ceramics. The alumina powder is dispersed in an aqueous solution then poured into a gypsum mould. The mould removes the water from the solution leaving the powder in a tightly packed green state. Because of the diversity in the sizes and shapes of the moulds, the ceramic bodies can take on any number of shapes [3].

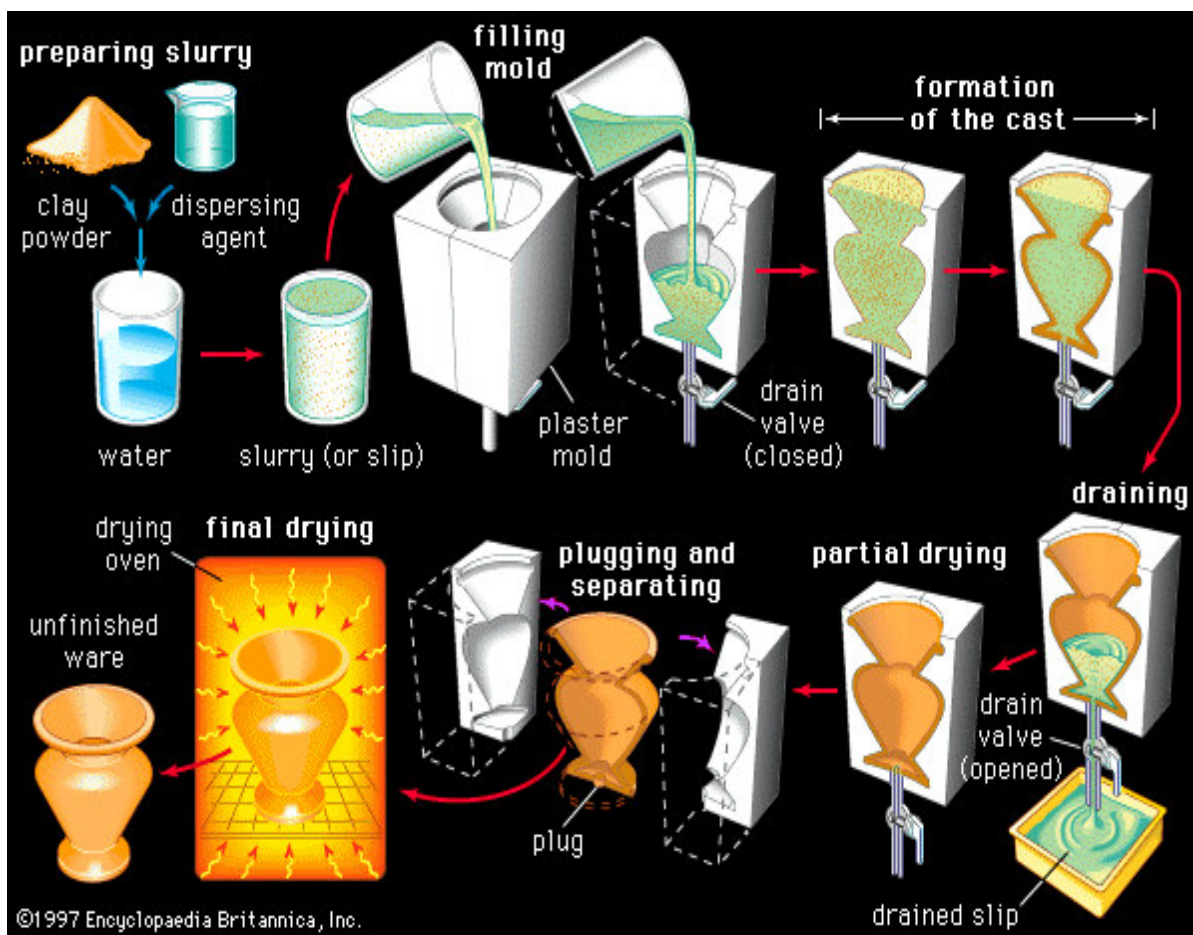


Figure (2-1): Show the sample preparation steps by slip casting technique [3].

2.2.1 Mould making

The most commonly used porous mould material for slip casting is gypsum ($\text{CaSO}_4 \cdot 2\text{H}_2\text{O}$) formed from the reaction between Plaster of Paris ($\text{CaSO}_4 \cdot 0.5\text{H}_2\text{O}$) and water [4]:



This technology is used because of the ability to fabricate moulds with good surface smoothness and details, short setting time, small dimensional expansion (about 0.17%) on setting which aids release from models and relatively low cost. A range of (60/100) to (80/100) water/plaster weight ratio is used in slurries for production moulds [3].

The mould must satisfy the following three requirements:-

1. The casting mould must be so porous as to absorb a liquid such as water, alcohol, etc. as a solvent for the slip, though it is not a disadvantage that a part of the casting mould fails to absorb the solvent [3].
2. Mould material must have such strength above a given level as to ensure the mould-making work, for example, compression strength of at least ($3\text{-}4\text{kgf/cm}^2$) [3].
3. The strength of the casting mould must be considerably lowered within a shape maintainable range by heating. More specifically, a compression strength of about (1kgf/cm^2) can be maintained [3].

2.2.2 Slurry preparation

The next important thing required in case of casting process is to disperse the ceramic powders in an aqueous medium which has to fulfill several requirements such as suspended particles should not be settle fast under the effect of gravity and should be able to remain in suspended state or else segregation can occur and may cause density inhomogeneities in the casted bodies [24].

Secondly, the slurries should be easily reproduced and must be insensitive to slight variations in solids content, chemical composition and time durations. For the casting of alumina based bodies generally slip with high solid content is preferred which not only ensures reasonable casting rates but also reduce energy consumption, which is required, in the subsequent drying stages due to the lower moisture content that has to be removed [25].

The use of very fine particles, which is the prevailing trend in ceramic processing, enhances sintering rates of the bodies. However use of both fine powder and high solid content in the slip leads to increase in the viscosity because the increases of particle-particle interactions that increase complexities [4].

The tendency of ceramic powders to agglomerate which is due to the intra-particle Vander Waals forces made unstable, but that can be eliminated with the addition of appropriate dispersants which alter the powder surface properties and made a stable slurry as shown in the figure (2-2) [26].

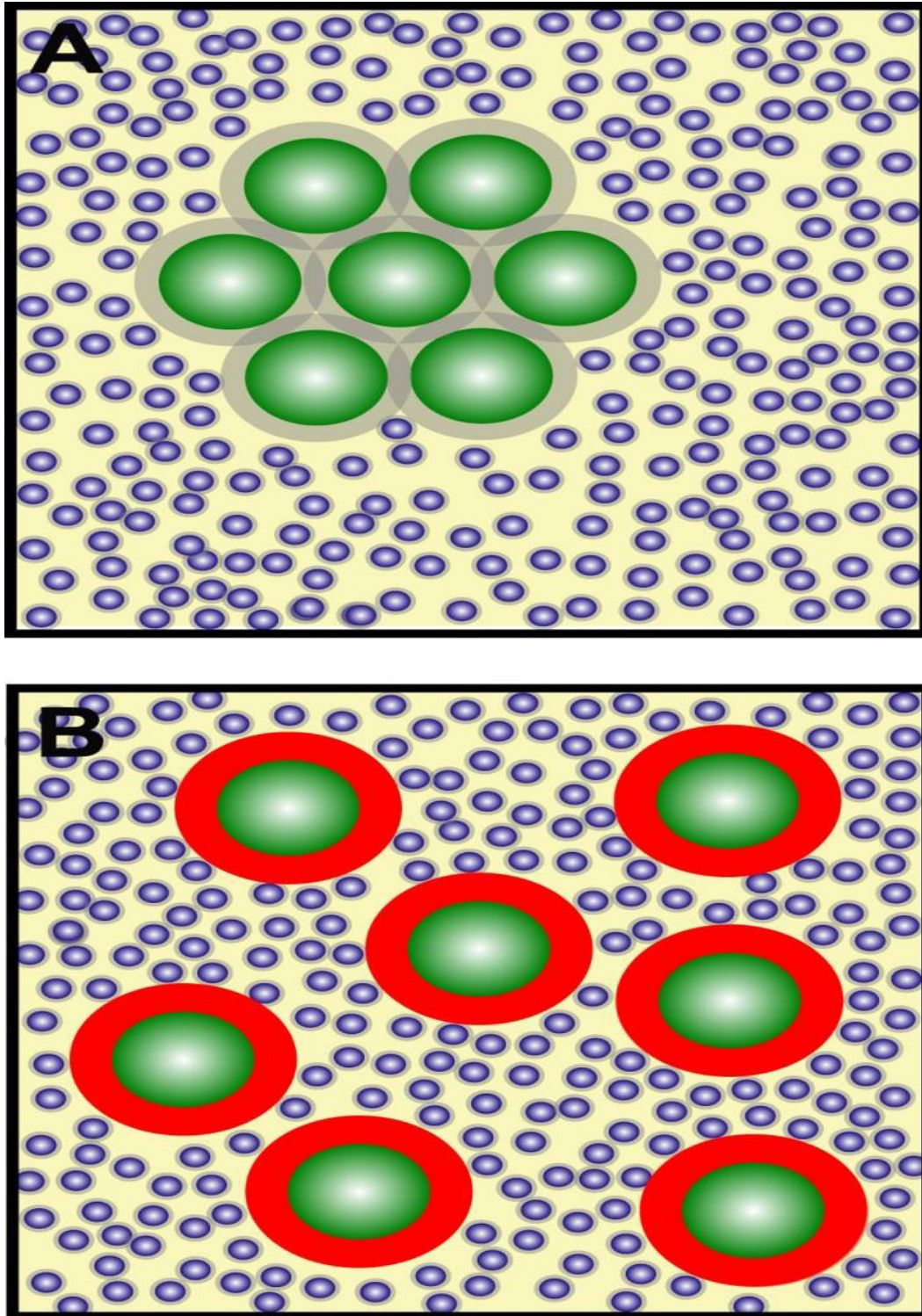


Figure (2-2): (A) unstable and (B) stable colloidal dispersion [26].

Theoretical concept

These dispersants modify net Charge at the particle surface and that development affects the distribution of ions in the neighboring interfacial region, resulting in an increased concentration of (counter ions – ions) of Charge opposite to that of the particle - close to the surface. Thus an electrical double layer is formed in the region of the particle-liquid interface [27].

The double layer (figure (2-4)) may be considered to consist of two parts [27]:

- An inner region of strongly bound ions known as the Stern layer
- An outer layer of loosely associated ions called the diffuse layer.

The potential in this region, therefore, decays as the distance from the surface increases until, at sufficient distance, it reaches the bulk solution value, conventionally taken as zero [27].

As the particle moves through solution, due to gravity or an applied voltage, the ions move with it. At some distance from the particle there exists a boundary, beyond which ions do not move with the particle. This is known as the surface of hydrodynamic shear, or the slipping plane, and exists somewhere within the diffuse layer. It is the potential that exists at the slipping plane that is defined as the zeta potential (figure (2-4)) [27].

The velocity of a particle in an electric field is dependent on [27]:

- ❖ the strength of the electric field
- ❖ the dielectric constant of the liquid
- ❖ the viscosity of the liquid
- ❖ the zeta potential

By directly measuring the electrophoretic mobility of a particle, the zeta potential may then be determined using the Henry Equation [27]:

Theoretical concept

$$U_E = \frac{2\epsilon z f(Ka)}{3\eta}$$

Where (ϵ) is the dielectric constant, (z) is the zeta potential, ($f(Ka)$) is Henry's function, and (η) is the viscosity. Henry's function generally has value of either (1.5) or (1.0). If measuring zeta potential in a non-polar solvent, the Huckel approximation is used, where $f(Ka)$ is set to (1.0).

The zeta potential is crucial in determining the stability of a colloidal suspension. When all the particles have a large negative or large positive they will repel each other, and so the suspension will be stable. If the zeta potential is low the tendency for flocculation is increased. Another important consideration when discussing zeta potentials is pH as shown in figure (2-3); in fact, quoting a zeta potential without an accompanying pH is almost meaningless [27].

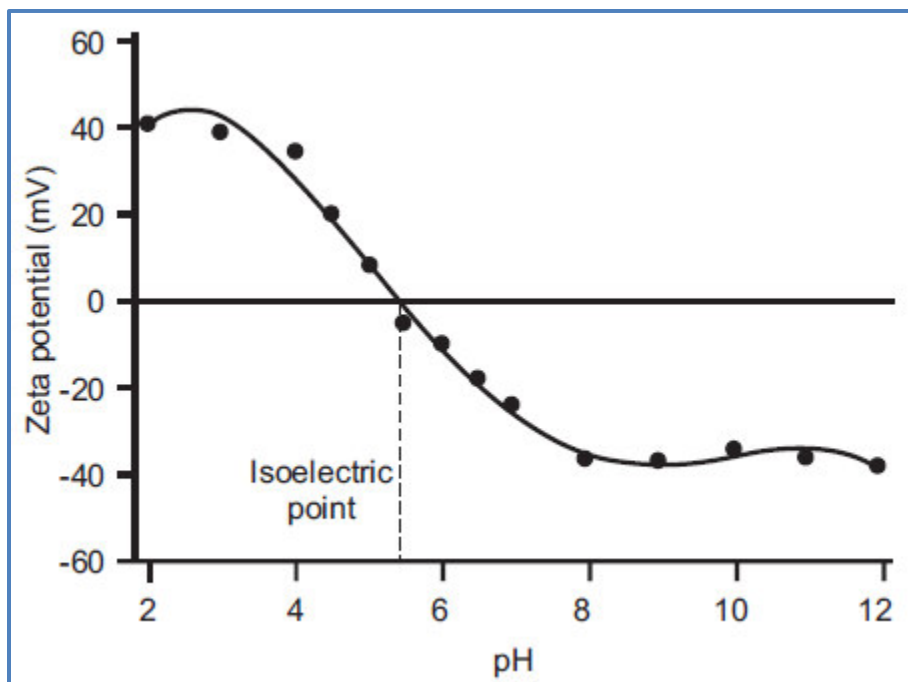


Figure (2-3): Zeta potential vs. pH for slurries [27].

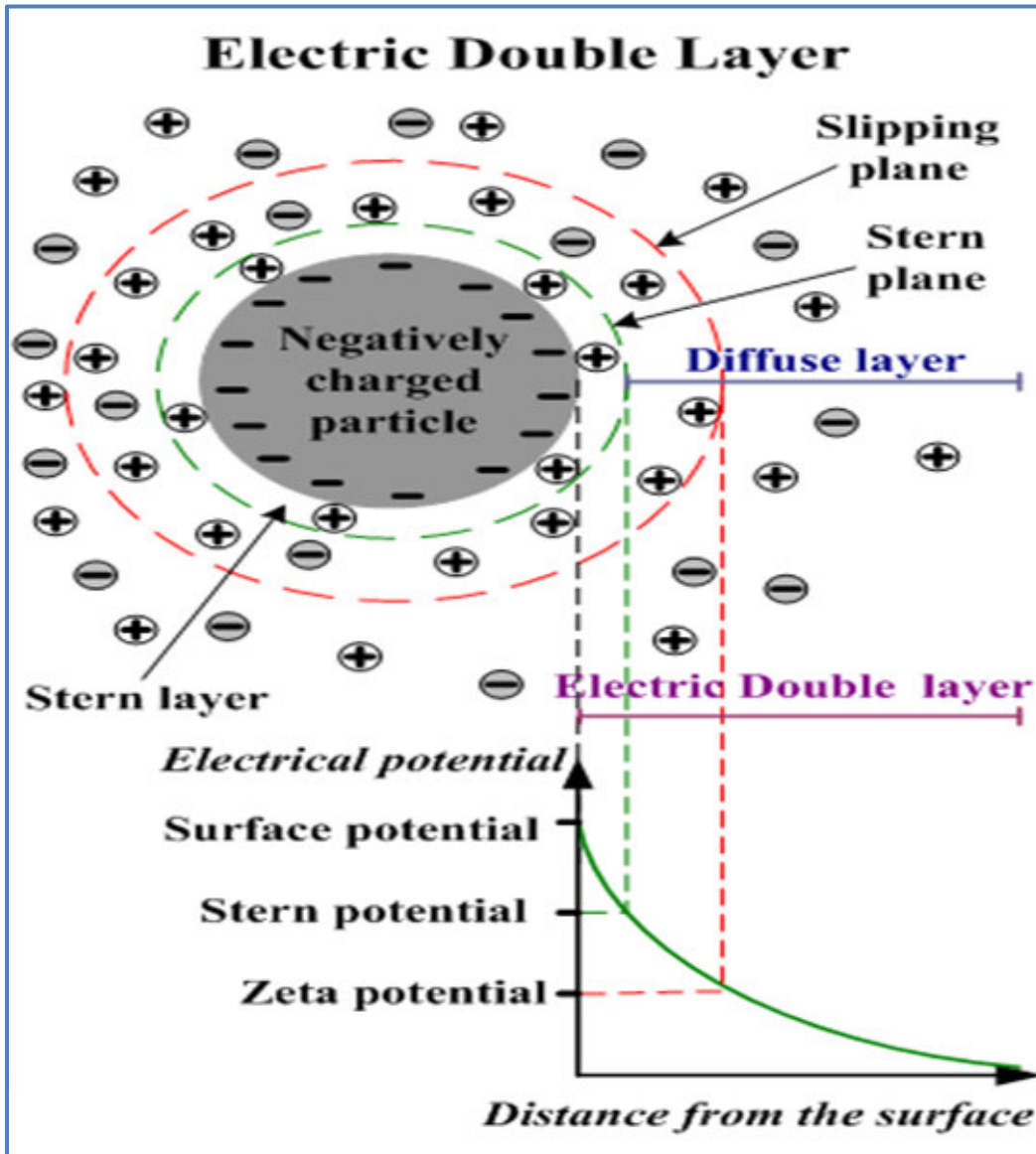


Figure (2-4): Double layer colloidal process [27, 28].

These modifications ensure the suspension of particles within the slurry without being getting settled or forming thick lumpy masses [26].

Combining the attractive van der Waals interaction and the repulsive double-layer repulsion is the foundation of the well-known (DLVO) theory, which provides an overall net interaction energy, as illustrated in figure (2-5) [28, 29].

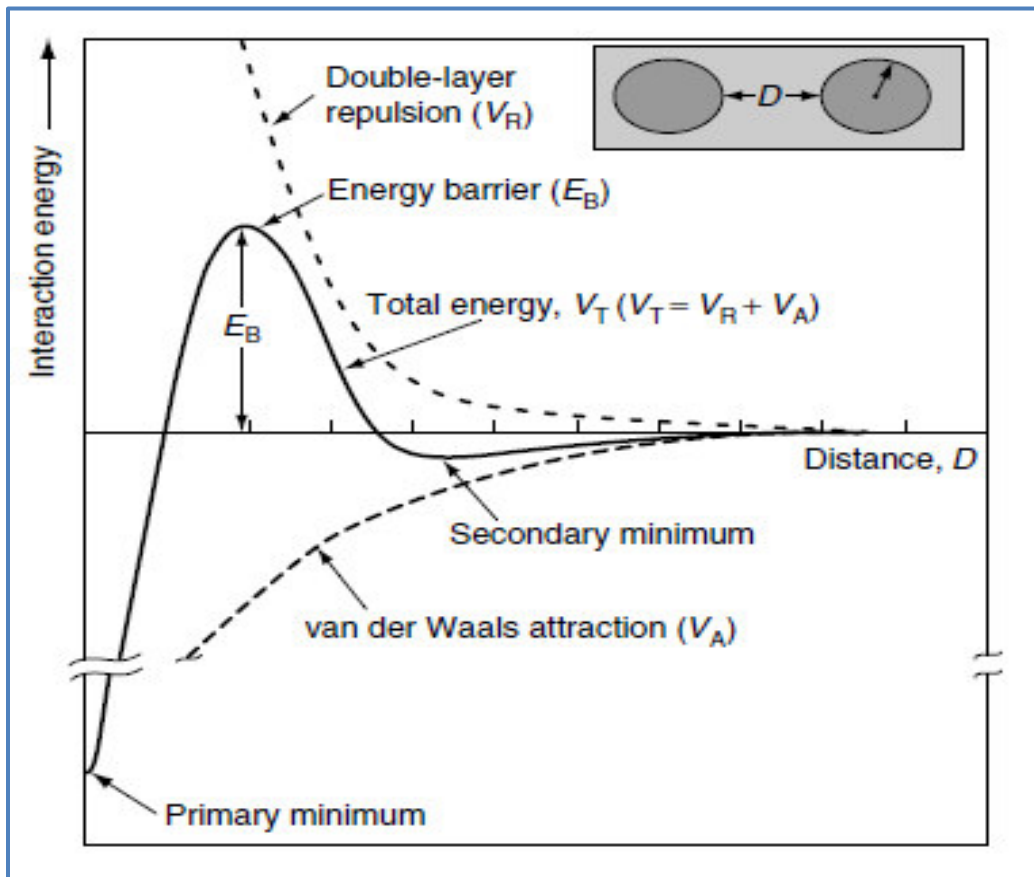


Figure (2-5): Schematic energy versus distance curves for double layer repulsion and van der Waals attraction [28].

Various dispersants are available for the stabilization of oxide powder slurries (alumina, titania, zirconia, etc.) but Sodium carboxymethylcellulose (Na-CMC) was used. This was performed according to the existing reports claiming the effectiveness of (Na- CMC) in slip casting of high purity alumina, acting as a deflocculant, binder and fluxing agent with low residual sodium upon burnout, albeit for sub-micron powders [30, 31].

2.2.3 Casting the slurry

The slurry is then poured into a porous mold that removes the liquid (it diffuses out through the mold) and leaves a particulate compact in the mold. This process is known as slip casting [32, 33].

When the slip is poured into the mould, the plaster begins to absorb the water out of the slip (figure (2-6)) at a rate controlled by release agents on the surface of the mold, the moisture content of the mold, and by the ambient relative humidity in the casting shop. The absorption causes the clay to form and thicken where it is in contact with the surfaces of the mould, removing deleterious air gaps and controlling shrinkage of the casting. The cast piece remains in the mould until it dries sufficiently to attain a “leathery” consistency. At this point, the clay casting will separate easily from the plaster surfaces and can be removed from the mould [34].

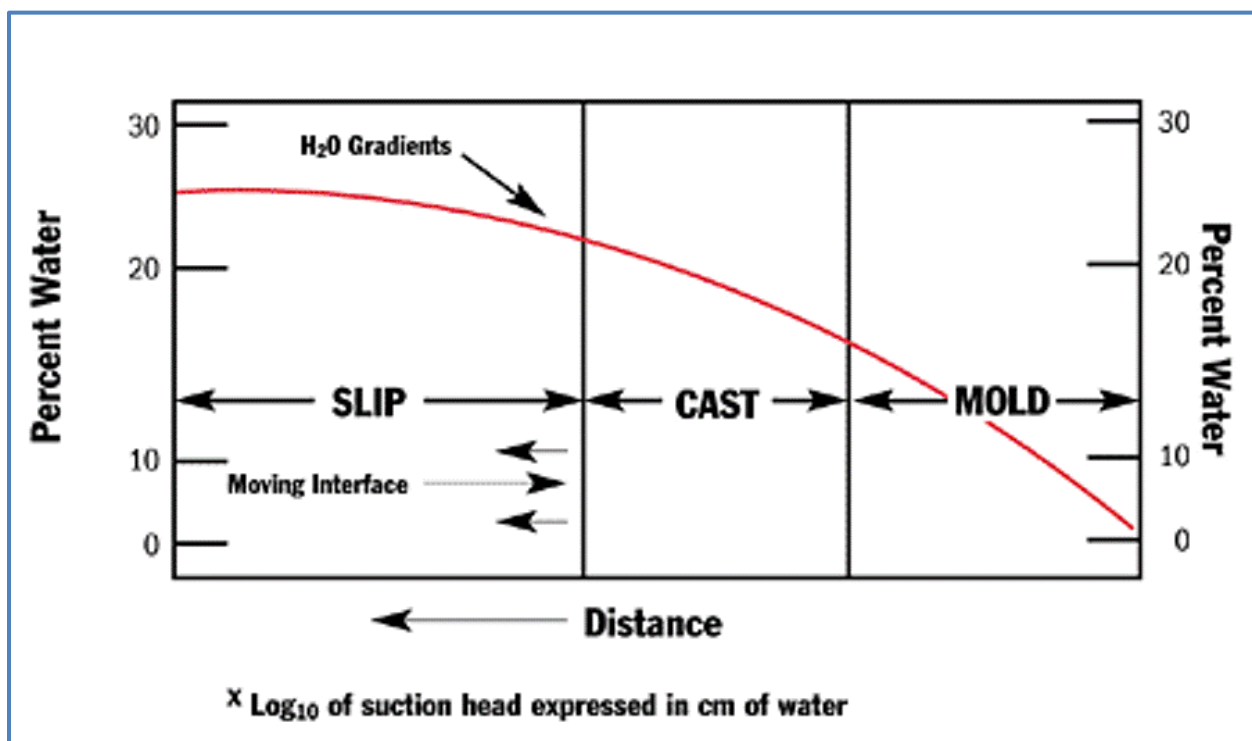


Figure (2-6): Water distribution in slip casting [34].

Theoretical concept

The common casting methods involve drain casting and solid casting; hollow bodies such as crucibles are prepared by drain casting where consolidated layer of solids, referred to as a cast, forms on the walls of the mold (Figure (2-7)). After a sufficient thickness of the cast is formed, the surplus slip is poured out and the mold and cast are allowed to dry. Normally, the cast shrinks away from the mold during drying and can be easily removed [33, 34].

In a solid cast mould, ceramic objects such as handles and platters are surrounded by plaster on all sides with a reservoir for slip, and are removed when the solid piece is held within (figure (2-8)) [34].

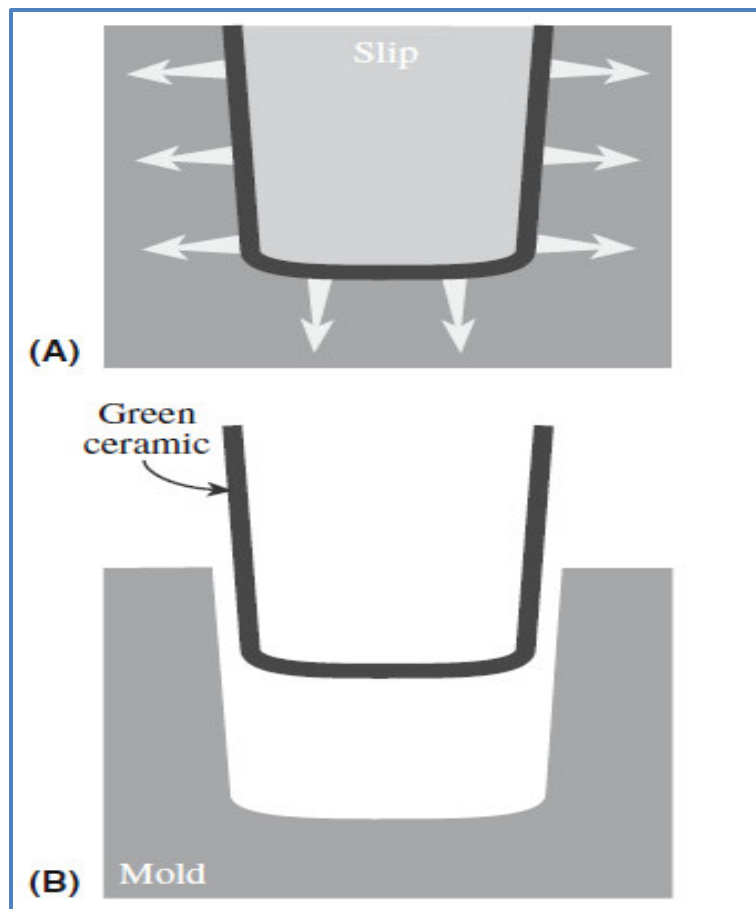


Figure (2-7): Schematic diagram of the drain casting system: (a) initial system (b) after the formation of a thin cast [34].

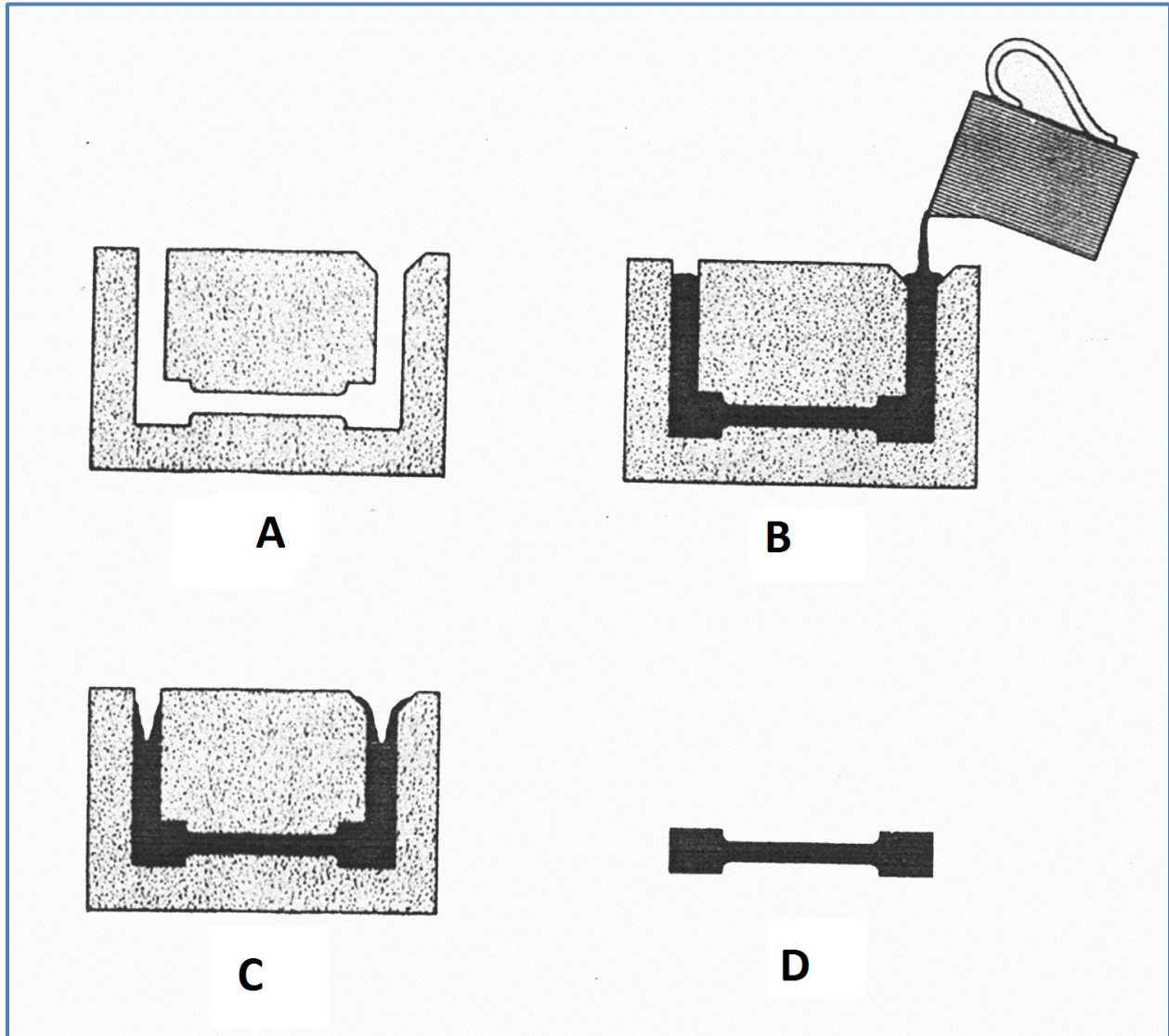


Figure (2-8): Schematic diagram of the solid casting system [34]:

- (a) The plaster of Paris mould**
- (b) Initial system**
- (c) The mould absorb the water from the slip**
- (d) The solid piece is taken out**

2.3 Crystal Structure of Materials

2.3.1 Alumina

Polycrystalline alumina, (Al_2O_3) is a ceramic material. The alumina exists with different phases depending on the alumina purity and its mechanical and physical properties [35]. Alumina (α -phase) is a thermodynamically stable phase, which can be used as a coating to keep the material surface safe from wear. Alumina has other properties for example; mechanical properties, chemical inertness, and thermal stability and these properties provide useful applications for the alumina [36]. Polycrystalline alumina was used as catalyst and catalyst support due to the alumina having a small grain size and high surface area [35, 37].

The alumina phases are (γ , θ , and α phase) which represent the crystalline phases that are important in the alumina structure. The α -phase is stable at high temperature (i.e. melting temperature for this phase is (2051 °C)) but the other phases do not always exist in the alumina [35].

The polycrystalline alumina (α -phase), is formed at the high temperature of about (1000 °C). The properties for the (α -alumina) are not the same for other phases, which gives the alumina phases a wide range for applications [35]. Table (2-1) shows the melting temperature for these phases.

The (α -alumina) has a hexagonal structure but the (γ -alumina) has a spinel structure.

Theoretical concept

Table 2-1: The phases of the alumina and their physical properties at different melting temperatures [21].

Alumina phase	Density kg/m ³	Melting point °C
α alumina	3980	2051
γ alumina	3200	$\gamma \rightarrow \delta$: 700–800
θ alumina	3560	$\theta \rightarrow \alpha$: 1050

The (α -phase) alumina is stable at high temperatures and also, other phases are transformed to α -phase at high temperature. At the specific temperature the (γ and θ) phases are transformed to the corundum phase as shown in Figure (2-9). The (α -alumina) does not change to the (γ) and (θ) phases and the (α -phase) is thermodynamically stable at (1000 °C) [35, 38].

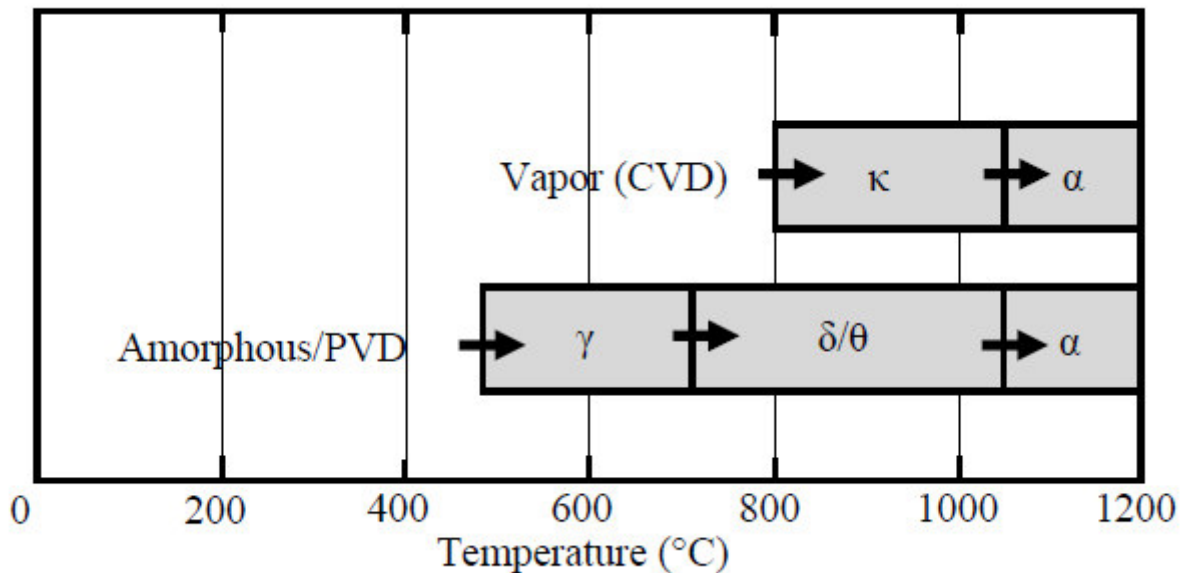


Figure (2-9): The alumina phases (i.e. α , γ , and θ phases) and the transition stages at different temperatures [35].

2.3.1.1 γ -Alumina

The (γ - Al_2O_3) phase is an unstable phase and it is transformed to the (θ -alumina) phase at a temperature of (700–800) °C. This phase of alumina was used as a catalyst and catalyst support as the (γ - Al_2O_3) unit cell has a large specific area and also has a low surface energy [39]. This phase is not used in the high temperature applications because this phase transforms to the stable phase at high temperature (i.e. α -alumina) [40].

The lattice structure for the (γ - Al_2O_3) phase has two different lattices, the first lattice is comprised of aluminium ions and it is formed from octahedral and tetrahedral interstitial locations and the oxygen lattice is formed with the face centre cubic structure are shown in figure (2-10) [40].

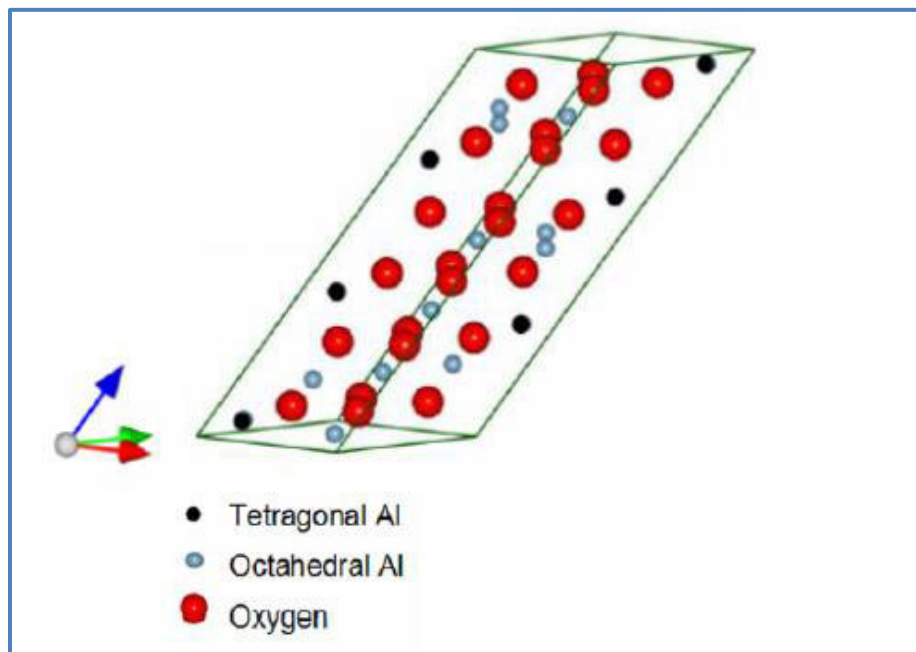


Figure (2-10): The face centre cubic structure for the oxygen lattice and the octahedral and tetrahedral structure for the aluminium lattice. The whole structure forms the (γ -alumina) phase structure [41].

2.3.1.2 α -Alumina

Polycrystalline (α -phase alumina) is used as a structural ceramic due to it having good mechanical properties and also excellent thermal properties at high temperatures. Polycrystalline alumina also has a high strength and these properties are provided during developing, processing, and optimizing the polycrystalline alumina. The alumina was used in parts for many applications instead of the other ceramics due to its high strength [42]. There are many ceramics that have been used as structural ceramics for example Titania (TiO_2), Zirconia (ZrO_2), Magnesia (MgO), Ytria (Y_2O_3) and alumina–magnesia spinel (MgAl_2O_4). In gas turbine applications, non-oxide ceramics have been used, for example, silicon carbide (SiC), and silicon nitride (Si_3N_4) [38]. When the (α - Al_2O_3) phase is single crystal, it is called sapphire and has also been used in structural ceramics [38]. The polycrystalline alumina lattice for the α -phase has large oxygen ions with arrangement (A–B–A–B) to form the (HCP) sublattice as shows in figure (2-11) [8].

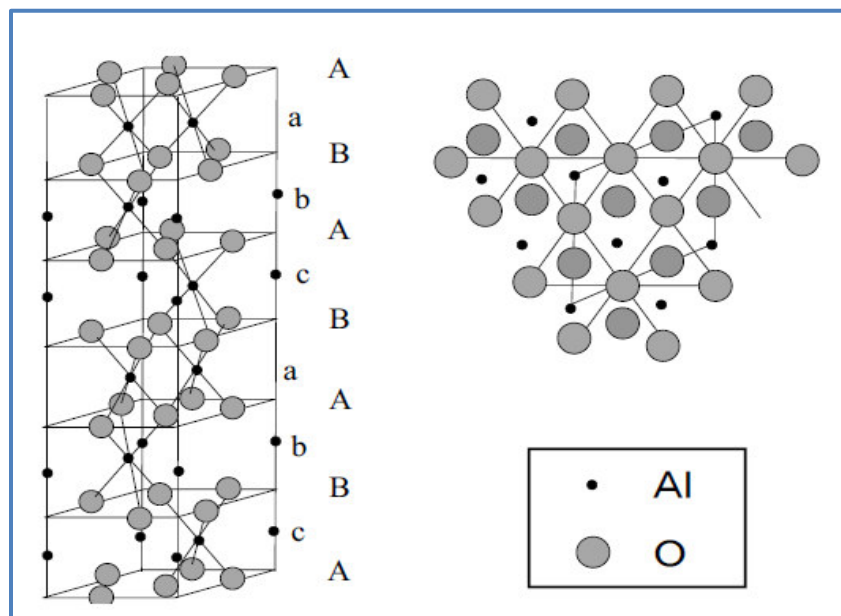


Figure (2-11): Shows the unit cell for the (α -alumina) phase [8].

2.3.2 Kaolin

Very pure kaolins have compositions of $\text{Al}_2\text{O}_3 \cdot 2\text{SiO}_2 \cdot 2\text{H}_2\text{O}$ called "Kaolinite", formed by weathering of feldspathic rocks, granites, etc. The kaolin raw material contains besides clay mineral "Kaolinite", other oxide fluxes such as TiO_2 , MgO , Fe_2O_3 , K_2O , Na_2O , CaO , etc. [43].

Kaolinite consists of a single silica tetrahedral sheet and a single alumina octahedral sheet combined to form the kaolinite unit layer (Figure (2-12)). These unit layers are stacked on top of each other [44]. The kaolinite structure doesn't have interlayer cations, this leads to no swelling, and the water (H_2O) is chemically-bound in the structure as (OH) ions [45]. There is no substitution in these layers. Therefore the layers have no charge and no adsorbed cations (Figure (2-13)) [46].

The crystal structure of kaolinite is triclinic, with cell data: $a = 5.15 \text{ \AA}$, $b = 8.95 \text{ \AA}$, $c = 7.39 \text{ \AA}$ and $\alpha = 91.8^\circ$, $\beta = 104.5^\circ$, $\gamma = 90^\circ$ [47].

The plastic property of clay occurs because of the crystal structure of kaolinite, the unit cell being a hexagonal assembly of thin ionic and covalently bonded layers (Figure (2-14)). Thus with water added to the clay, the plates of the crystal can be made to slide easily over each other [48].

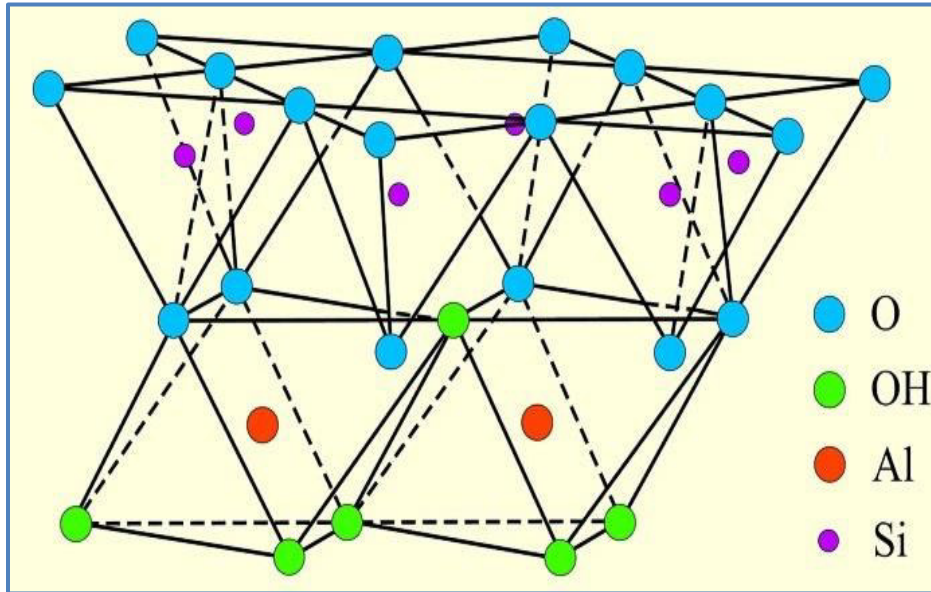


Figure (2-12): Structure of kaolinite [45].

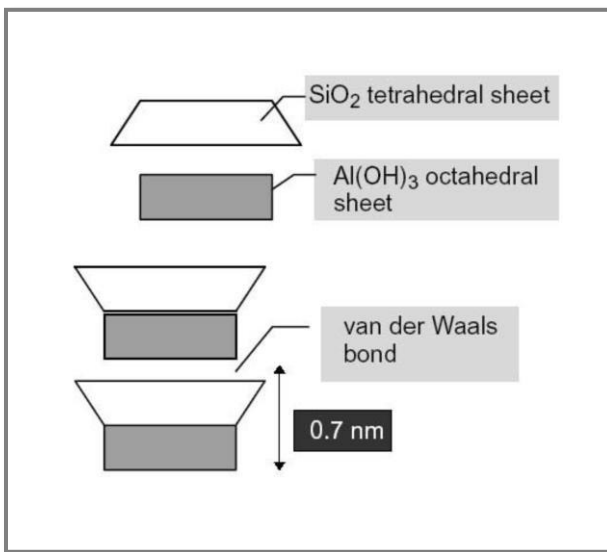


Figure (2-13): Schematic representation of kaolinite structure [46].

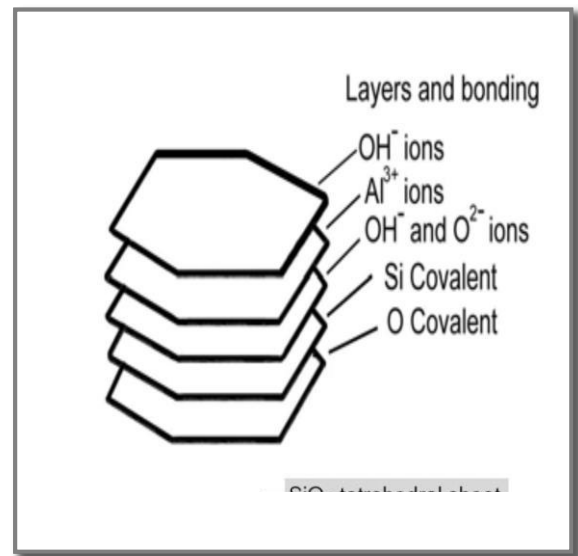


Figure (2-14): Kaolinite Plates [48].

2.4 Characteristic of α - alumina

Polycrystalline alumina has good mechanical properties and these properties provide alumina with significant applications [49]. The melting temperature for α -alumina is about $(2050 \pm 4 \text{ }^\circ\text{C})$. It has a good creep resistance due to alumina being stable at high temperature and it also has excellent compressive strength [49]. Polycrystalline alumina is used in medical and high temperature applications and electronics applications [42].

Table (2.2): (99.9%) alumina mechanical and physical properties [32, 50].

Properties	Units of Measure	value
Density	g/cc	3.93
Porosity	% (%)	0
Color	—	ivory
Flexural Strength	MPa	410
Compressive Strength	MPa	2900
Elastic Modulus	GPa	385
Poisson's Ratio	—	0.23
Hardness	Kg/mm ²	1440
Thermal Conductivity	W/m [•] K	31
Specific Heat capacity	J/kg-K	840

2.5 Mullite

The mullite is the only stable crystalline phase in the aluminosilicate system under normal atmospheric pressure. The crystal structure of mullite is orthorhombic. It consists of (AlO_6) octahedral chains, parallel to the (c-axis), which are cross-linked by the $((\text{Al,Si})\text{O}_4)$ tetrahedral chains [51, 52].

The high levels of the functional properties of aluminosilicate ceramics depend on the general content of mullite, on its structural and morphological state [53, 54]. The industrial methods for producing aluminosilicate ceramics are based on the highest formations of mullite quantity. This is achieved by using the refractory clays with high amount of SiO_2 and (Al_2O_3) . The kaolin is an example of such clay [55, 56]. The mullite ceramic can be achieved from alumina and silica oxides mixing with refractory clay in certain ratios [56, 57].

The flow complex of physical-chemical processes is important at the time of sintering at the high temperatures. These are dehydration, decomposition of the components of the mass, combustion of organic impurities, the reaction between the components of the mass with the formation of other crystalline phases and polymorphic transformations [58].

The kaolinite and other minerals of clay are converted into mullite and cristobalite, quartz into various modifications of silica. When kaolin is heated, its important minerals – kaolinite is transformed to mullite by several steps according to the following reaction scheme (figure (2-15)) [51].

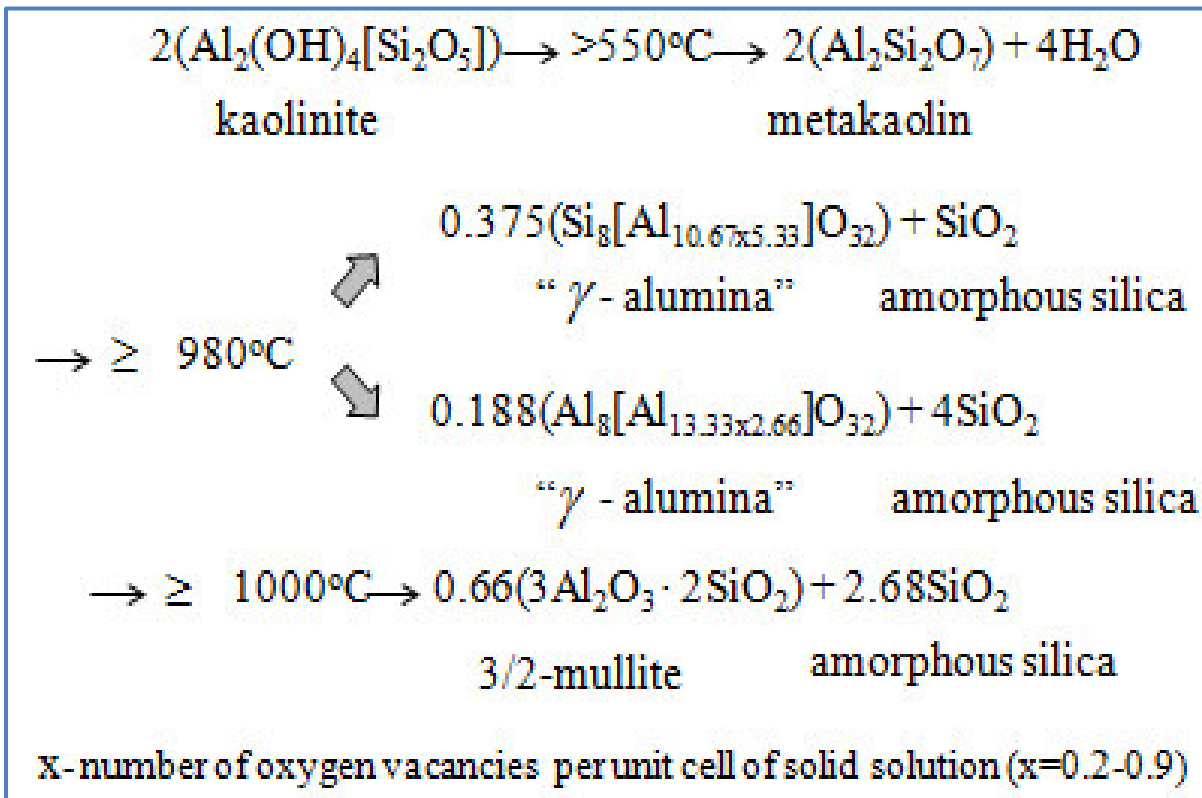


Figure (2-15): Kaolinite phases transformation in the time of kaolin heating [51].

The mullite ceramics have high mechanical strength, chemical stability and high refractoriness. The mullites are produced by heat treatment of the starting materials, essentially via solid-state reactions. These mullites tend to have “stoichiometric”, i.e., (3/2-composition) $(3\text{Al}_2\text{O}_3 \cdot 2\text{SiO}_2)$ [58].

2.6 Physical Properties

2.6.1 Density of Powder

Pycnometer method is a very precise procedure for determining the density of powders and this method is more labor-intensive and far more time-consuming than the buoyancy and displacement methods. The density of powder calculated by applied the following equation [59]:

$$G_t = \frac{P_s}{P_{w,t}} = \frac{M_s}{M_{p,w,t} - (M_{p,w,s,t} - M_s)} \quad (2-1)$$

Where:

ρ_s : the density of the soil solids g/cm³,

$\rho_{w,t}$: the density of water at the test temperature (T_t), g/ml or g/cm³.

M_s : the mass of the oven dry soil solids (g).

$M_{pws,t}$: the mass of pycnometer, water and soil solids at the test temperature, (T_t), g.

In this test we use the pycnometer assimilates (25ml) and sensitive balance max (350g) as shown in (Figure (2.16)) (ASTM D854-10) [60].

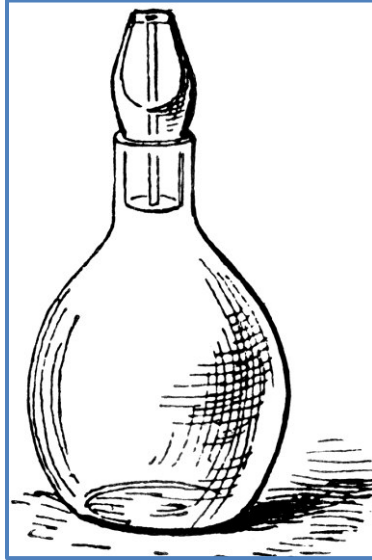


Figure (2-16): Pycnometer [60].

2.6.2 Mass Losses

In alumina slip casting ceramic the mass losses are often referred to as ‘moisture’ (MOI) and ‘loss on ignition’ (LOI) respectively [61]. Total losses for sample are calculated by [62]:

$$L.O.I = \frac{m_o - m}{m_o} * 100 \% \quad (2-2)$$

Where;

m_o : Sample wet mass

m : Sample fired mass

Loss calculation on ignition is very important to the evaluation of density after firing of product [62].

2.6.3 Shrinkage

Shrinkage occurs because the particles approach together. Volume Calculation or linear shrinkage is necessary to find out the amount of the decreasing or increasing in the dimension to be taken into consideration when designing the mould or die [50].

Total linear shrinkage (L.S) after drying and firing of ceramic specimens as a percentage of plastic length, is as follows [62]:

$$\% \text{ linear shrinkage} = \frac{L_0 - L}{L_0} * 100 \% \quad (2-3)$$

Where L_0 : initial length of test specimen (before firing)

L: fired length of test specimen.

Also (ASTM C326) [63]:

$$\% \text{ Volume shrinkage} = [1 - (1 - \frac{L.S}{100})^3] \quad (2-4)$$

Theoretical concept

2.6.4 Density, Porosity and Water absorption

Archimedes Principle states that the buoyant force on a submerged object is equal to the weight of the fluid that is displaced by the object [64].

Density, porosity and water absorption (BD , AP and A) can be measured using the Archimedes buoyancy technique with dry weights (W_d), soaked weights (W_s) and immersed weights (W_i) in water (mercury, xylene or denatured alcohol if the refractory is water sensitive) (Figure (2-17)) [64].

Various standard test methods are based on this procedure (ISO 5017, ASTM C20, BS 1902- 308, and SANS 5905 using mercury).



Figure (2-17): Laboratory Archimedes setup [65].

2.6.4.1 Bulk density

Bulk (or Apparent) density (BD) is mass divided by bulk volume where bulk volume is the volume of solid and of open and closed porosity.

Bulk Density can be calculated as follows (ASTM C20 – 00) [65]:

$$BD = \frac{W_d}{W_d - W_i} \quad (2-5)$$

2.6.4.2. Apparent porosity

Apparent porosity (% AP) is open pore volume as a percentage of Bulk Volume.

The apparent porosity calculates from the Dry, Soaked and Suspended weights as follows (ASTM C20 – 00) [65]:

$$\% A.P = \frac{W_s - W_d}{W_s - W_i} * 100 \quad (2-6)$$

2.6.4.3 Water absorption

This property is particularly important in ceramic, as well as being important for durability. It can be used to predict ceramic durability to resist corrosion.

The water absorption is determined by dividing the specimens change in weight by their dry weight (ASTM C20 – 00) [65].

$$\% A = \frac{W_s - W_d}{W_d} * 100 \quad (2-7)$$

2.6.5 Thermal conductivity

The thermal conductivity measurements (K in W/m.k units) are carried out by using Lee's method [66]. Lee's disk method is used to measure the thermal conductivity of the specimen whose thickness (ds) is small relative to its diameter (D). Since the crosssectional area of the disk, ($A = 4\pi D^2$) is large compared with the exposed area of the edge ($s a = \pi Dd$), the aspect ratio removes the need to account for heat loss from the edge of the die. Using a thin specimen also means that the system will reach thermal equilibrium more quickly [62].

The heat transfer (Q) across the thickness of the specimen (Ignoring heat losses from the edge of the disk) is given by [62]:

$$Q = KA \frac{(Tu - Tm)}{ds} \quad (2-8)$$

Where, (Tu – Tm) is the temperature difference across the specimen (figure (2-18 a)). The thin specimen is placed between two brass disks in conjunction with a heat source in figure (2-18b) [62].

Because of the low thermal conductivity of the ceramic compared with that of brass, the temperature of brass disk (1) can be assumed to be very close to that of one surface of the ceramic specimen. Similarly, the temperature of brass disk (2) can be assumed to approach that of the other surface of the specimen. In this way the temperature difference across the specimen, ($T_U - T_M$), can be measured [62].

At equilibrium, heat entering the brass disk (2) equals the rate of heat loss due to cooling. The heat loss can be determined by measuring the cooling rate at the equilibrium temperature (Tm) (with the brass disk (2) covered with a pad of

Theoretical concept

insulation as in Fig. (2-18c)). If the disk cools at a rate of (dt/dT) then the rate of heat loss is given by [62]:

$$\frac{dQ}{dt} = mCp \frac{dT}{dt} \quad (2-9)$$

Where (m) is the mass of the brass disk and (Cp) is the specific heat capacity of brass [67].

Assuming, that the heat flow in the specimen is the mean of the quantities of heat flowing into it and out of it, therefore [62]:

$$K \frac{(Tu - Tm)}{ds} = h \left(Tm + \frac{2}{r} \left(dm + \frac{1}{4} ds \right) Tm + \frac{1}{2r} ds Tu \right) \quad (2-10)$$

where, (T_U) : temperature of disk (U), (T_M) : temperature of disk (M), (r) : radius of the disk, (d_M) : thickness of the disk (M), (ds) : thickness of the disk (S) (specimen) and (h) : heat loss per $(\text{second}/\text{cm}^2)$ for one degree in excess of temperature of disk over that of the enclosure, determined from following equation [62]:

$$h = \frac{H_t}{\pi r \left[(T_c - T_M)r + 2 \left[d_M T_M + \frac{1}{2} d_s (T_M + T_U) + d_U T_U + d_c T_c \right] \right]} \quad (2-11)$$

Where d_c and T_c : thickness and temperature of disk(c) respectively.

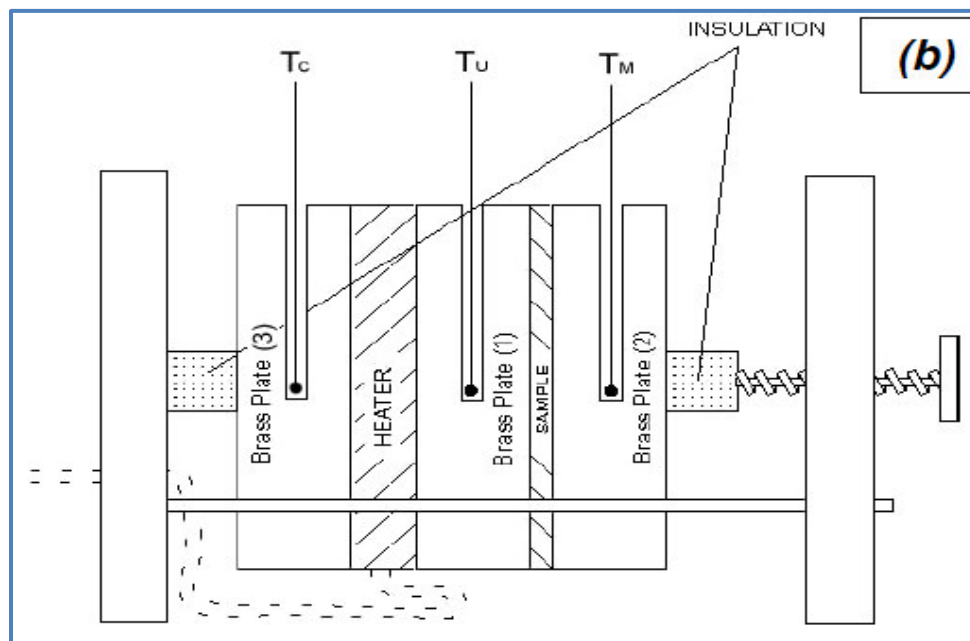
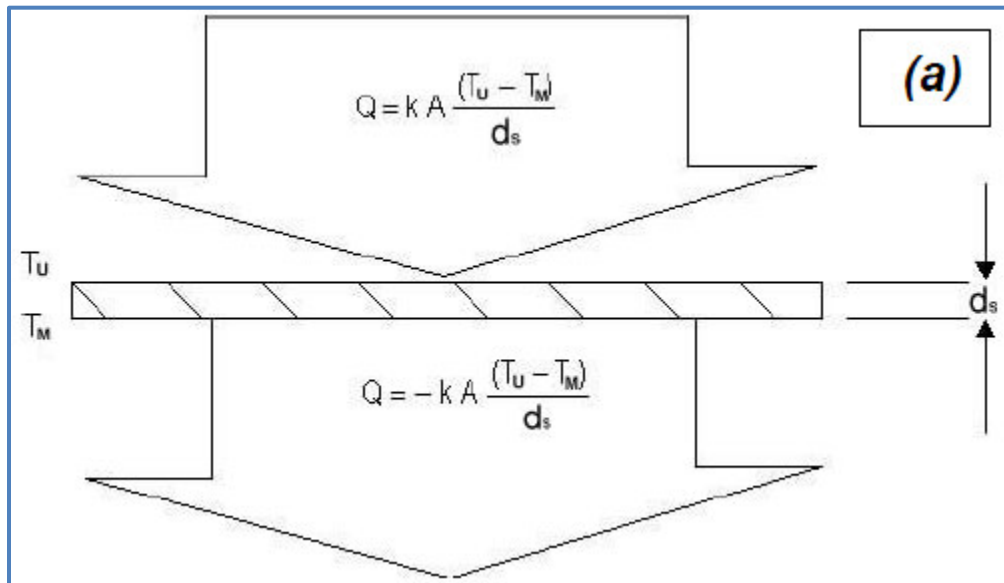
Lee's disk system is isolated from external effects by using glass desiccator's. When the system is linked to an electric power supply; then the power in watt is [62]:

$$H_t = I V \quad (2-12)$$

Theoretical concept

Where V : is The Voltage (6 V) and I is the current equal to 0.25 A.

The dimensions of device is ($r = 20.7$ mm) and ($d_M = d_U = d_C = 13$ mm).



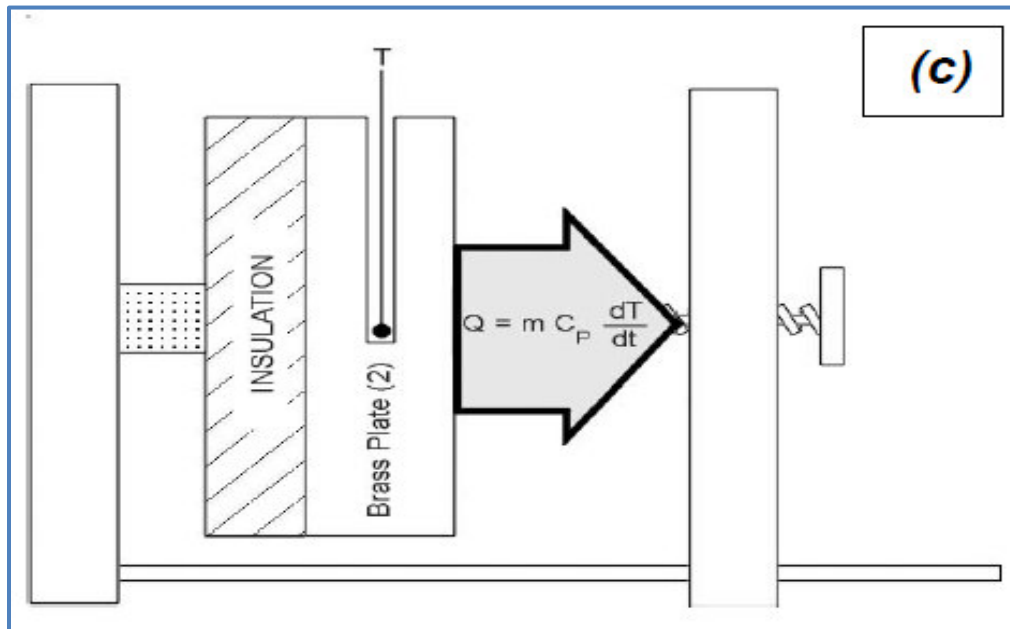


Figure (2-18): Lee's Disk, for measurement of the thermal conductivity [62]:

(a) Heat transfer, Q , across the thickness(x) of the specimen. (b) Diagram of Lee's Disk apparatus. (c) Measuring heat loss.

2.7 mechanical Properties

2.7.1 Hardness

Hardness is a key parameter in the choice of ceramic for abrasives, tool bits, bearings, wear resistant applications, and resistance to particulate erosion and ballistic impact [68].

The hardness of a material is related to the material characteristics which give stiffness and strength. Hardness is an important characteristic of a material, as it contributes to resistance to erosion/wear processes. At high temperature, however, engineering alloys become "Softer" and so ceramics are often used to give wear resistance [69]. The hardness of a material may be specified in terms of some standard test [48].

Shore hardness is a general method for measuring the bulk hardness of a material. Although hardness testing does not give a direct measurement of any performance properties, hardness correlates with strength, wear resistance, and other properties. Hardness testing is widely used for material evaluation due to its simplicity and low cost relative to direct measurement of many properties (ASTM D2240 – 05) [70].

The Shore A scale is used for 'softer' rubber samples while the Shore D scale is used for 'harder' ones, and it's used here because of the high porosity in the slip casting ceramics. Shore hardness is tested with an instrument called Durometer. Durometer utilizes an indenter loaded by a calibrated spring. The measured hardness is determined by the penetration depth of the indenter under the load [70].

Theoretical concept

Two different indenter shapes and two different spring loads are used for two Shore scales (A and D). The loading forces of Shore A: (822 g), Shore D: (4536 g) as shown in figure (2.19) [70].

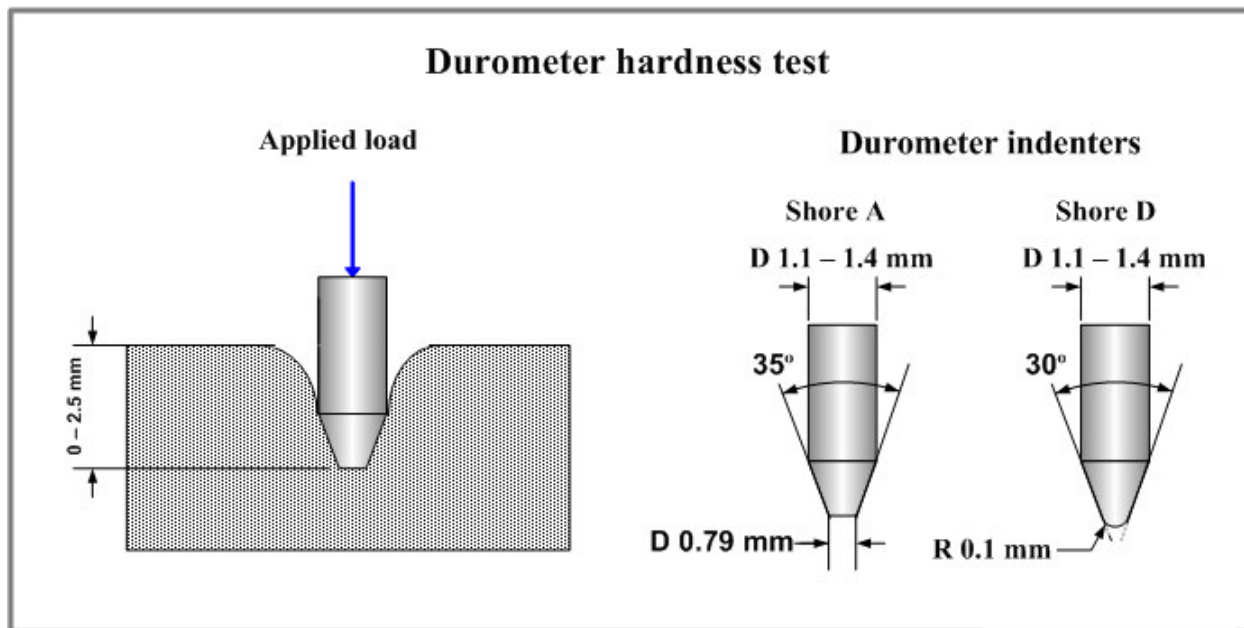


Figure (2-19): Durometer hardness testers (A and D) [70].

2.7.2 Strength and Compressive Strength

For compressive stresses, there is no stress amplification associated with any existent flaws. For this reason, brittle ceramics display much high strengths in compression than in tension (on the order of a factor of 10), and they are generally utilized when load conditions are compressive [71].

Tensile testing of ceramics is not only time consuming but it is also expensive to fabricate the specimens. Therefore, the easier to- handle transverse bending or flexure test is commonly used for determining the strength of ceramics [72].

Theoretical concept

The stress distribution should be independent of length, provided a uniform compression stress applied [62].

Compressive Strength can be calculated from this equation [62]:

$$\text{Compressive Strength} = \frac{F}{A} \quad (2-13)$$

Where: (F) is the applied load and (A) is the area of the specimen.

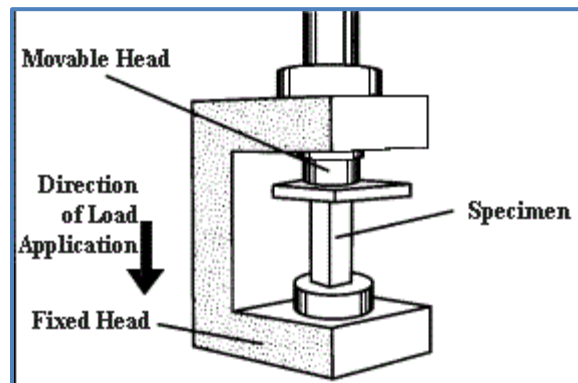


Figure (2-20): Compression strength test [82].

2.7.3 Bending Strength

The stress at fracture using flexure test is known as the flexural strength, modulus of rupture, fracture strength, or bend strength, an important mechanical parameter for brittle ceramics [71].

In ceramic materials, the conventional tensile test cannot be used because of the problems of preparing suitable test pieces and effectively holding them in the test machines. The materials are in the forms of beams and bent by three-point bending figure (2-21).

Theoretical concept

For a rectangular cross-section specimen [62]:

$$\text{Flexural strength} = \frac{3FD}{2bd^2} \quad (2-14)$$

Where:

b: is the breadth of the section and (d) its depth

Flexural strength values for materials tend to be about twice their tensile strength values. Because cracks and flaws tend to close up in compression, brittle materials tend to be much stronger in compression than tension [43].

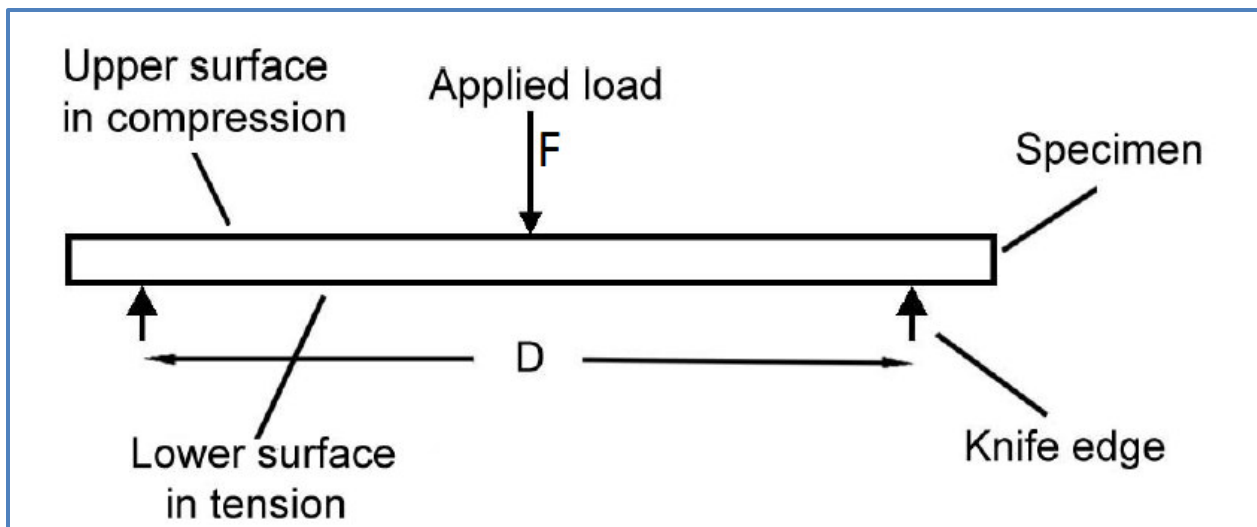


Figure (2-21): Three Point loading for modulus of rupture test [62].

During bending, a specimen is subjected to both compressive and tensile stresses [71]. Although bending strength is independent of the orientation of the test specimen, higher values are obtained in the pressing direction [72].

2.8 Factors Affecting Mechanical Properties

The strength of ceramic bodies depends on a number of factors including the mechanical testing method, strain rate, temperature, impurity level and size distribution of microstructural defects [62].

2.8.1 Grain size and distribution:

Flexural strength of a sintered body is strongly dependent on particles and grain size distribution [72]. Agglomerates and large grains cause degradation in strength. During sintering, the rapid densification regions containing agglomerates can induce stresses within the surrounding compact facilitating the formation of the voids and cracks. Isotropic large grains often produce mismatch in thermal expansion and elastic modulus and act as flaws in a homogenous matrix.

Typically, the strength of ceramics shows an inverse correlation to the average grain size G . The strength can be expressed as [73]:

$$\sigma = (\sigma_o + k_1 G^{-0.5}) e^{-nP} \quad (2-15)$$

Where (σ) is true strength, (σ_o) is strength with no micropores, (k_1) and (n) are constants, (G) is grain size, and (P) is porosity.

A schematic of the dependence is shown in figure (2-22) where the fracture strength is plotted versus ($G^{-0.5}$) [74].

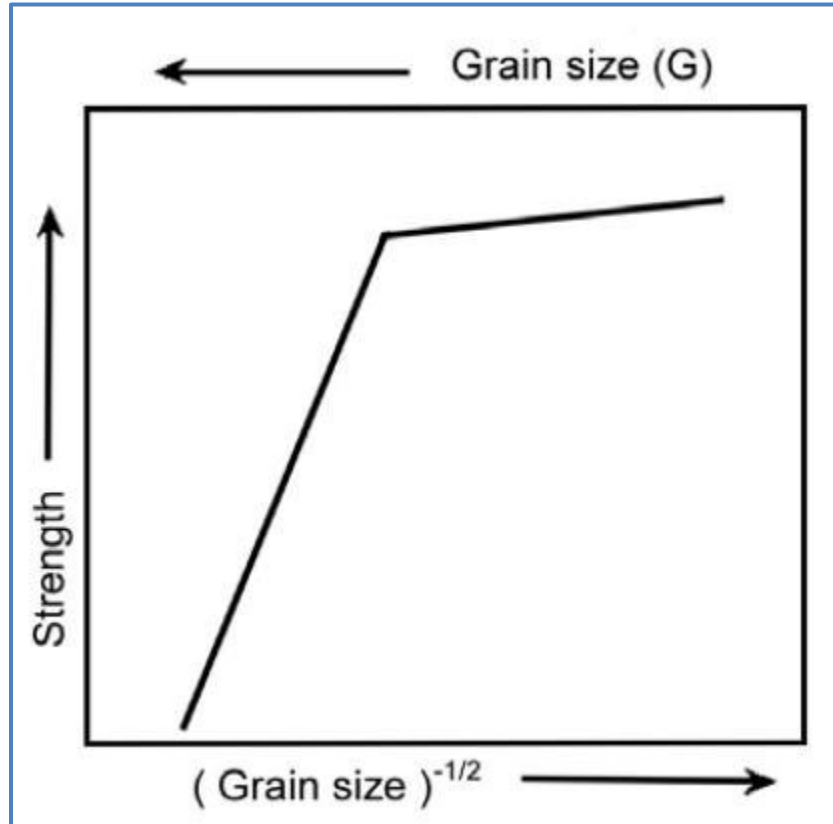


Figure (2-22): Schematic relationship between grain size and strength for a number of ceramics [62].

2.8.2 Porosity Effects

The major effect of the structure in most ceramics is the result of porosity. Pores are usually quite deleterious to the strength of ceramics not only because they reduce the crosssectional area over which the load is applied, but more importantly because they act as stress concentrators (for an isolated spherical pore, the stress is increased by factor of 2). Experimentally, it is found that the strength of porous ceramics is decreased in a way that is nearly exponential with porosity. Various specific analytical relationships have been suggested for the effect of porosity. An empirical suggestion by Ryskewitsch is [75]:

$$\sigma_p = \sigma_o \exp(-B P) \quad (2-16)$$

Where:

(P), (σ_p) and (σ_o) are respectively, the volume fraction of the pores and the strength of the specimen with and without porosity. (B) is a constant and depends on the distribution and morphology of the pores, (where B is in the range 4 to 7). Data for several wall-characterized materials illustrating the strong effect of porosity are included in Figure (2-23) [75].

For strength, the pore size is sometimes a more important parameter than the amount of porosity [76]. For many materials the flaw size can be related to the grain size or pore size. It is the largest flaw that affects strength and thus the relative sizes of pores and grains dictate which of these are important. In fully dense materials there are no large pores and the flaw size is usually related to the grain size [77].

The degree of the influence of pore volume on flexural strength is demonstrated in Figure (2-24) [71].

Hardness decreases when porosity increases [54], in relation to the fracture of the walls between contiguous pores. No firm theoretical analysis exists to explain $H=f(P)$ but empirical exponential law Soroka and Sereda generally has proved valid [62]:

$$\frac{H}{H_o} \approx \exp(-A P) \quad (2-17)$$

Theoretical concept

Where (H_0), (H) hardness of dense material and porous and ($A \approx 10$), it must also be pointed out that (H) depends on the load applied to the indenter. This dependence becomes more pronounced when (P) increases. To reduce the scattering of data the size of the indentation must be much larger than the size of the pores [78].

Few bibliographical data on the influence of (P) on hardness are available [76].

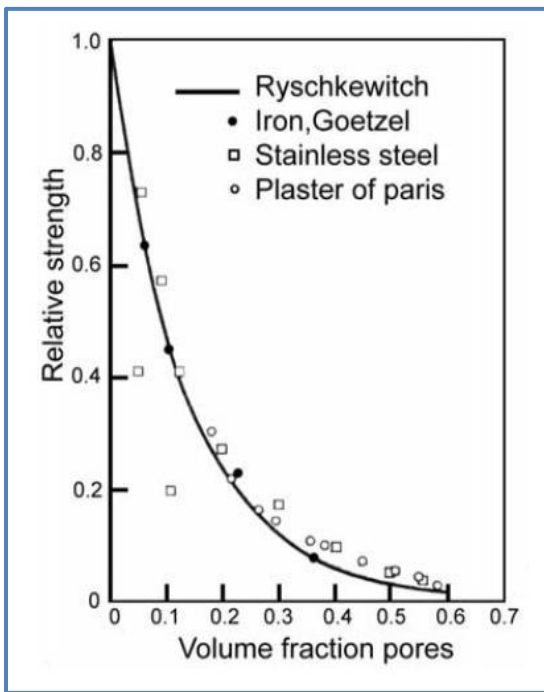


Figure 2-23: Effect of porosity on the fracture strength of ceramics [75].

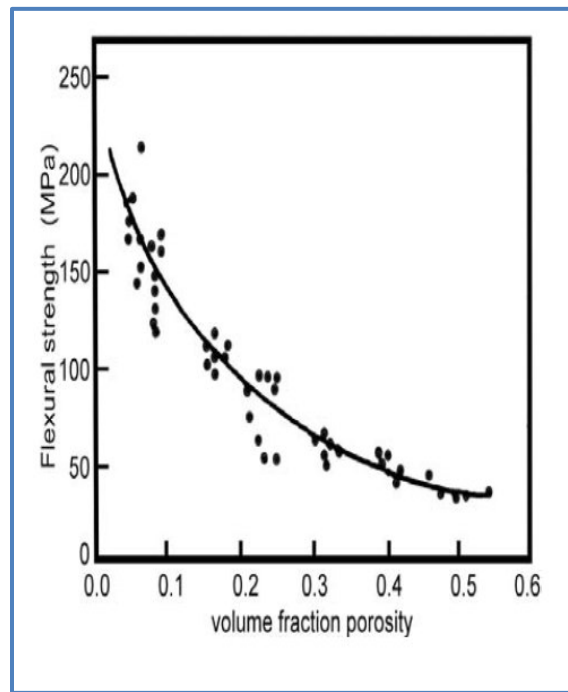
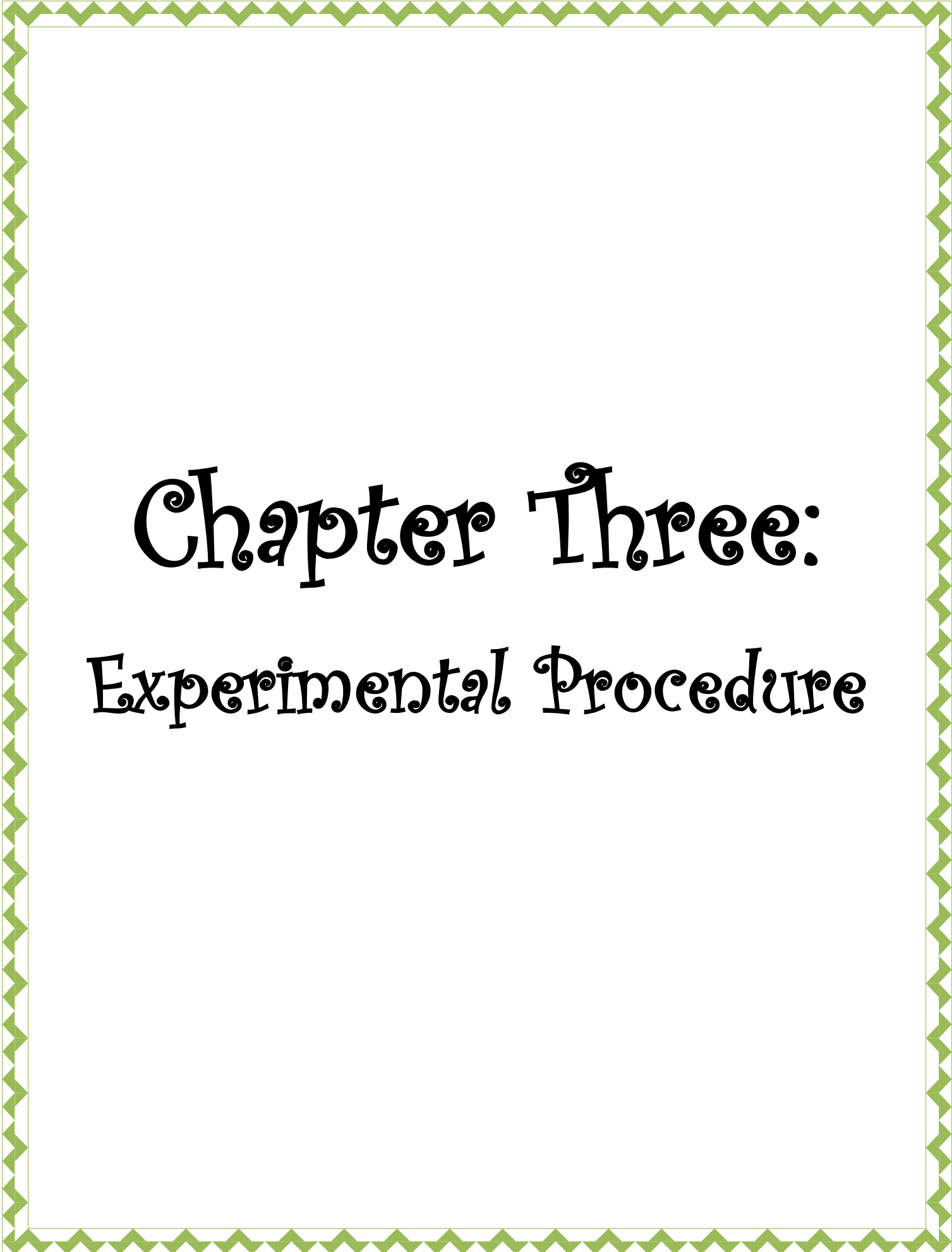


Figure 2-24: The influence of porosity on the flexural strength for ceramics (Al₂O₃) [71].



Chapter Three:

Experimental Procedure

3. Chapter Three: Experimental Procedure

3.1 Introduction

Powder processing is a collective term for technologies which produce objects starting from fine powders without melting and consolidate them by sintering. The temperature of sintering is generally no more than about two-thirds of the melting point [62].

Powder processing technologies are used generally in the manufacturing of ceramics, because of their high melting point, producing hard and brittle ceramic components [79].

For the preparation of samples through slip casting: fine powders were used such as micro alumina, nano alumina and kaolinite; Dispersant used is Sodium carboxymethylcellulose (Na-CMC); Solvent used is distilled water and moulds prepared from Plaster of Paris were used for the casting. The flow chart of the overall experiment has been shown in two different flow chart refer figure (3-1) and figure (3-2)

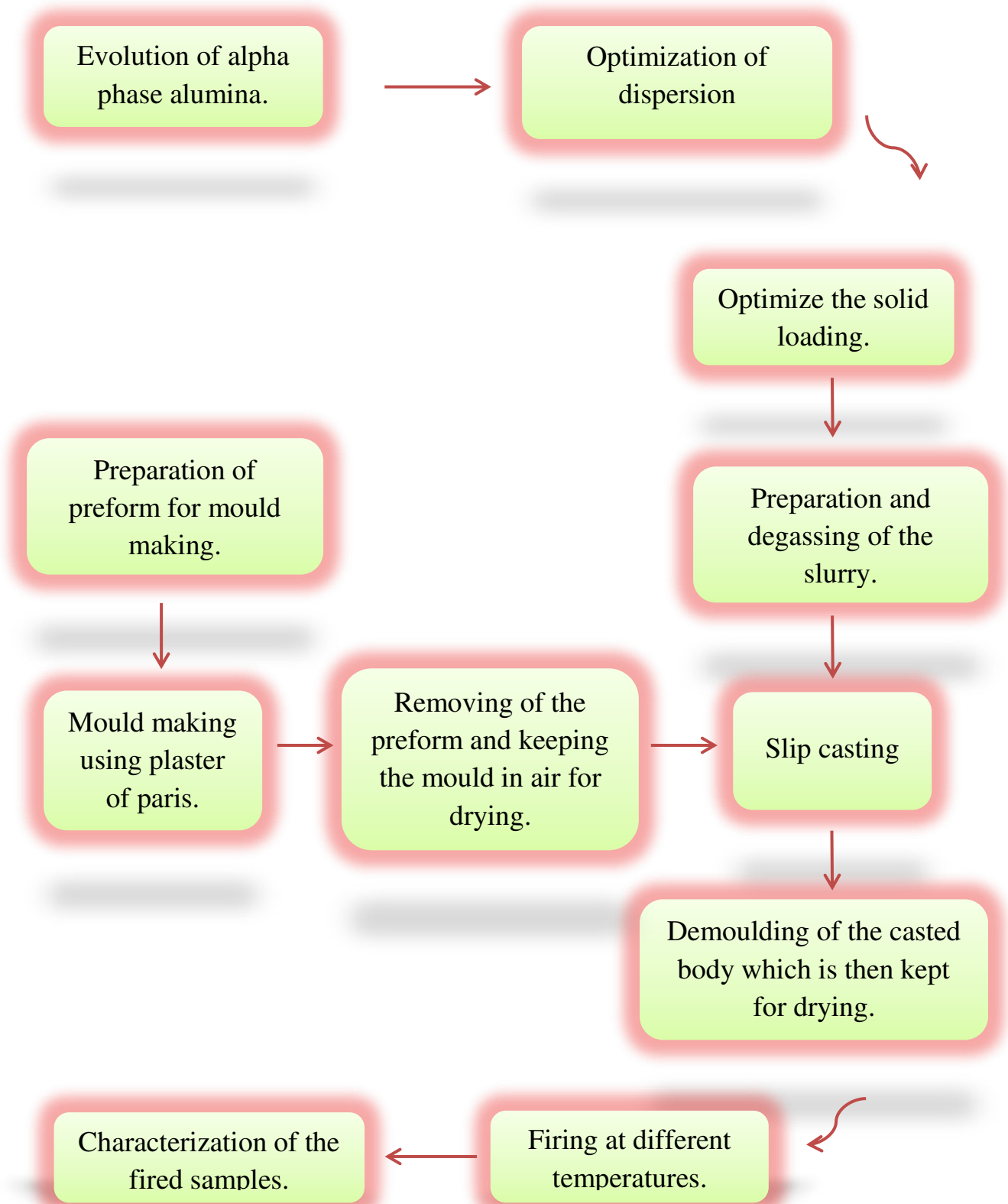


Figure (3-1): Flow chart of the overall experimentation.

Experimental Procedure

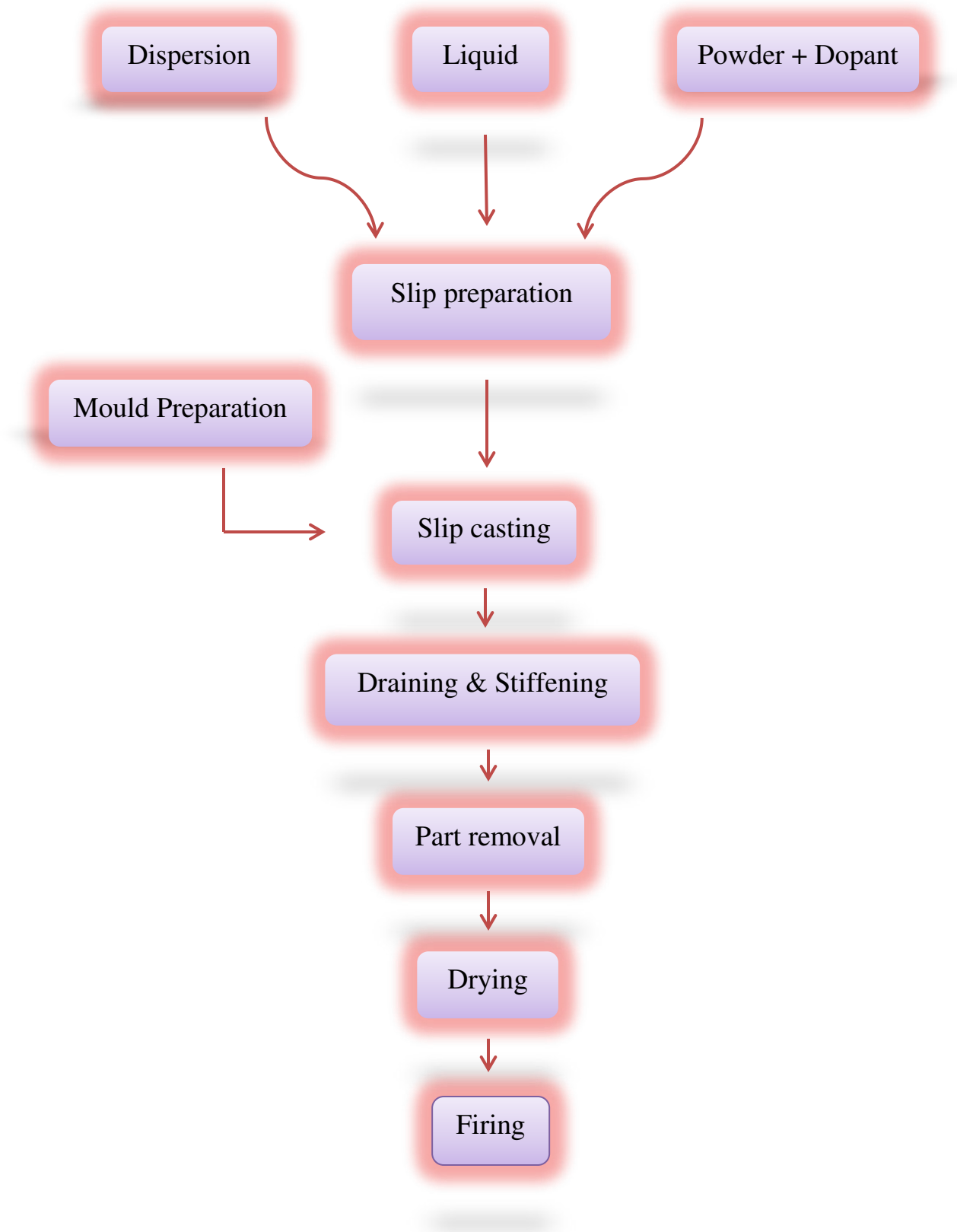


Figure (3-2): Flow chart of the slip casting process in general.

3.2 Materials

3.2.1 Micro Alumina

The raw materials used for this work were a commercial micro Aluminum dioxide powder (Al_2O_3) German origin, prepared by Merck Company. The figure (3-3) represents x-ray analysis (XRD-6000, SHIMADZU) of the micro alumina powder and the specifications are shown in table (3-1) [16].

Table (3-1): Specifications of micro alumina *.

Density	Purity%	Mean particle size	Type	Color
3.22 (g/cm^3)	99.99	10 (μm)	γ	White

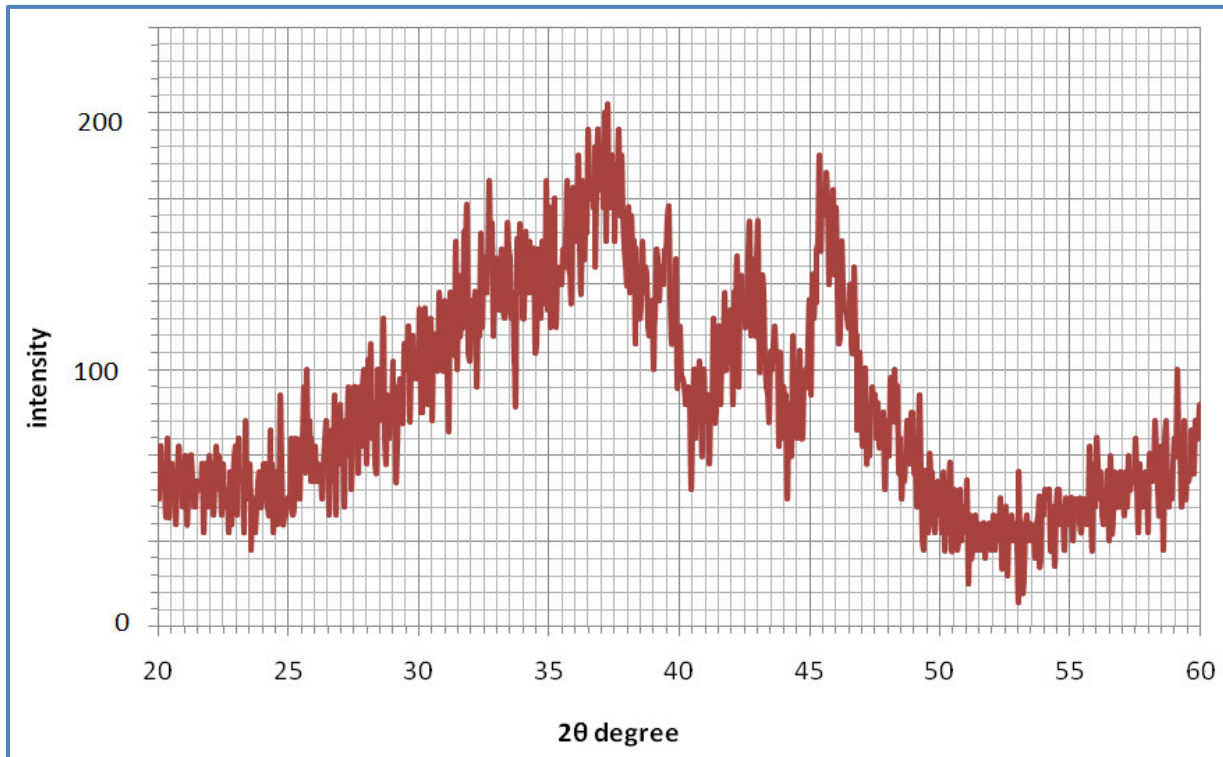


Figure (3-3): XRD pattern for the micro gamma alumina powder.

* By the Merck Company.

3.2.2 Nano Alumina Powder

Nano Aluminum dioxide powder (Al_2O_3) an English origin, prepared by Nanoshell Company. The figure (3-4) represents x-ray analysis (XRD-6000, SHIMADZU) of the nano alumina powder and the specifications are shown in table (3-2) [16].

Table (3-2): Specifications of nano alumina by the manufacturer.

Product	Al_2O_3 (white powder, alpha type, crystalline structure)
Particle size	30 nm
Mfg. method	SOL-GEL
Purity	99.99
True density	3.97 g/cm³
Morphology	Spherical
Specific surface area	~25 m²/g

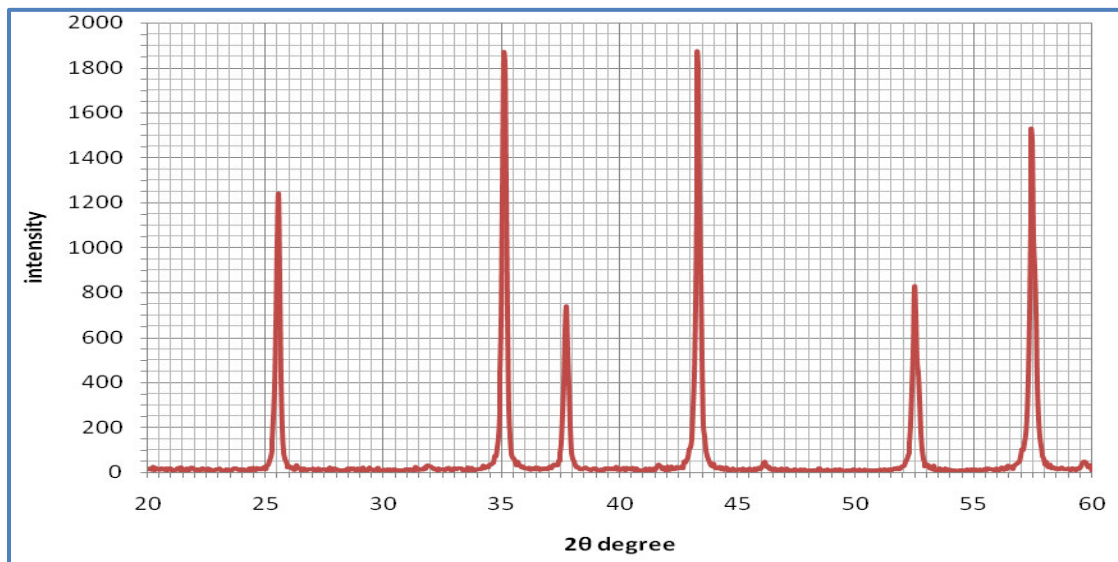


Figure (3-4): XRD pattern for the nano alpha alumina powder.

*** By the Merck Company.**

3.2.3 Kaolinite

Kaolinite micro powder ($\text{Al}_2\text{Si}_2\text{O}_5(\text{OH})_4$), prepared by (LTD Chemicals Dearborn) Company. The figure (3-5) represents x-ray analysis (XRD-6000, SHIMADZU) of the micro Kaolinite powder and the specifications are shown in table (3-3) [52].

Table (3-3): Specifications of micro Kaolinite *.

Product	Kaolinite powder ($\text{Al}_2\text{Si}_2\text{O}_5(\text{OH})_4$)
Color	Grayish white
Particle size	20 μm
Calculated density	2.57 g/cm^3

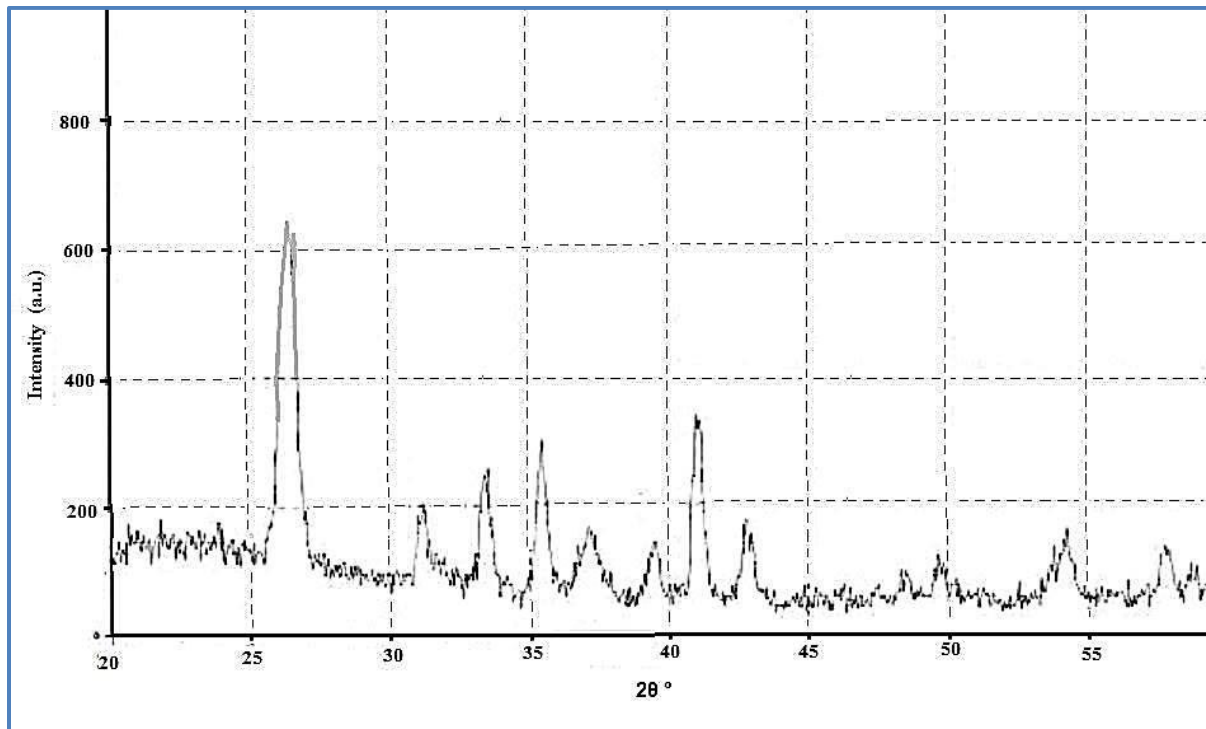


Figure (3-5): XRD pattern for the micro kaolinite powder fired at 1300 °C.

* By the LTD Chemicals Dearborn Company.

3.3 Obtainment of Alpha Phase Alumina

All alumina phases involved in transformation sequences, which all have in common that they end in the (α phase) at high temperature. The transformations to the (α phase) are irreversible and typically take place at above (1000 °C) [68, 69].

Figure (3-6) represents x-ray analysis (XRD-6000, SHIMADZU) of the (α) phase alumina which transformed from (γ) alumina at (1100 °C) [16].

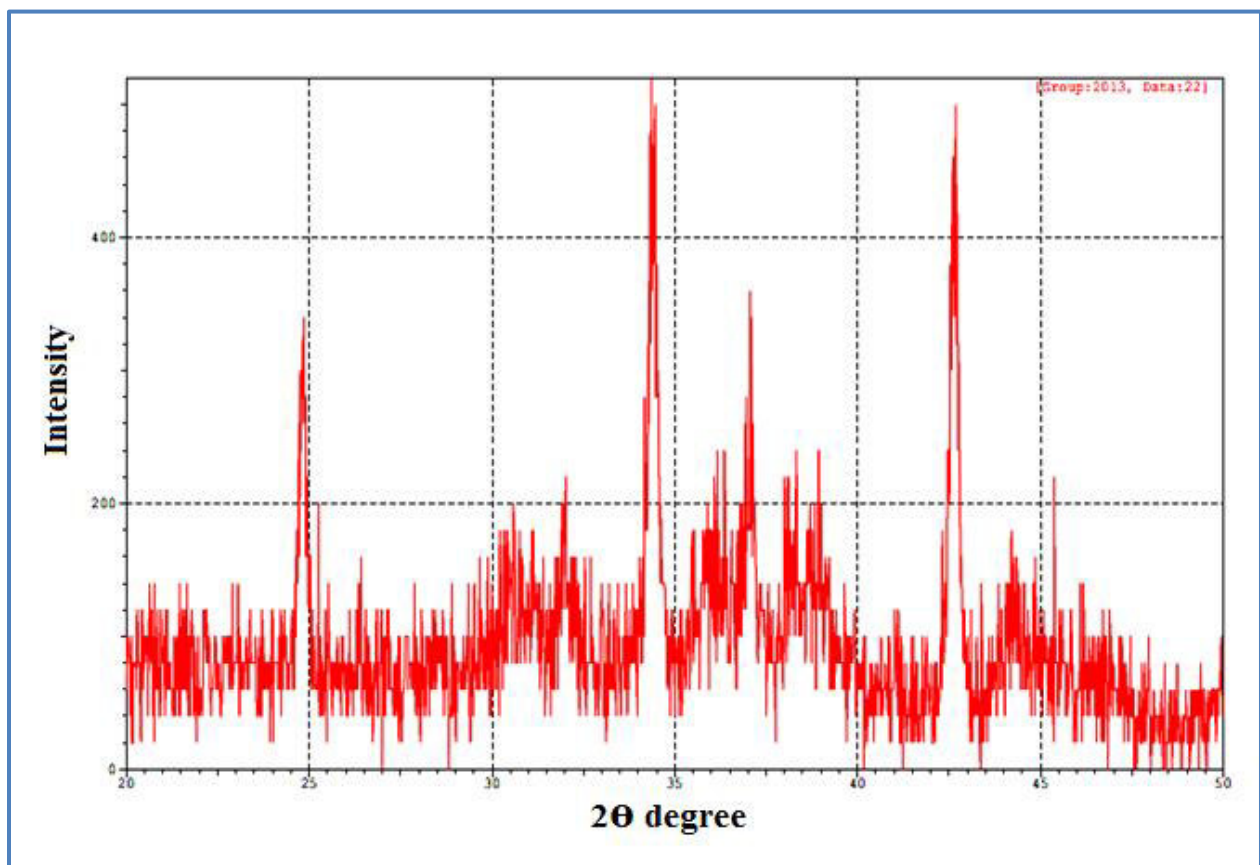


Figure (3-6): X-ray analysis of the (α phase) micro alumina.

3.4 Green Body Fabrication by slip casting

3.4.1 Mould Making

(ASTM C59 / C59M - 00) was used as standard to make the Gypsum mould [88].

The mixture is prepared using water and Plaster of Paris in the ratio (3:4) such that the negative imprint can be casted over the mould.

A glass plate is taken over in which the Vaseline oil is applied. This Vaseline oil acts as a lubricant and does not allow the mould to stick on the glass. Then a hollow cubic made from plywood was used as a container which puts over the glass plate, piece of rubber takes the form of the sample (preforms) put over the glass plate at the center of the hollow cubic and this helps in uniform drying during the casting process Vaseline oil is also applied over the preforms.

Artificial clay was used to cover the gap between the cubic and the glass plate to avoid leakage of slurry from the holes as seen in figure (3-7). Then the prepared mixture was slowly poured into the hollow cubical box to a certain height predefined. The body is kept for air drying for about (2 h). After (2 h) the body is removed from the wood box and kept for air drying for (24 h). Then the mould was kept in a drier at (60 to 70) °C for complete removal of water deposited at the pores.

Thereafter the preforms were carefully removed using a blade and forceps as seen in figure (3-7). The mould inner surface was polished using a sand paper after drying.



Figure (3-7): Pictures of mould preparation and the mould prepared for a bar sample.

3.4.2 Optimization of the Slurry

Optimization of the slip is necessary as it controls the stability, viscosity and many other casting phenomenon such casing rates, defects generated during casting process and many more. The slurry is optimized by studying its properties so as to get a slip which is stable i.e. the suspended particles do not agglomerate or do not settle with changing time. The slip is obtained by preparing samples with different dispersants and different percentage of dispersant. We were found experimentally that (Na-CMC) is the most preferred dispersant at the value of (0.33 ml) for each gram of powder (figures (3-8) and (3-9)), when the density of (Na-CMC) solution is (1.17 g/cm³).

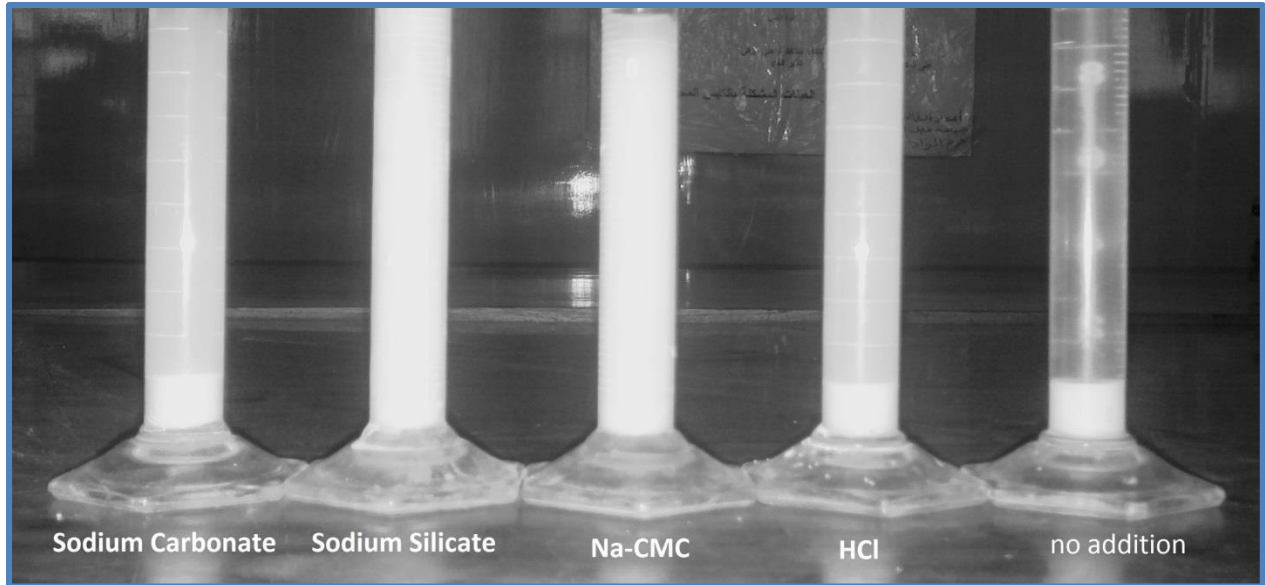


Figure (3-8): Obtainment of the preferable dispersant.

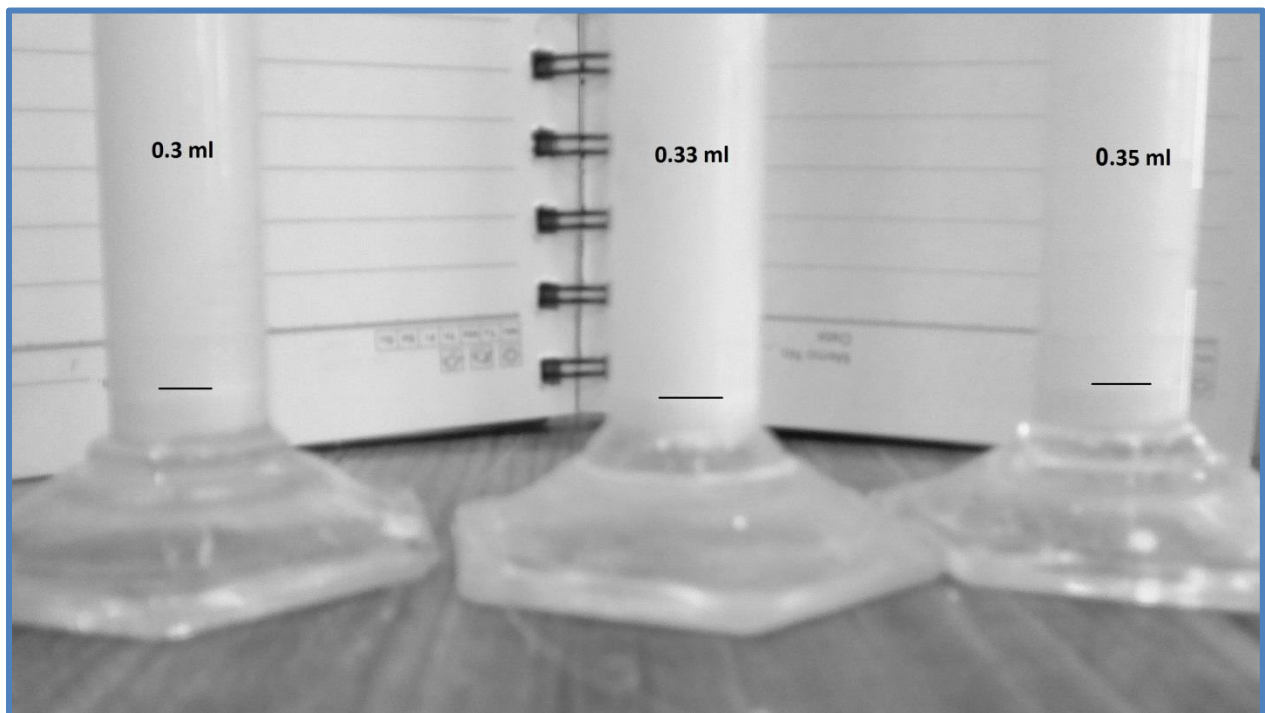


Figure (3-9): Obtainment of the preferable value of (Na-CMC) dispersant.

Experimental Procedure

Three different alumina slurries are made with different solid content (50 – 70) wt. % by the addition of powder and dispersant slowly to the distilled water and mixing them by magnetic stirrer for (45 minutes) as shown in figure (3-10).

The alumina – kaolinite slurries solid content chosen to be (60 wt. %), three different weight percentage of kaolinite (mean particle size 20 μm) to alumina (mean particle size 10 μm) ((5, 10 and 15) wt. %) was used. By addition of nano alumina powder (mean particle size 30 nm) to (alumina – kaolinite) slurries the solid content chosen to be (50 wt. %) because of the large number of particles that available in the Nano powders. Table (3-4) shows the samples names, solid content and the raw materials composition of each sample type.

TABLE (3-4): The raw materials compositions of samples.

Samples type	Solid Content wt.%	Fine Alumina (~ 10 μm) wt.%	Nano Alumina (30 nm) wt.%	Fine Kaolinite (~ 20μm) wt.%
A	50	50	-	-
B	60	60	-	-
C	70	70	-	-
B1	60	55	-	5
B2	60	50	-	10
B3	60	45	-	15
B4, B5	50	25	25	10



Figure (3-10): Pictures depicting the slip preparation.

3.4.3 Casting Process and De-moulding

Once the slip prepared, it casted in the plaster moulds, the casting method that used here is both the solid casting and the drain casting methods.

After casting the body, the casted body was kept away from an air draft or under direct sunlight to dry at room temperature. After (24 h) the mould is tapped slowly so as to remove the casted bodies (figure (3-11 A and B)).

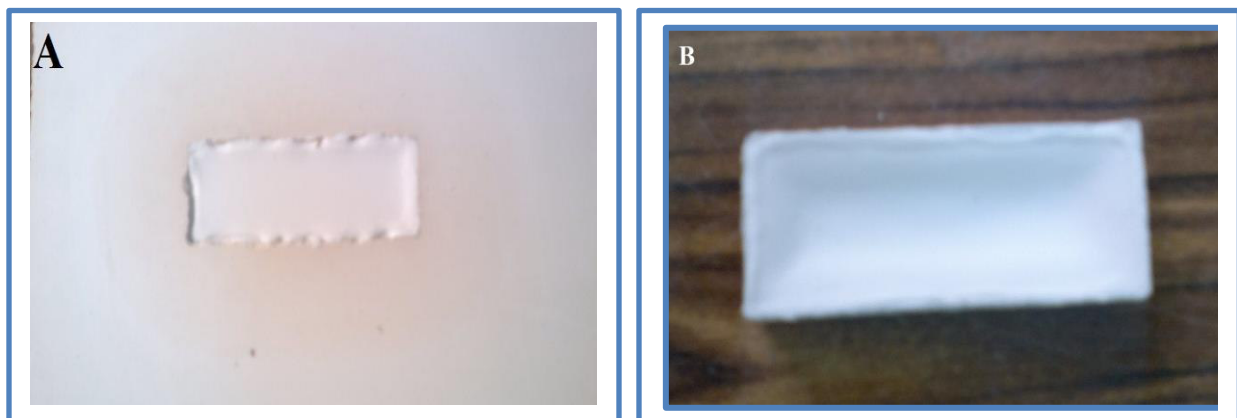


Figure (3-11): The cast A) in the mould. B) After de-moulding.

3.5 Drying and Shaping

The casted body is kept for air drying either under direct sunlight or at room temperature depending on the initial strength of the body. Then the sample is transferred to oven (made by (JRAD) company) for oven drying which is kept at about (60 °C) for (24 h) [2]. So the overall drying process takes nearly about (2-3) days. After the bodies have dried up they are brought into shape by polishing their surfaces using a sand paper. Now the sample is ready to be fired.

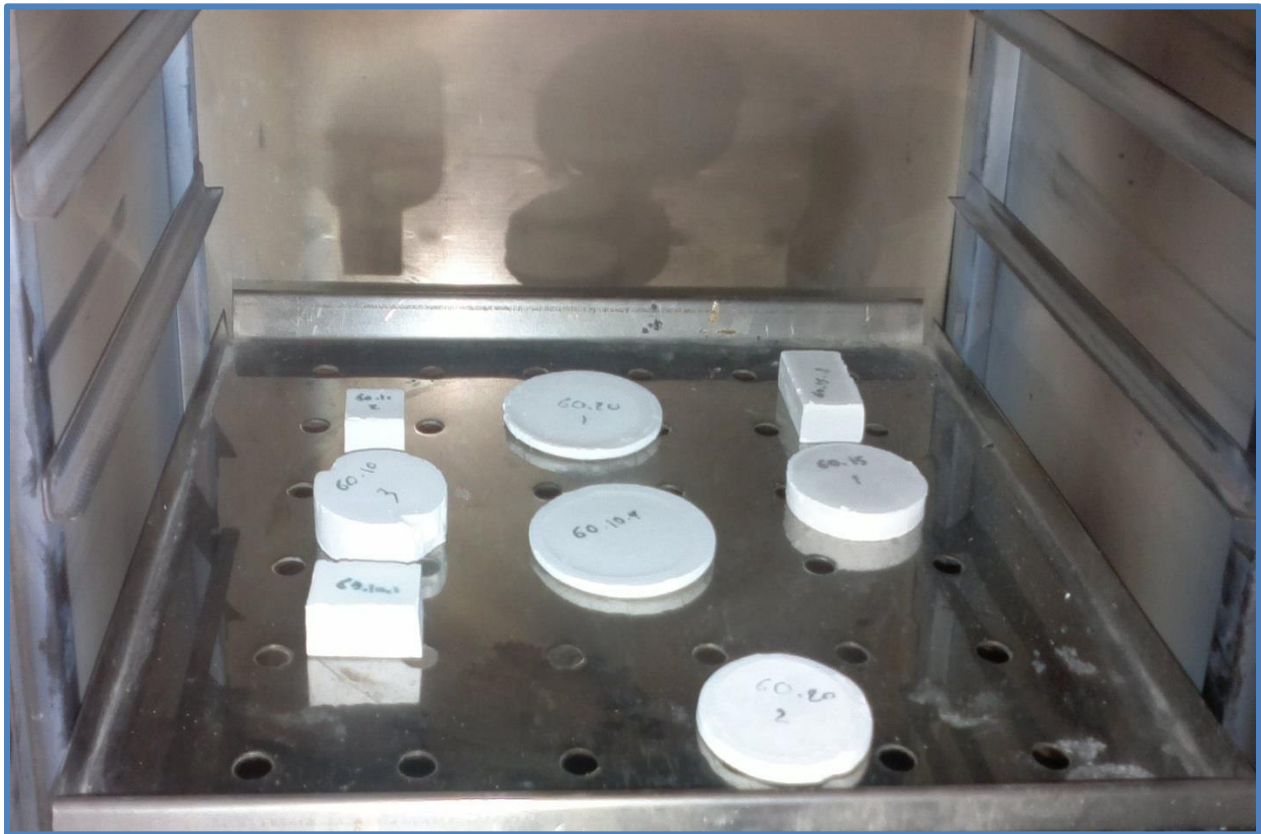


Figure (3-12): Samples oven drying.

3.6 Firing Program

The samples were fired in an English origin furnace made by (carbolite) company (figure (3-13)) in three steps:

- ❖ **The first step:** Temperature rising from the room temperature with a heating rate of (10 °C/min) and Settled at (500 °C) for (2 hours).
- ❖ **The second step:** Temperature rising with a heating rate of (10 °C/min) from (500 °C) and Settled at (1100 °C) for (2 hours).
- ❖ **The third step:** Temperature rising from (1100 °C) with heating rate of (6 °C/min) and Settled at (1600 °C) for (2 hours) for the samples (A, B, C, B1, B2 and B3), but Settled at (1450 and 1550) °C for (2 hours) for (B4 and B5) samples respectively.

Figure (3-14) shows the Firing Program of this work, the sintering temperature of each sample's type is shown in table (3-5).

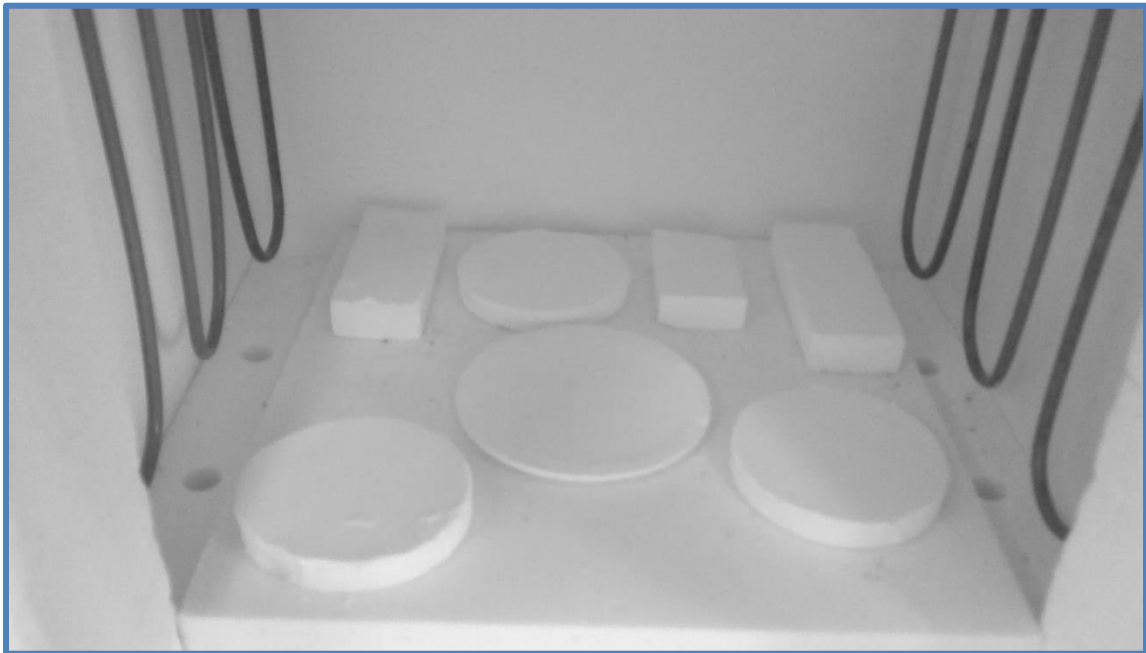


Figure (3-13): Samples firing.

Table (3-5): The sintering temperature of each sample's type.

Samples Type	Sintering temperature °C
A	1600
B	1600
C	1600
B1	1600
B2	1600
B3	1600
B4	1450
B5	1550

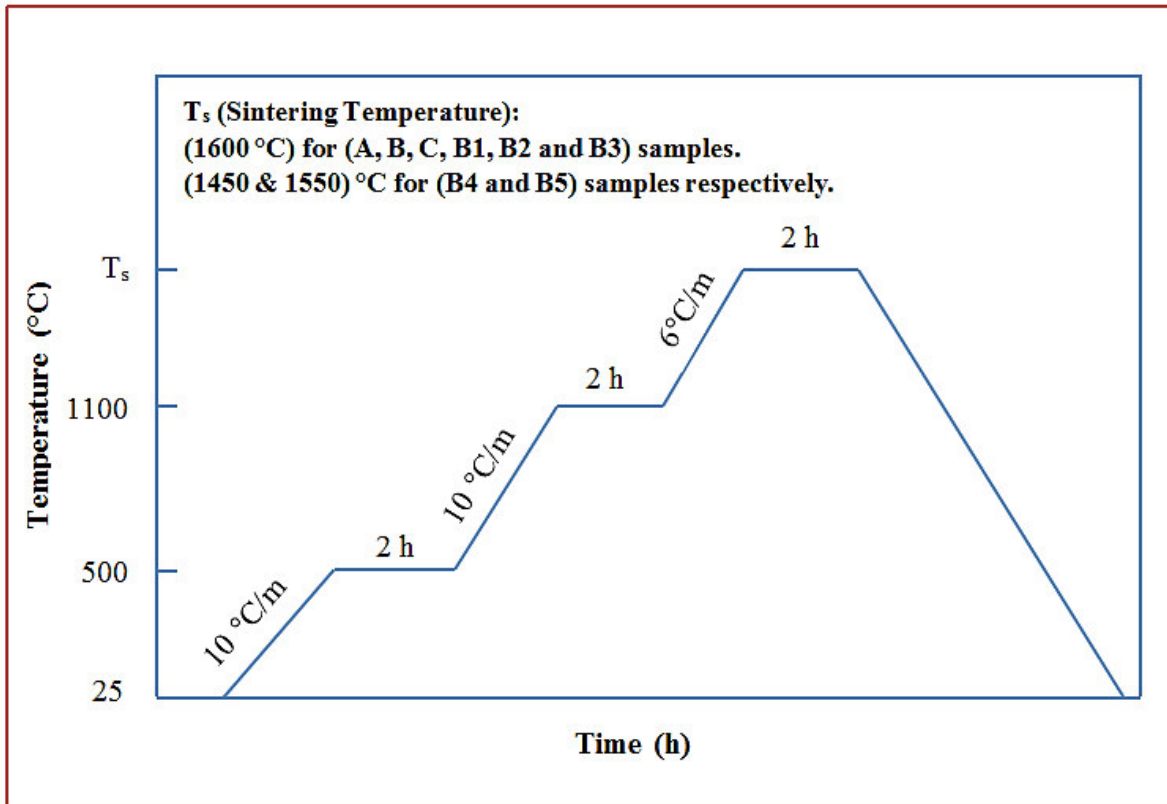


Figure (3-14): The firing program.

3.7 Procedure of Measurements

All the tests were calculated by taking the average of over (4) specimens.

3.7.1 Physical Testing

3.7.1.1 Mass Losses

(AS 2879.1—2000) was used as a standard to test this determination of loss of mass on heating of aluminum oxide at (60°C) and further loss of mass on ignition at sintering temperature . These mass losses are often referred to as moisture (MOI) and loss on ignition (LOI) respectively [61]. Equation (2-2) is used to calculate it.

3.7.1.2 Linear Shrinkage

(ASTM C326 – 09) was used as standard to test the linear shrinkage of the specimens, and the (L.S.) is calculated by equation (2-3).

3.7.1.3 Bulk Density (BD)

This test was determined according to the (ASTM C20 – 00). The Bulk Density was calculated by using equation (2-5).

3.7.1.4 Apparent Porosity (% AP)

This test was determined according to the (ASTM C20 – 00). The apparent porosity (% AP) was calculated by using equation (2-6).

3.7.1.5 Water Absorption

This test was determined according to the (ASTM C20 – 00). The water absorption was calculated by using equation (2-7).

3.7.1.6 Thermal Conductivity

Lee's disk method is used to measure the thermal conductivity of the specimens. The Lee's disk apparatus made by (Griffin and George) company was used (figure (3-15)). The thermal conductivity is calculated by the equation (2-10).



Figure (3-15): The Lee's disk apparatus.

3.7.1.7 Density of Powder

This test was determined according to the (ASTM D854-10). The pycnometer assimilates (25ml) and sensitive balance max (350g) was used as shown in figure (3-16).

The experimental procedure is:

1. Determine the weight of empty, dry pycnometer
2. Fill about (1/3) of pycnometer volume with the powder and measure the weight.
3. Empty pycnometer and fill it with distilled water only. Use the filter paper to dry the spare water again and measure the weight.
4. Fill the pycnometer with the powder and water and as well as the capillary hole of pycnometer and measure the total weight.
5. Apply equation (2-1).



Figure (3-16): Pycnometer (25ml).

3.7.2 Mechanical Testing

3.7.2.1 Compressive Strength

(ASTM standard-C773) was used as a standard to test the compressive strength of ceramic specimens [82], and this compressive strength is calculated from the equation (2-13). The force was applied perpendicular and continuously on the specimen by using hydraulic testing compression machine, maximum force (7.5 kN) as shown in figure (3-17).

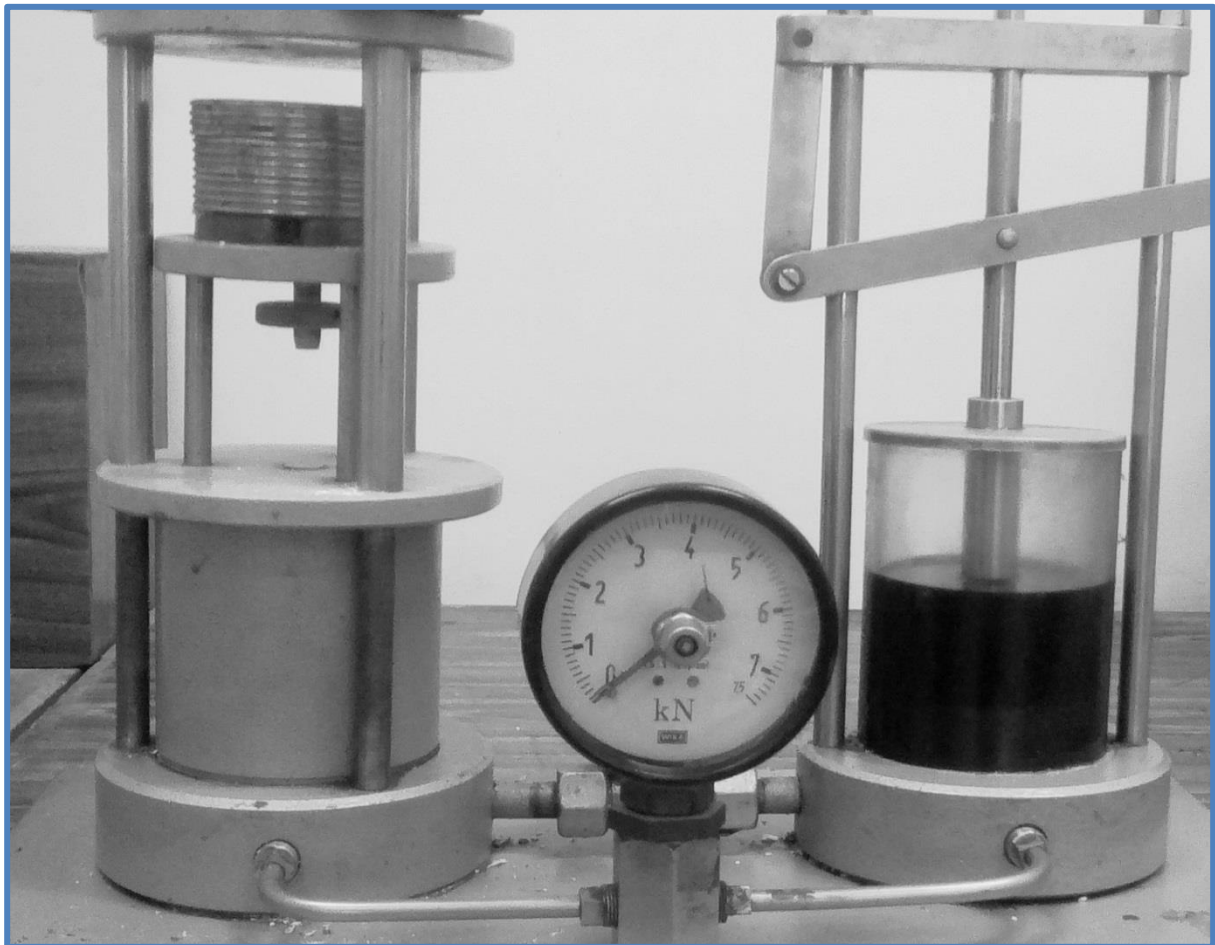


Figure (3-17): Hydraulic testing compression machine.

3.7.2.2 Flexural Strength

Flexural strength was measured in a (3-point bending) test (figure (3-18)) [46]. The dimensions of bar-shaped specimens are ($6 \times 2 \times 1 \text{ cm}^3$), and equation (2-14) was used to calculate the bending strength for the specimens (ASTM C1674 – 11) [83].



Figure (3-18): A (3-Point) bending tester.

3.7.2.3 Hardness

(TH210) Shore (D) hardness tester (figure (3-19)) was used to measure the hardness of the high porous specimens (ASTM D2240 – 05). The hardness was calculated by taking the average of each surface hardness value of the specimens.



Figure (3-19): Shore (D) hardness tester.



Chapter Four:

Results and Discussion

4. Chapter Four: Results and Discussion

4.1 Introduction

This chapter deals with the experimental results and discussion of the effects of four parameters (solid concentration, kaolinite addition, nano sizealumina addition and sintering temperature) on physical (linear shrinkage (L.S.), loss on ignition (L.O.I), bulk density (BD), apparent porosity, water absorption (W.A) and thermal conductivity (K)) and mechanical (hardness, compressive strength and bending strength) properties of the samples.

4.2 Effects of Solid Concentration

The figures (4-1), (4-2), (4-3) and (4-4) explain the effect of solid concentration (specimens (A, B and C)) on the linear shrinkage, bulk density, apparent porosity and water absorption respectively.

Linear shrinkage percentage varies with solid concentration for the samples, the dimensions shrinkage increase slightly when solid concentration is increased, this increasing is due to the lower compaction during forming process in case of higher solid concentration which lead to increase the distance among the particles and that causes a higher shrinkage value in the higher solid concentration samples [18, 84].

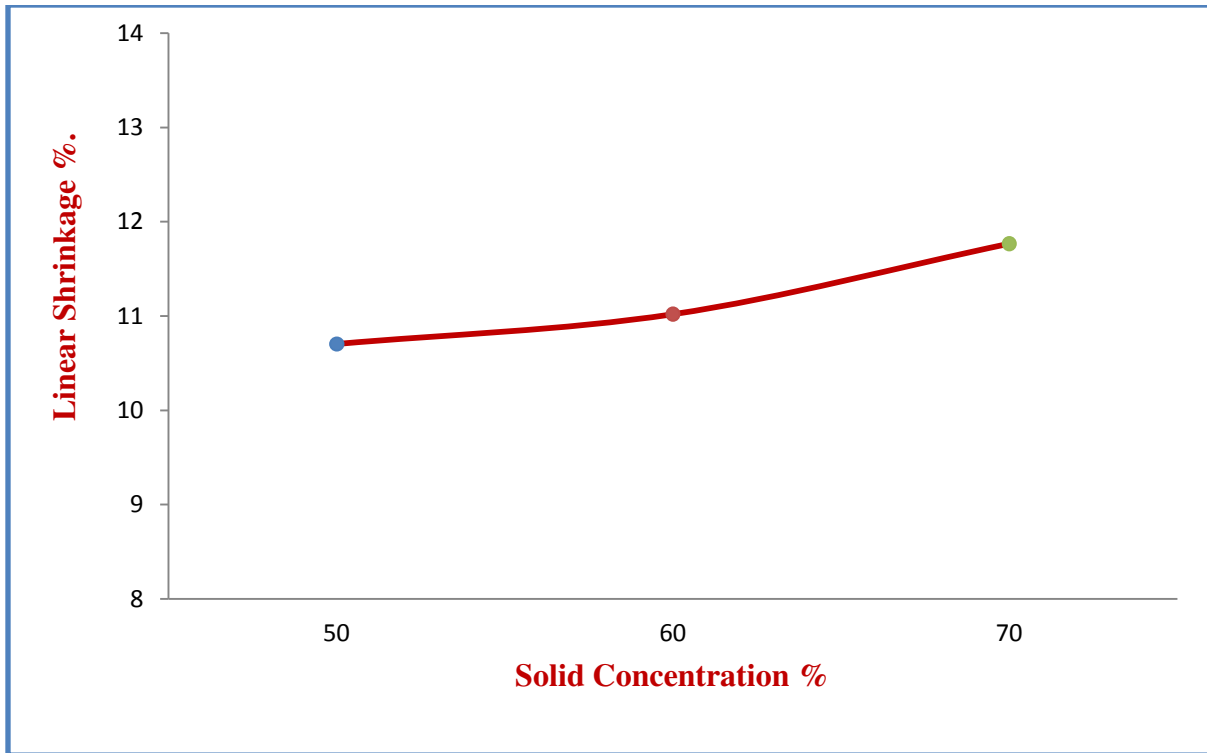


Figure (4-1): Effect of solid concentration on the linear shrinkage.

The bulk density is decreasing in a small amount by the increasing of solid concentration. In the case of apparent porosity and water absorption, they are decreasing in a small amount with increasing of the solid concentration [18]. This decreasing of bulk density, apparent porosity and water absorption is due to the decreasing of casting rate and slurry stability which leads to make sediments and conglomerates in the cast of higher solid concentration [11, 84].

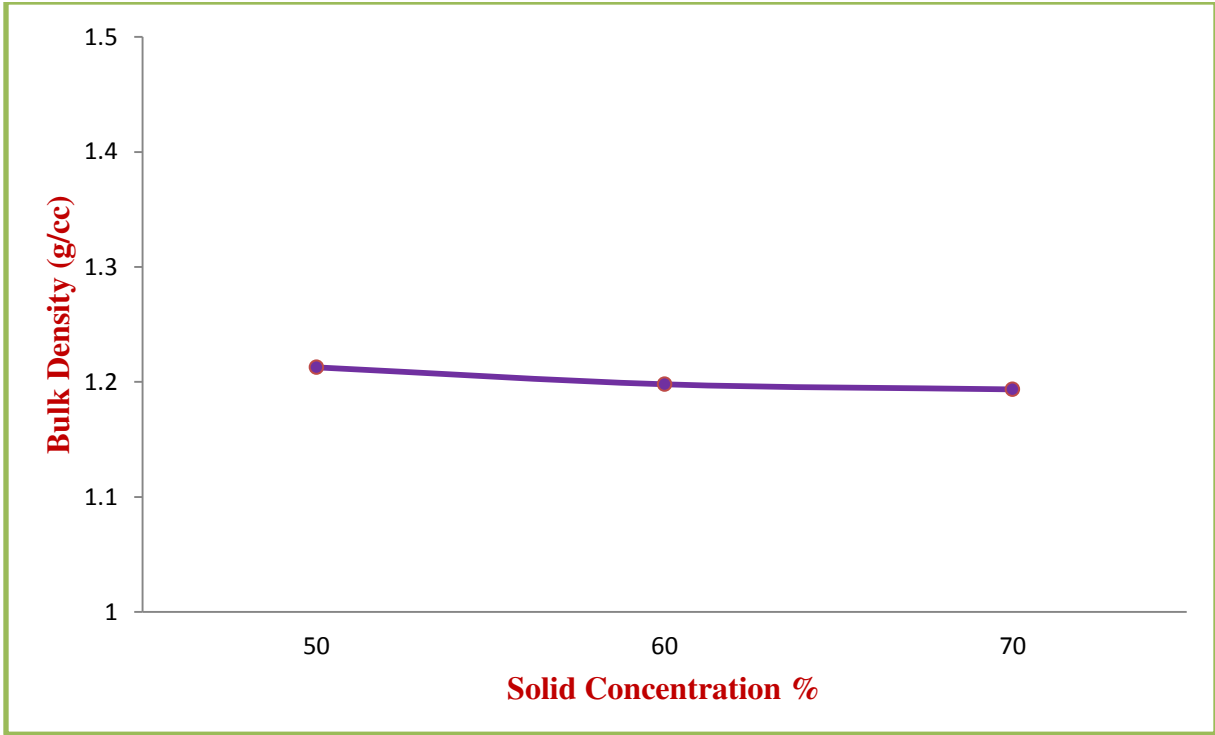


Figure (4-2): Effect of solid concentration on the bulk density.

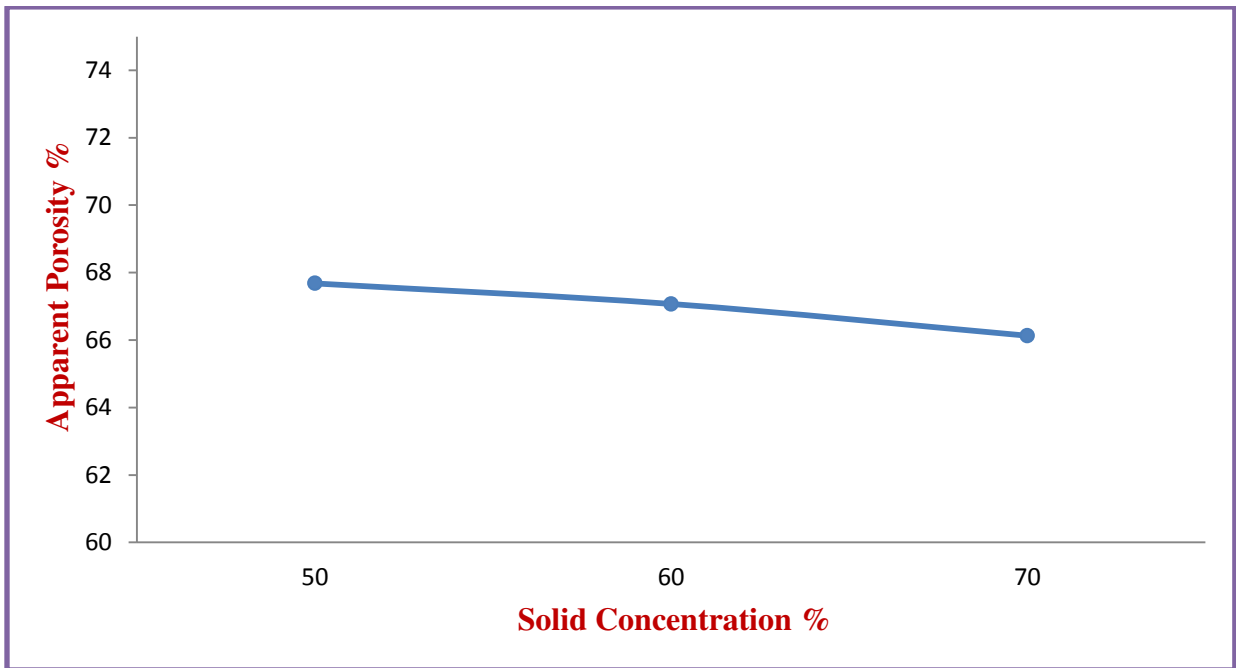


Figure (4-3): Effect of solid concentration on the apparent porosity.

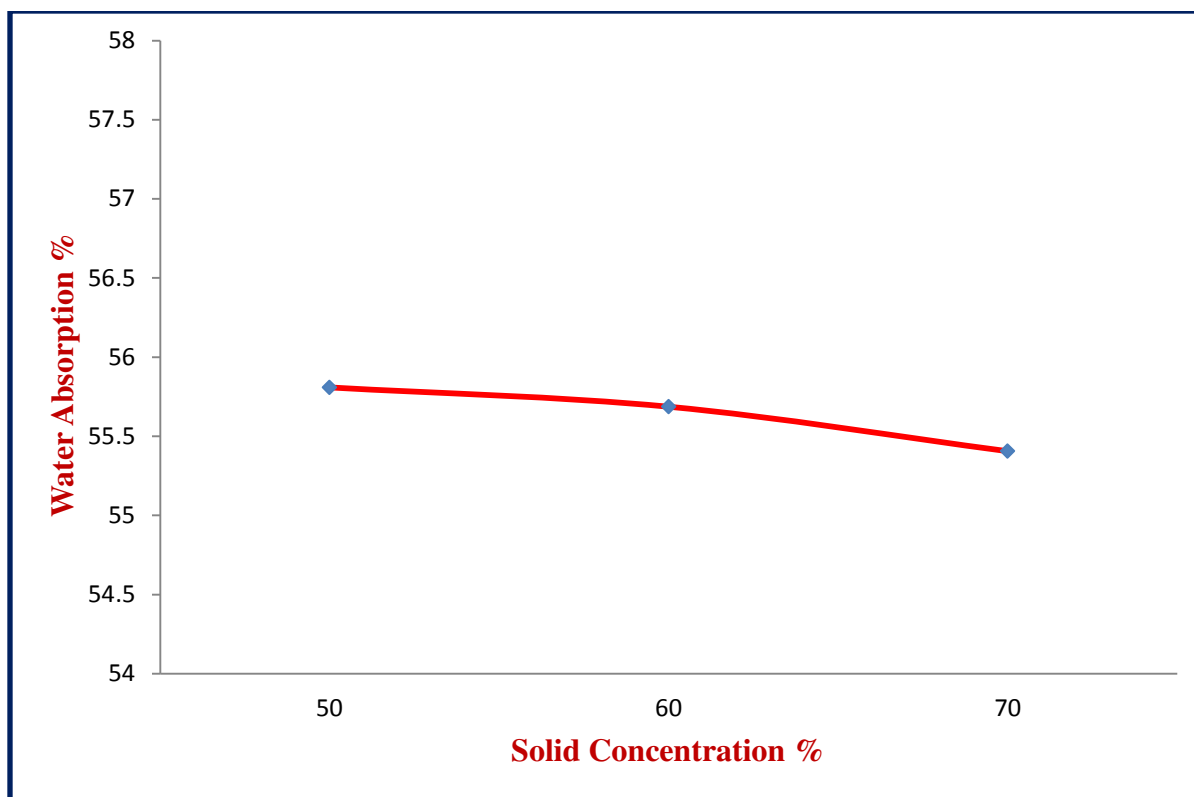


Figure (4-4): Effect of solid concentration on the water absorption.

4.3 Effects of Kaolinite Additions

Physical and mechanical properties were measured to explain the effects of kaolinite additions on micro alumina samples (B, B1, B2 and B3).

4.3.1 Linear Shrinkage

Figure (4-5), shows the linear shrinkage percentage variations with kaolinite additions. Clearly, dimension shrinkage increases when kaolinite addition is increased. This is due to high shrinkage of kaolinite (28%) in comparison with that of alumina (less than 1%) [85, 86].

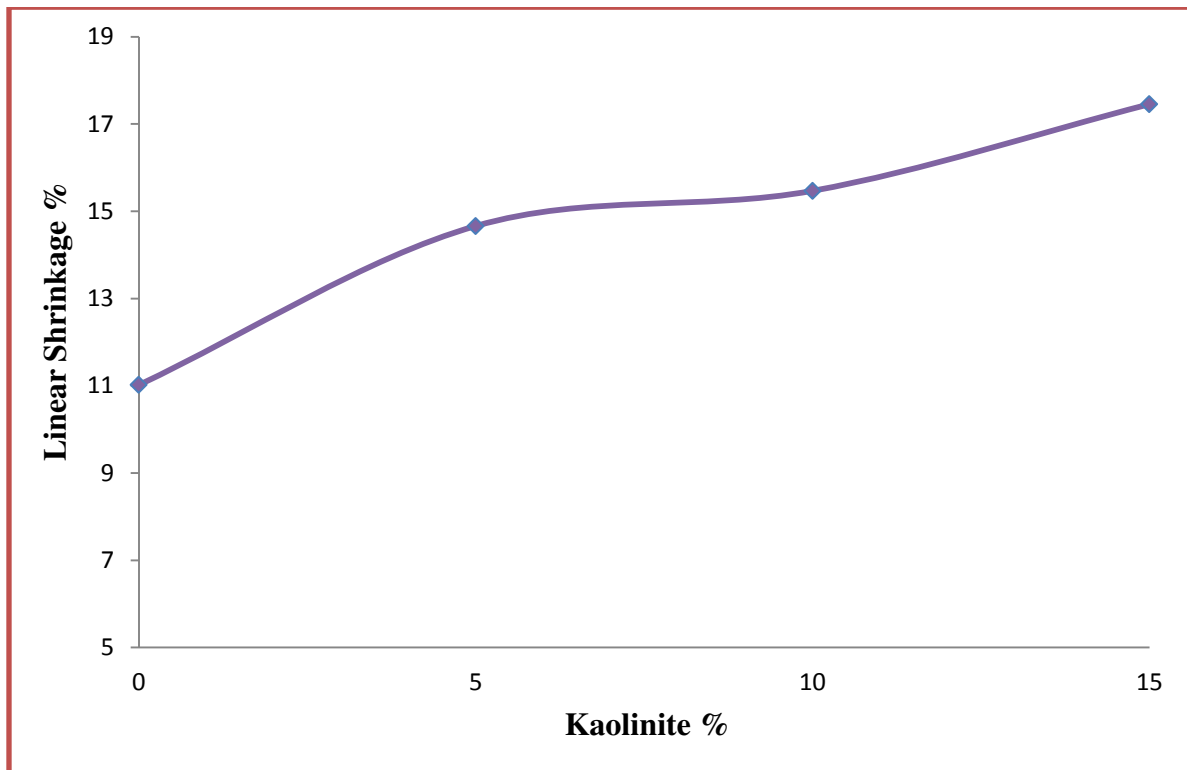


Figure (4-5): Effect of kaolinite percentage additions on shrinkage.

4.3.2 Mass Loss

Mass loss is shown in figure (4-6) for the specimens, it is decreasing with increasing kaolinite additions, this is natural situation because of the decreasing of moisture by increasing of kaolinite ratio [61].

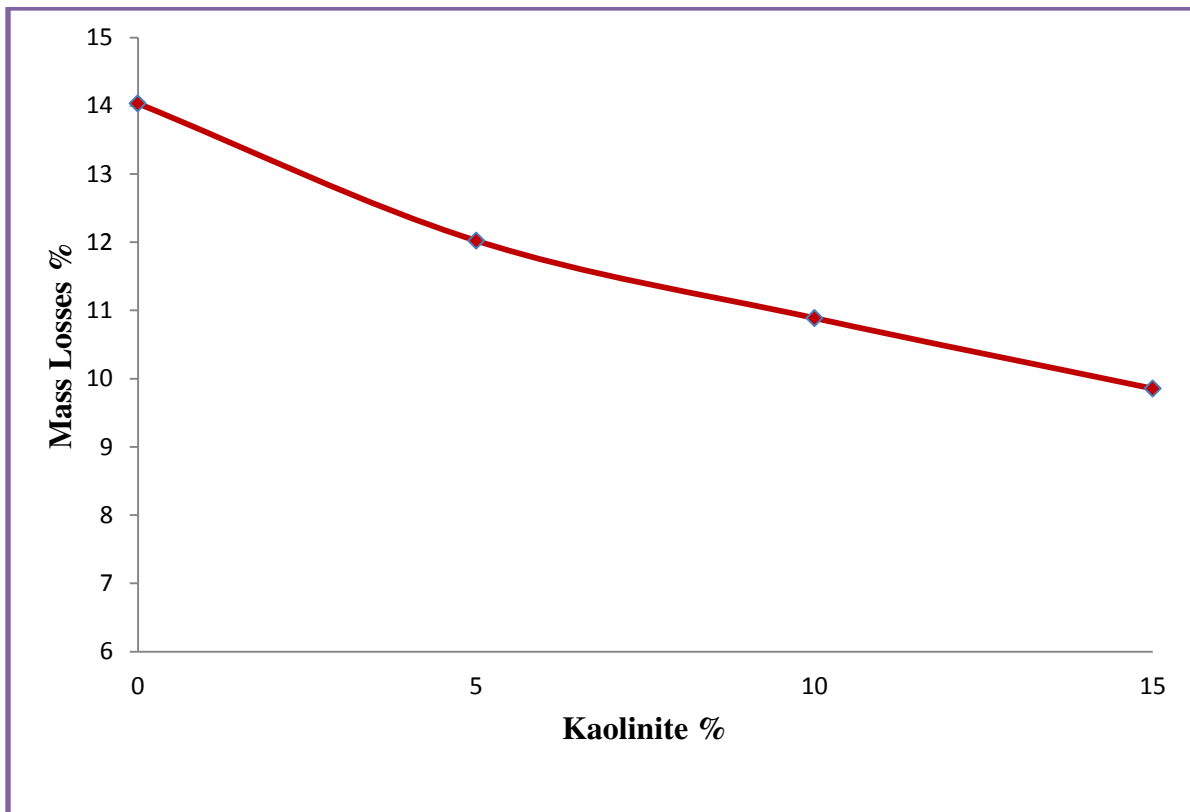


Figure (4-6): Effect of kaolinite percentage additions on loss on ignition.

4.3.3 Density, Porosity and Water Absorption

Lower density of additive materials leads to decreasing the density of the specimen. But here in the case of (alumina – kaolinite) cast the contrary was occurred, and that is a normal situation because of two main reasons; the first is the low percentage addition of kaolinite (5 – 15)%, and the second is the effect of casting rate which increase by the increasing of kaolinite ratio because of the plastic property of clay, and that leads to increase in the density because of the high reduction of porosity during forming process [11, 18]. Therefore the density is increasing with increasing of kaolinite and that is clear in figure (4-7). Figure (4-8) and (4-9) shows the decreases of porosity and water absorption respectively with kaolin additions for the same reason.

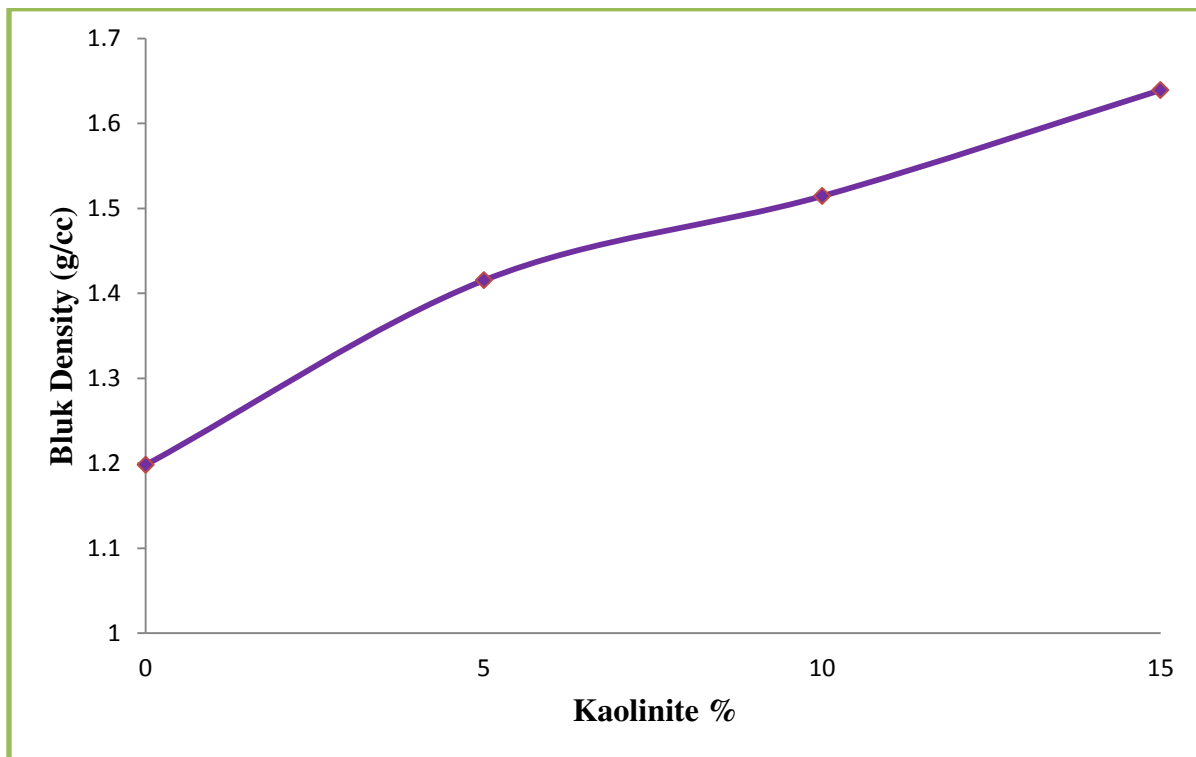


Figure (4-7): Effect of kaolinite percentage additions on bulk density.

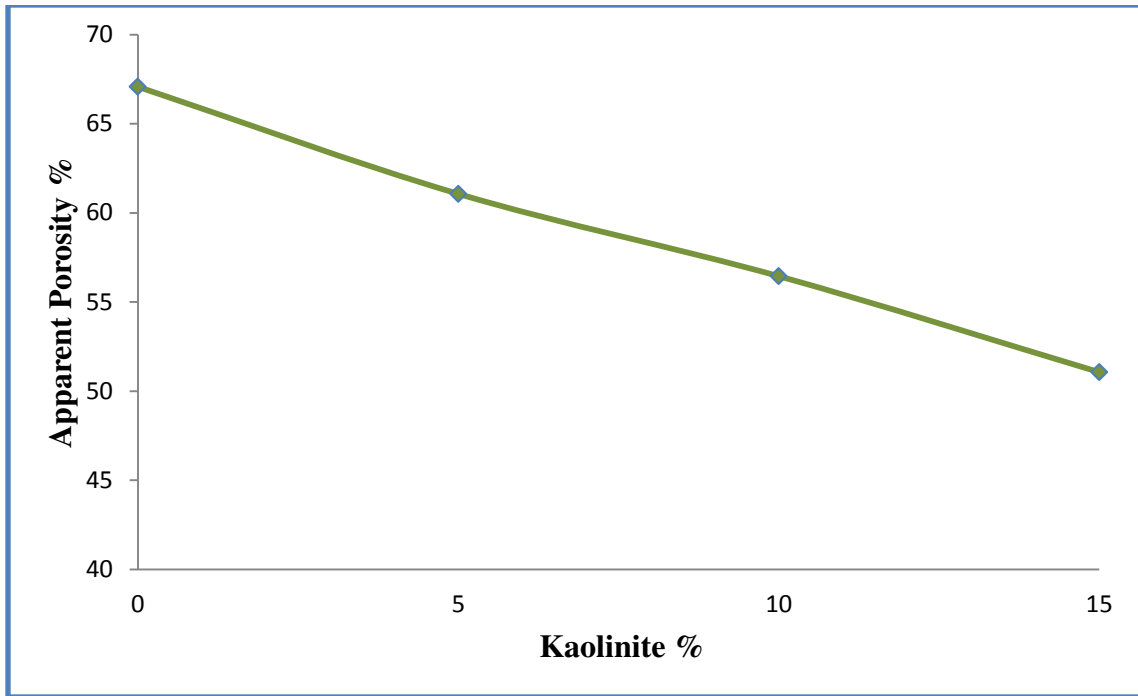


Figure (4-8): Effect of kaolinite percentage additions on apparent porosity.

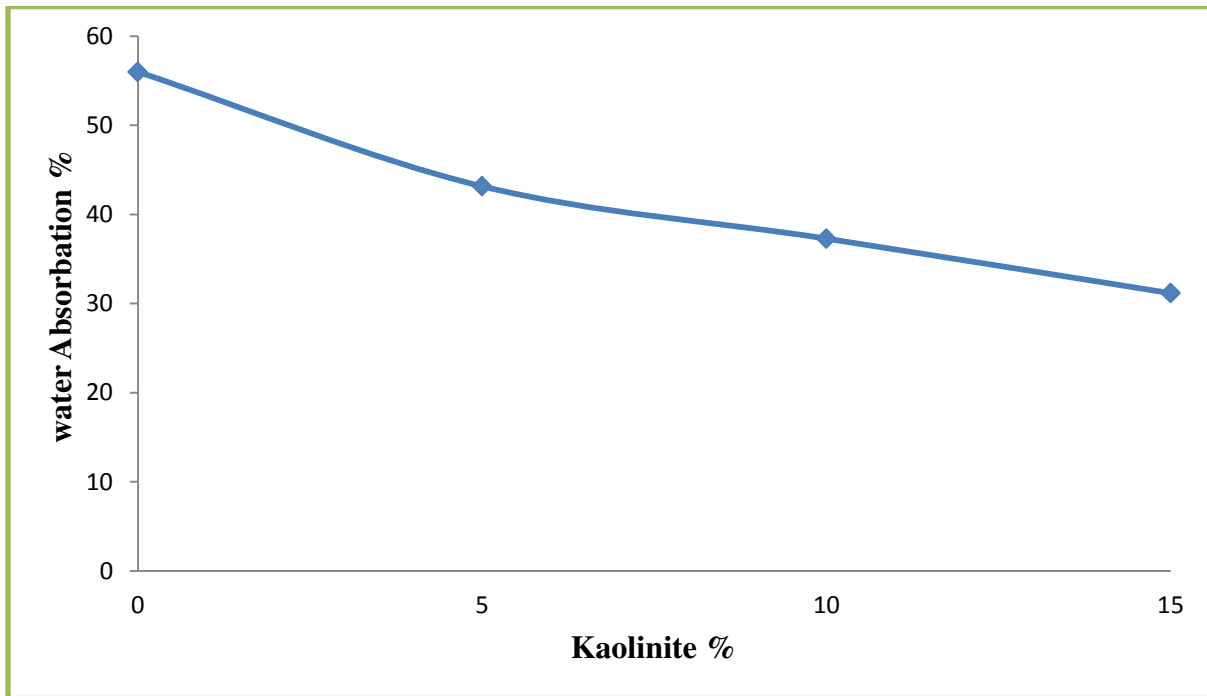


Figure (4-9): Effect of kaolinite percentage additions on water absorption.

4.3.4 Thermal Conductivity

Thermal conductivity of alumina samples, naturally, decreases with clay additions [62]. But here the thermal conductivity increases with kaolinite additions, the main cause is the increase in kaolinite ratio which leads to decrease the porosity and consequently increases thermal conductivity (figure (4-10)) [62].

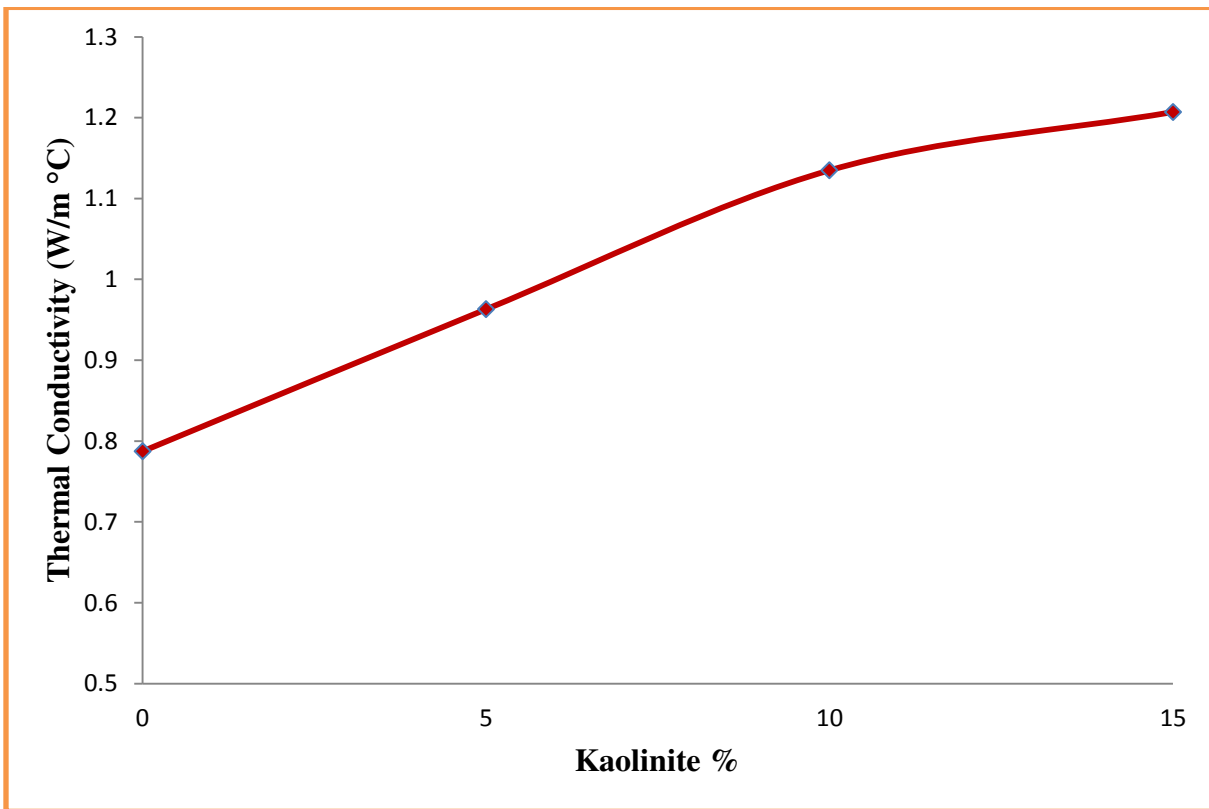


Figure (4-10): Effect of kaolinite percentage additions on thermal conductivity.

4.3.5 Mechanical Properties

The compressive strength increase with increasing kaolinite content (figure (4-11)). This increasing start with comparatively large value (at 5% addition) then increase in kaolinite addition leads to increase in the strength of ceramic products, because of the bigger amount of glass phase and higher density at the highr percentage of kaolinite [87].

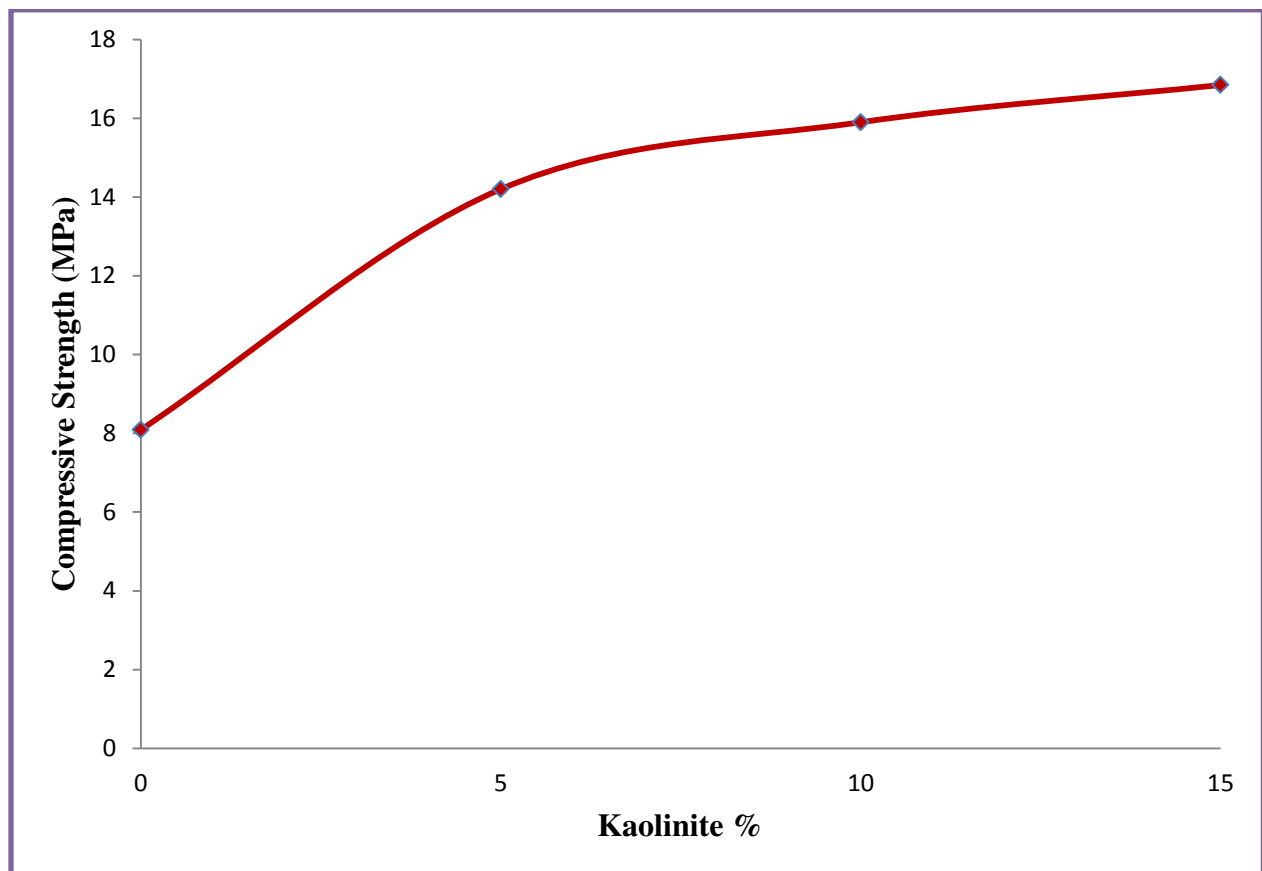


Figure (4-11): Effect of kaolinite percentage additions on compressive strength .

Bending Strength increases with clay addition which increases with a semi-linear form as shown in figure (4-12), this is due to lower porosity and higher density at the highr percentage of kaolinite [62, 87].

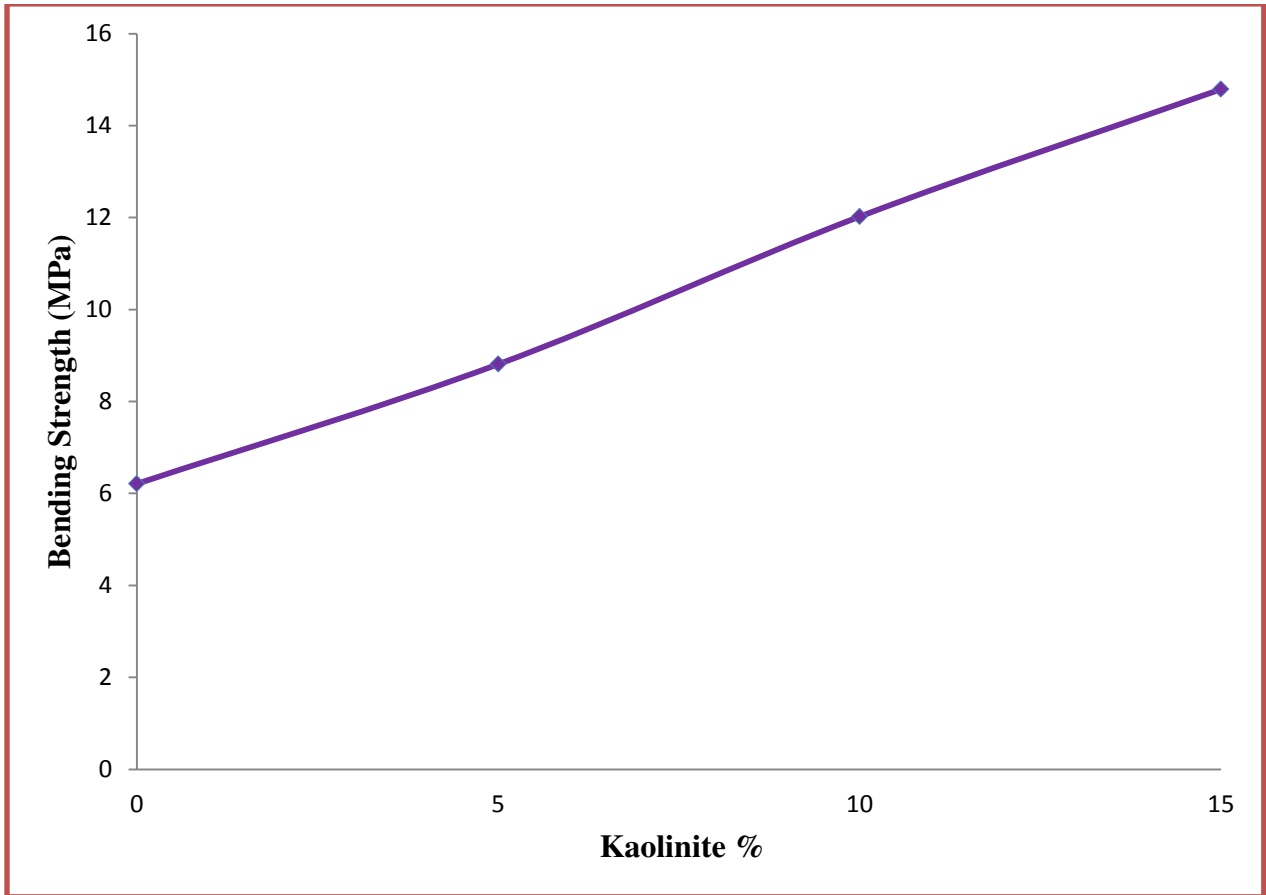


Figure (4-12): Effect of kaolinite percentage additions on bending strength.

Figure (4-13), shows the shore (D) hardness variations with kaolinite additions. Clearly, hardness increases when kaolinite addition is increased. Raising and lowering hardness can be explained on the basis of decreasing and increasing the porosity [62]. This is an important factor affecting the hardness. This increasing of hardness lead to increase wear resistance in addition to increase abarasive resistance of ceramic products.

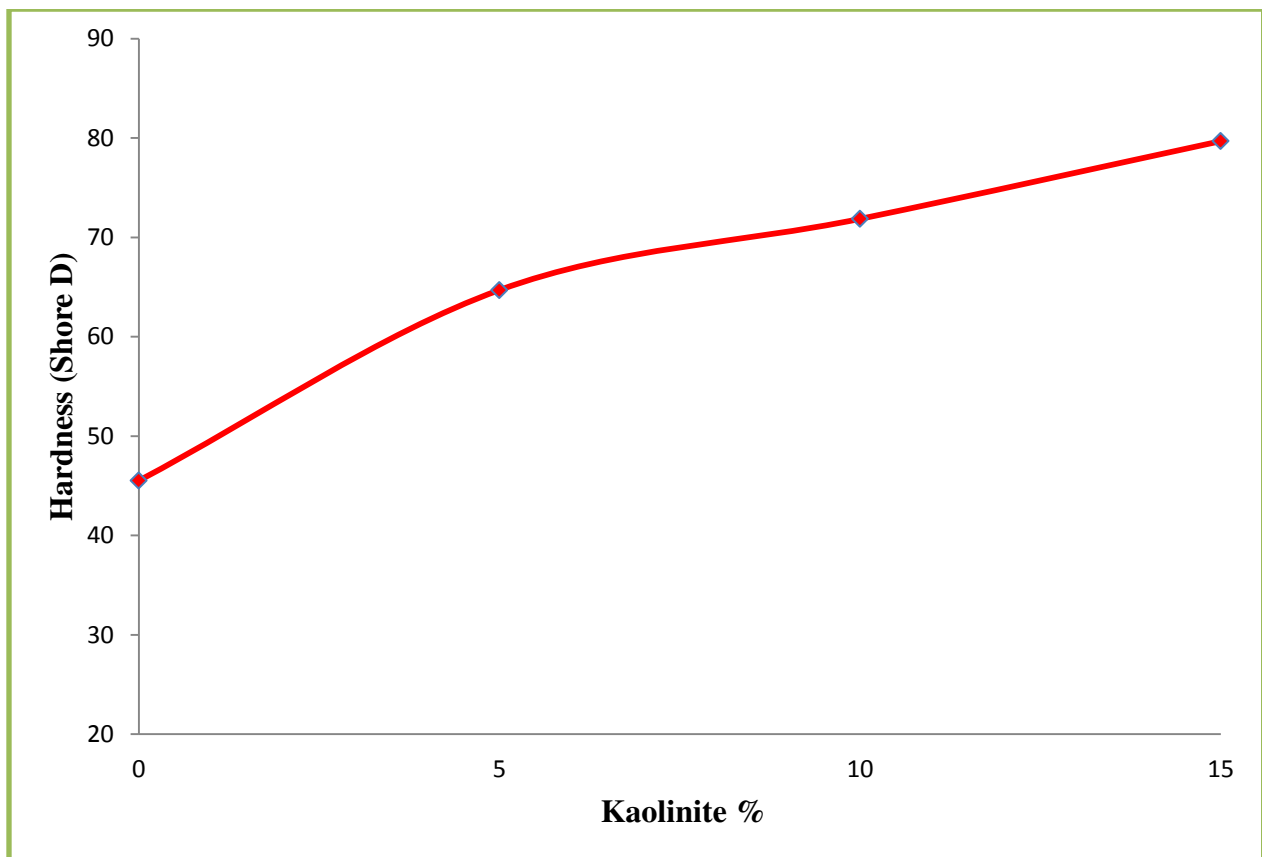


Figure (4-13): Effect of kaolinite percentage additions on hardness.

4.4 Effects of Nano Powder

Nano alumina powder has strong effect on all physical and mechanical properties. Table (4-1) represent a comparison between the samples (B2 and B5) in order to understand the effects of nano powder (nano alumina) on the (alumina-kaolinite) samples.

Loss of mass for (nano- micro) powder (B5 samples) is lower than that of micro powder (B2 samples). And the same case for shrinkge, porosity and water absorption. Density increasing for (nano- micro) powder, that increasing in density lead to increase the thermal conductivity and mechanical properties [62, 87]. This is a natural situation because of the reduction of porosity during casting process where high compaction of (nano-micro) powders occurs [62].

Table (4-1): Effects of nano alumina on the (alumina-kaolinite) samples.

No.	Properties	Units of Measure	Value	
			B5	B2
1	Loss On Ignition	%	9.064	10.888
2	Linear Shrinkage	%	14.325	15.467
3	Bulk Density	g/cm ³	1.739	1.514
3	Apparent Porosity	%	51.416	56.445
5	Water Absorption	%	29.543	37.276
6	Thermal Conductivity	W/m °C	1.293	1.134
7	Bending Strength	MPa	20	12.02
8	Compressive Strength	MPa	33.8	15.898
9	Hardness	Shore D	85.5	71.86

4.5 Effects of Sintering Temperature

Sintering temperature is one of the most effective parameters on all properties of ceramic bodies. Table (4-2) represent a comparison between the samples (B4 and B5) in order to understand the effects of sintering temperature on the (alumina-kaolinite) samples where (B4) samples sintered at (1450 °C) and (B5) samples sintered at (1550 °C).

Mass loss percentage increases with increasing the sintering temperature. And the dimension shrinkage increases when sintering temperature is increased. The bulk density increases by the increasing of the sintering temperature, so that the mechanical properties increases [62, 86].

The contrary occurs in the case of apparent porosity and water absorption where they are decreasing with increasing of sintering temperature. This is a natural situation because of the higher amount of liquid phase and the higher sintering that's occurs in the particles [62].

Table (4-2): Effects of sintering temperature on the (alumina-kaolinite) samples.

No.	Properties	Units of Measure	Value	
			B4 (1450 °C)	B5 (1550 °C)
1	Loss On Ignition	%	8.550	9.064
2	Linear Shrinkage	%	9.102	14.325
3	Bulk Density	g/cm ³	1.402	1.739
3	Apparent Porosity	%	63.603	51.416
5	Water Absorption	%	45.348	29.543
6	Thermal Conductivity	W/m °C	0.821	1.293
7	Bending Strength	MPa	11.7	20
8	Compressive Strength	MPa	15.449	33.8
9	Hardness	Shore D	70.3	85.5



Chapter Five:

Conclusions and Recommendations

5. Chapter Five: Conclusions and Recommendations

5.1 Conclusions

The following conclusions were found during this study:

- The high porosity of samples as well as their good mechanical properties and low thermal conductivity make a possibility of using it in the thermal insulation, filters, light Blocks, spark plugs and furnaces lining.
- Among many dispersants available here the (Na-CMC) was act as a good dispersant and binder, the best ratio of (Na-CMC) solution (density 1.17 g/cm³) is found to be (0.33 ml) for each gram of solid.
- The Kaolinite acts as a binder for the alumina particle.
- The decreasing of casting rate lead to increase the density and decrease the porosity.
- The increasing of kaolinite additions lead to decrease the casting rate because of its plastic property.
- The use of nano particle and the kaolinite additions improve the mechanical properties of the samples.

5.2 Recommendations

- ❖ Studying other properties of the samples such as structural, electrical, thermal and other mechanical properties.
- ❖ Studying the rheological properties of slurries.
- ❖ Studying the effect of Zeta potential of slurries on the physical properties and showing the relation between zeta potential and pH of the slurries.
- ❖ Using another dispersant such as (darvan C) and compare it with (Na-CMC).
- ❖ Using other dopants such as Zirconia, Magnesia and Titania.
- ❖ Applying a magnetic field during the casting and show its effects.
- ❖ Using a different mixing ratio of water to plaster to show its effects on the casting rate.
- ❖ Determining the particle size of powders by laser diffraction method.



References

References:

- [1]. R. Pampuch, "Constitution and Properties of Ceramic Materials", PWN-Polish Scientific Publishers, Warsaw; Elsevier, Amsterdam, (1991).
- [2]. A.G. Lamas, M. Almeida, H.M.M. Diz, "Slip-casting of alumina bodies with differential porosities", *Journal of the American Ceramic Society*, 85, (2002), (pp. 3126 – 3132).
- [3]. T. Natori, T. Shimaguchi, T. Yamada, "Method of forming cast article by slip casting", United states patent, 4,883, 621, (1989).
- [4]. J. S. Reed, *Principles of Ceramics Processing*, 2nd edition Wiley, New York (1995).
- [5]. W.H. Gitzen, "Alumina as a Ceramic Material", *The American Ceramic Society*, Westerville, (1970), (pp. 13-18).
- [6]. J.M. Andersson, "Controlling the Formation and Stability of Alumina Phases", *Plasma and Coatings Physics Division*, Linköping University, Sweden (2005).
- [7]. K. Nakano, "Alumina Powders and Their Prices", *Ceramics*, 36, (2001) (pp. 248-253).
- [8]. T. Shirai, H. Watanabe, M. Fuji and M. Takahashi, *Journal of Nagoya Institute of Technology*, 9, (2009) (pp. 23 - 31).
- [9]. A. Tsetsekou , C. Agrafiotis , A. Miliadis, "Optimization of the rheological properties of alumina slurries for ceramic processing applications Part I: Slip-casting ", *Journal of the European Ceramic Society*, 21, (2001) (pp. 363-373).
- [10]. C.Y. Chen, G.S. Lan, W.H. Tuan, "Preparation of mullite by the reaction sintering of kaolinite and alumina" *Journal of the European Ceramic Society*, 20, (2000), (pp. 2519-2525).

- [11]. Y. Zhang, J. Binner , "Enhanced casting rate by dynamic heating during slip casting "Journal of the European Ceramic Society, 22, (2002), (pp. 135–142).
- [12]. L. Braginsky, V. Shklover, H. Hofmann, P. Bowen, "High-temperature thermal conductivity of porous Al₂O₃ nanostructures "Physical Review B, 70, (2004), (pp. 134- 139).
- [13]. M. Hashiba, A. Harada, N.Adachi, S. Obata, O. Sakurada, K. Hiramatsu "Near-Net-Shape Fabrication of Porous Alumina-Spinel Castings "Materials Transactions, 46, 12 (2005), (pp. 2647- 2650).
- [14] Y. J. Shin, Ch.Ch. Su, Y. H. Shen, "Dispersion of aqueous nano-sized alumina suspensions using cationic polyelectrolyte "Materials Research Bulletin, 41, (2006), (pp. 1964-1971).
- [15] I. Zedniková, J. Andertová, J. Havrda, "Length changes of slip casting Alumina-Zirconia ceramics "Ceramics-Silikáty, 51, 3, (2007), (pp. 142-146).
- [16] S. Cava, S.M. Tebcherani, I.A. Souza, S.A. Pianaro, C.A. Paskocimas, E. Longo, J.A. Varela, "Structural characterization of phase transition of Al₂O₃ nanopowders obtained by polymeric precursor method "Materials Chemistry and Physics, 103, (2007), (pp. 394-399).
- [17] P. Silakate, A. Nuntiya, S. Larpkittaworn, "Effect of Flocculation of Alumina Slip on the Pore Size Distribution of Cast Alumina by Polyacrylamide (PAM) "Chiang Mai J. Sci., 35, 1, (2008) 17-22.
- [18] C. Falamaki, M. Beyhaghi, "Slip casting process for the manufacture of tubular alumina microfiltration membranes" Materials Science-Poland, 27, 2, (2009), (pp. 427-441).

- [19] Sun Yi hua, Xiong Wei hao, Li Chen hui," Fabrication of ultrahigh density ZnO-Al₂O₃ ceramic composites by slip casting "Trans. Nonferrous Met. Soc. China, 20, (2010), (pp. 624-631).
- [20] Li Zhang, Jef Vleugels, Omer Van der Biest, "Slip Casting of Alumina Suspensions in a Strong Magnetic Field "Journal of the American Ceramic Society, 93, 10, (2010), (pp. 3148-3152).
- [21]. Vlack, L. H. van, "Physical Ceramics for Engineers", USA: Addison Wesley Publishing Company, Inc., 1964
- [22]. P. Wray, "Structure and Properties of Ceramics", University of Tennessee state, (2009).
- [23]. J. D. Mccrummen, Master Thesis, Montana State University, (2001).
- [24]. A. Tsetsekou, C. Agrafiotis, A. Miliias; "Optimization of the rheological properties of alumina slurries for ceramic processing applications", Part I: Slip-casting, J. of the European Ceramic Society, 21, (2001), (pp. 363-373).
- [25]. C. H. Schilling and I. A. Aksay, Slip casting, In Engineered Materials Handbook, 4, Ceramics and Glasses, American Technical Publishers, Herts, (1991) (pp. 153-160).
- [26]. R. G. Horn, "Surface forces and their action in ceramic materials", J. Am. Ceram. Soc., 73(5), (1990), (pp. 1117-1135).
- [27]. R.J. Hunter, "Zeta Potential in Colloids Science", Academic Press, NY, (1981).
- [28]. W. B. Russel, D. A. Saville and W. R. Schowalter, Colloidal Dispersions, Cambridge University Press, Cambridge, UK, (1989).
- [29] J. N. Israelachvili, Intermolecular and Surface Forces, 2nd ed., Academic Press, London, (1992).

- [30] A.J. Ruys and C.C. Sorrel, "Slip Casting of High-Purity Al₂O₃ Using Sodium Carboxymethylcellulose as Deflocculant/Binder.", *Am. Ceram. Soc., Bull*, 69, (1990), (pp. 828-832).
- [31] A.J. Ruys and C.C. Sorrel, "Slip casting alumina with Na-CMC", *Bulletin of the American Ceramic Society*", *Am. Ceram. Soc., Bull*, 75, (1996), (pp. 66-73).
- [32] C. B. Carter and M. G. Norton, "Ceramic Materials Science and Engineering", (2007).
- [33] M. N. Rahaman, "Ceramic Processing and Sintering", 2nd ed. (2003).
- [34]. K. Bodišováb, M. Micháلكováb, J. Sedláčeka, "Alumina/MWCNTs composites by aqueous slip casting and pressureless sintering", *Ceramics International*, 39, (2013), (pp. 6543-6550).
- [35]. I. Levin, D. Brandon, *Metastable Alumina Polymorphs: Crystal Structures and Transition Sequences*. *J. Am. Ceram. Soc.*, 1998. 81, (8), (pp. 1995–2012).
- [36]. E. Dorre, H. Hubner,, *Alumina-Processing Properties and Applications*. Berlin: Springer-Verlag. 73, (1984), (pp. 251-267).
- [37]. Z. R. Ismagilov, R. A. Shkraabina, N. A. Koryabkina, *New technology for production of spherical alumina supports for fluidized bed combustion*. *Catalysis Today*, 47, (1999), (pp. 51-71).
- [38]. W. H. Gitzen, *Alumina as a ceramic material*, Columbus: The American Ceramic Society. (1970).
- [39]. S. Vasefi, M. Parvari, "Alkaline earth metal oxides on γ -Al₂O₃ supported Co catalyst and their application to mercaptan oxidation", *Korean Journal of Chemical Engineering*, 27 (2), (2010), (pp. 422-430).
- [40]. J. M. McHale, A. Auronx, A. J. Perrotta, A. Navrotsky, "Surface Energies and Thermodynamic Phase Stability in Nanocrystalline Aluminas", *Science*, 277 (8), (1997), (pp. 777-788).
- [41]. K. Jiang, D. Music, K. Sarakinos, J. Schneider, "Study of effects of

- substitutional additives on the phase stability of γ –alumina”. *Journal of Physics: Condensed Matter*, 22, 505502, (2010), (pp. 8-17).
- [42]. M. A. Aswad, Doctoral Thesis, University Of Manchester, (2012).
- [43]. W. Rayan and C. Radford, “White Wares Production Testing and Quality Control”, Pergamon Press, U.K (1987) (p256-259).
- [44]. W.Gerhartz, "Ullmann's Encyclopedia Of Industrial Chemistry", Verlagsgesellschaft , Germany, 7, (1987), (pp. 109-111).
- [45]. R. Tantatherdtam, Doctoral Thesis, The Pennsylvania State University, (2003).
- [46]. J.K. Mitchell, “Fundamentals of Soil Behavior”, 2nd Edition, JohnWiley & Sons, Inc., New York (1993).
- [47]. C. Detellier, S. Letaief, “Kaolinite–Polymer Nanocomposites”, *Journal of Developments in Clay Science*, 5, (2013), (pp. 707-719).
- [48]. W. Bolton, "Engineering Materials Technology", 3rded. , Butterworth Heinemann, Oxford, (1998), (pp. 291, 294).
- [49]. M. A. Aswad and T.J. Marrow, “Intergranular Crack Nucleation in Polycrystalline Alumina”, *Journal of Engineering Fracture Mechanics* (2011).
- [50]. A. Ito, Y. You, H. Katsui and T. Goto, “Growth and microstructure of β -alumina films by laser chemical vapor deposition”, *Journal of the European Ceramic Society*, 33, (2013), (pp. 2655-2661).
- [51]. L. Mahnicka, “Influence of Raw Materials Ratio and Sintering Temperature on the Properties of the Refractory Mullite-Corundum Ceramics”, *World Academy of Science, Engineering and Technology*, 63, (2012).
- [52]. H. Lu, W. Wang, W. Tuan and M. Lin, “Acicular Mullite Crystals in Vitrified Kaolin”, *J. Am. Ceram. Soc.*, 87, (2004), (pp.1843–1847).
- [53]. K. Okada, “Activation energy of mullitization from various starting materials” *J. Eur. Ceram. Soc.*, 28, (2008) (pp. 377-382).

References

- [54]. R. Svinka, V. Svinka, G. Bula, T. Juettner and E. Palcevskis, "Influence of suspensions rheology on the properties of light weight high temperature materials" *Adv. Sci. Technol.*, 45, (2006) (pp. 2266-2271).
- [55] T. Juettner, H. Moertel, V. Svinka, R. Svinka, "Structure of kaoline– alumina based foam ceramics for high temperature applications", *J. Eur. Ceram. Soc.*, 27, (2007) (pp. 1435-1441).
- [56] H. J. Kleebe, F. Siegelin, T. Straubinger and G. Ziegler, "Conversion of Al₂O₃–SiO₂ powder mixtures to 3:2 mullite following the stable or metastable phase diagram", *J. Eur. Ceram. Soc.*, 21, (2001), (pp. 2521-2533).
- [57] A. Aras, "The change of phase composition in kaolinite- and illiterich clay based ceramic bodies." *Appl. Clay Sci.*, 24, (2004) (pp. 257-269).
- [58] H. Schneider, S. Komarneni. "Mullite" Wiley - VCH Verlag GmbH & Co.KGaA, (2005), (pp. 180-190).
- [59]. R. J. A. Soldozian, master Thesis, University Of Technology, (2012).
- [60]. ASTM D854 – 10, "Standard Test Methods for Specific Gravity of Soil Solids by Water Pycnometer1", *Annual Book of ASTM Standards*, (2010).
- [61]. AS 2879.1, "THE IMPORTANCE AND TESTING OF DENSITY / POROSITY / PERMEABILITY / PORE SIZE FOR REFRACTORIES", (2010).
- [62]. S. A. Z. Al-Jeboori, Doctoral Thesis, University of Technology, (2005).
- [63]. ASTM C326 – 09, "Standard Test Method for Drying and Firing Shrinkages of Ceramic Whiteware Clays", *Annual Book of ASTM Standards*, (2009).
- [64]. S.C. Carniglia, and G.L. Barna, "Handbook of Industrial Refractories Technology", Noyes Publications, United Sates of America (1992).
- [65]. ASTM C20 – 00, "Standard Test Methods for Apparent Porosity, Water Absorption, Apparent Specific Gravity, and Bulk Density of Burned Refractory Brick and Shapes by Boiling Water", (2010).

References

- [66] E. Grimsehl, "A Text Book of Physics", 2nd ed., Blackie and Sons Lemet, (1944) (pp. 21-22).
- [67] T. Akrill, G. Bennet, C. Millar, "Physics", Edward Arnold Publishers Ltd, London, (1979), (pp. 118-119).
- [68]. F. franklin, Y. Wang, "Treatise on Materials Science and Technology", 9, Academic Press, New York, (1976) (pp. 254-255).
- [69]. G.W. Meetham and M.H. Van de Voorde, "Materials for High Temperature Engineering Applications", Springer, berlin (2000), (pp. 123-124).
- [70]. ASTM D2240 – 05, "Standard Test Method for Rubber Property - Durometer Hardness", (2010).
- [71]. W. D. Callister , " Materials Science and Engineering", 5th ed. , John Wiley , U.S.A , (2000), (pp. 406-407).
- [72]. P. Pastila, E. L. Curzio, "Determining the microstructure of some SiC-based hot gas filter materials", J. of the European Ceramic Society, 21, Sep. (2001) (pp. 1269-1272).
- [73] G. Zhong , Y. Hui, J. of Zhejiang University Science , 5, 8, (2004) (pp. 950-955).
- [74]. M.W. Barsoum, "Fundamentals of Ceramics", Mc Graw – hill, Singapore, (1997) (pp. 371-372).
- [75]. W. D. Kingery and H. R. Bowen and D. R. Uhlmann, "Introduction to Ceramics", 2nd ed., (1976) (pp. 499- 504).
- [76]. P. Boch , "RESISTANCE TO THERMAL FATIGUE AND STANDARDS" "Intereram" , No.3 ,(1984) (p 37-39).
- [77]. K. Othmer, "Encyclopedia of Chemical Technology", 3^{ed.}, 5, John wiley, U.S.A (1979), (pp. 276-277).
- [78]. P.Boch , J. C. Glandus, "Porosity effects on mechanical properties of ceramics", "Intereram" , 3, (1983) (pp. 33-36).

References

- [79]. S.F. Wang, J. Zhang, D.W. Luo, F. Gu, D.Y. Tang, Z.L. Dong, G.E.B. Tan, W.X. Que, T.S. Zhang, S. Li and L.B. Kong, “ceramics: Processing, materials and applications”, , J. of Progress in Solid State Chemistry, 41, (2013), (pp. 20-54).
- [80]. I. Levin and D. Brandon, “Metastable alumina polymorphs: Crystal structures and transition sequences”, J. Am. Ceram. Soc., 81, (1998) (pp. 1995-1999).
- [81]. W.H. Gitzen, “Alumina as a ceramic material”, The American Ceramic Society, Westerville, (1970), (pp. 17- 21).
- [82]. ASTM C773 – 88, “Standard Test Method for Compressive (Crushing) Strength of Fired White ware Materials”, Annual Book of ASTM Standards, (2011).
- [83]. ASTM C1674 - 11, “Standard Test Method for Flexural Strength of Advanced Ceramics with Engineered Porosity at Ambient Temperatures”, Annual Book of ASTM Standards, (2011).
- [84]. J. G. P. Binner and A. M. Murfin, “The Effect of micro wave energy on the slip casting of aqueous ceramic suspensions”, University of Nottingham, UK, (1997).
- [85]. N. Claussen, T. Le and S. Wu, “Low shrinkage reaction bonded alumina”, Journal of the European Ceramic Society, 5, 1, (1989), (pp. 29–35).
- [86]. H. Mohammed, “Reducing Kaolin Shrinkage by Using Kaolin Grog”, Journal of Babylon University, 18, 4, (2011), (pp. 713 -724).
- [87]. J. S. Magdeski, “The porosity dependence of mechanical properties of sintered alumina”, Journal of the University of Chemical Technology and Metallurgy, 45, 2, (2010), (143-148).
- [88]. ASTM C59 / C59M - 00, “Standard Specification for Gypsum Casting Plaster and Gypsum Molding Plaster”, Annual Book of ASTM Standards, (2011).

الخلاصة

في هذه الدراسة، تم تحقيق ظواهر فيزيائية متعلقة بانماء وتحول الاطوار البلورية لمسحوق الالومينا (Al_2O_3) من خلال التجارب والحسابات.

تم تشكيل العينات باستخدام طريقة الصب الانزلاقي. واحرقت هذه العينات بدرجات حرارة مختلفة (500, 1100, 1450, 1550, 1600) درجة سيليزية.

حضرت عينات الالومينا بنسب تشويب مختلفة لدراسة صفاتها الميكانيكية والفيزيائية المتعددة. قبل عملية الصب، تم تحضير عوالق من احجام حبيبية مختلفة وتراكيز بنسب وزنية متعددة (50 – 70) %، وبنسبة تشويب متعددة. المشوب الاساسي المستخدم هو مسحوق الكاؤولينايت بنسب تشوية مختلفة (0, 5, 10 و 15) %، حيث ان الكاؤولينايت احد المواد الخام التي تمتلك صفة اللدونة وميزة الربط.

المادة المشتتة التي تم استخراجها هي محلول (Na-CMC). حيث ان استقرارية العالق تعتمد بشكل مباشر على نسبة اضافة المشتت، افضل نسبة اضافة كانت (0.33 مل) لكل غرام واحد من المادة الصلبة.

زيادة التركيز الصلب في العوالق يؤدي الى نقصان الكثافة والمسامية وامتصاية الماء، بينما يؤدي الى زيادة في التقلص الحاصل في العينات.

زيادة نسب اضافة الكاؤولينات يؤدي الى نقصان في المسامية، امتصاية الماء والفقدان بالكتلة. بينما يؤدي الى زيادة التوصيلية الحرارية، الكثافة، التقلص والصفات الميكانيكية (مقاومة الانضغاط، مقاومة الانحناء والصلاة).

وتم ايضا دراسة تأثير كل من الحجم الحبيبي النانوي ودرجة حرارة التلبيبة على كل من الصفات الفيزيائية والميكانيكية.



جمهورية العراق
وزارة التعليم العالي والبحث العلمي
جامعة ديالى
كلية العلوم / قسم الفيزياء

دراسة خصائص الاجسام السيراميكية المحضرة من مساحيق مايكروية و نانوية بتقنية الصب الانزلاقي

رسالة مقدمة الى
مجلس كلية العلوم - جامعة ديالى وهي جزء من متطلبات نيل
درجة الماجستير علوم في الفيزياء

من

حيدر علي سلمان العبيدي

بإشراف

أ.د. صباح أنور
سلمان
أ.م.د. شهاب أحمد
زيدان

2013م

1435هـ